

STRATUS CONSULTING

Potential Hydrologic and Water Quality Alteration from Large-scale Mining of the Pebble Deposit in Bristol Bay, Alaska: Results from an Integrated Hydrologic Model of a Preliminary Mine Design

Review Draft

Prepared for:

Randall Hagenstein
State Director
The Nature Conservancy
715 L St # 100
Anchorage, AK 99501

The Nature Conservancy
Protecting nature. Preserving life.™

Review Draft
October 8, 2012

Potential Hydrologic and Water Quality Alteration from Large-scale Mining of the Pebble Deposit in Bristol Bay, Alaska: Results from an Integrated Hydrologic Model of a Preliminary Mine Design

Review Draft

Prepared for:

Randall Hagenstein
State Director
The Nature Conservancy
715 L St # 100
Anchorage, AK 99501

Prepared by:

Cameron Wobus
Ann Maest
Stratus Consulting Inc.
PO Box 4059
Boulder, CO 80306-4059

Bob Prucha
Integrated Hydro Systems, LLC
PO Box 3375
Boulder, CO 80307

Dave Albert
The Nature Conservancy
416 Harris Street, Suite 301.
Juneau, AK 99801

October 8, 2012
Confidential
SC13001

Contents

Abstract

Bristol Bay, Alaska is home to one of the most productive wild salmon fisheries on Earth, as well as one of the planet's largest undeveloped copper, gold, and molybdenum deposits. A mining group known as the Pebble Limited Partnership has invested hundreds of millions of dollars to develop the mineral resources in a project known as the Pebble Project, while the commercial fishing industry and some Alaska Native communities have expressed concern that such large-scale mining would create unacceptable risks to the ecosystem. To better understand and characterize potential risks to hydrologic processes and water quality in these watersheds, we built a hydrologic model of the deposit area using the integrated groundwater-surface water-climate code MIKE-SHE. Inputs to the model included information from publicly available sources, as well as documents released to the public by the mine proponents. A simple and realistic set of assumptions under baseline (i.e., pre-mine) conditions provided a good fit to measured streamflows and groundwater elevations without substantial adjustment of input variables. Potential effects of large-scale mining were evaluated by imposing a mine scenario that included an open pit mine, a tailings impoundment, and waste rock dumps in the headwaters of the three major streams draining the deposit area. Model results indicate that streamflows near the pit could decrease by more than 60% under this mining scenario, with more pronounced changes during spring and fall high flows. Water quality simulations tracking leachate from waste rock facilities indicate that in the absence of aggressive mitigation, leachate will migrate rapidly through shallow groundwater and inundate former headwater reaches. The resulting copper concentrations simulated in streams exceed relevant water quality standards for the protection of aquatic life under most flow conditions throughout the model domain. Simulations that include a system of active drains and pumps to capture waste rock leachate, likely required under permitting, indicate that even short-duration failures of such a system could lead to escape of leachate into surface waters, due to the high hydraulic conductivity of the unconsolidated glacial outwash surrounding the deposit. Resulting copper concentrations in receiving streams are predicted to exceed water quality criteria within days to weeks of a leachate collection system failure. The results are based on a preliminary 25-year mine design, whereas the 45-year resource is estimated to be approximately two times as large. Thus, our study shows that while some of the flow and water quality changes brought about by mining could be ameliorated by ambitious mitigation measures and water management plans, severe water quality effects could result from even a brief failure of these systems.

1. Introduction

The watersheds of Bristol Bay in southwestern Alaska rank among the most productive wild Pacific salmon (*Onchorhynchus* spp.) systems on Earth (Ruggerone et al., 2010). In the context of widespread declines in salmon stocks across the southern portions of their range (Lackey et al., 2006), these watersheds represent critical strongholds for future conservation of these species (Pinsky et al., 2009) and have supported sustainable commercial fisheries for more than 100 years (Hilborn et al., 2003).

The headwaters of the Nushagak and Kvichak rivers also contain a copper-gold-molybdenum ore body estimated at approximately 11.9 billion tons (Ghaffari et al., 2011), the potential development of which has raised concerns about downstream water quality, resident and anadromous fish, and other aquatic biota. Given the magnitude, history, and global significance of the salmon fishery in this region, a thorough estimation of ecological risk using the best available methodology is warranted (Suter et al., 2007).

The goal of this study was to develop and calibrate an integrated hydrologic model of the Pebble Project area and to improve the understanding of the potential effects of mining on existing hydrologic and water quality conditions. The hydrology of the Pebble area is characterized by complex surface water-groundwater interactions that vary in both space and time. The major streams draining the deposit area contain a number of gaining and losing reaches, and in some areas, streamflow is sustained by groundwater transfers from losing stream segments in other watersheds (Knight Piésold, 2011). Simulating these types of strongly coupled natural hydrologic conditions requires a fully integrated, physically based code with spatially explicit parameters. Such codes allow flows and solutes to be tracked within and among surface water, groundwater, and atmospheric systems based on the local physics, rather than being compartmentalized into separate surface water, groundwater, and atmospheric models.

The headwater streams draining the Pebble deposit have low background levels of dissolved copper, hardness, dissolved organic carbon (DOC), and alkalinity (SRK Consulting, 2011a). Under these conditions, aquatic biota are more susceptible to the toxic effects of metal releases because the background water quality conditions provide little assimilative or buffering capacity for additional metal loads (Meyer et al., 2007). One of the goals of the modeling exercise was to investigate the potential effects of mine-related releases on downstream water quality, especially changes in dissolved copper concentrations under a variety of flow conditions.

To evaluate hydrologic changes resulting from proposed large-scale mining, the model was constructed using available information on the topography, geology, and climate in the Pebble area, and was calibrated using publicly available information describing surface flows and groundwater elevations. Using the calibrated model, potential changes to the hydrology and geochemistry of the system associated with a preliminary mine design (Ghaffari et al., 2011)

were evaluated. Recognizing that water management and leachate collection systems would be required to minimize downstream effects, the simulations focused on changes in surface flows related to dewatering during mining operations, as well as potential changes in water quality related to downgradient movement of waste rock leachate in the event of short- or long-term failure of the leachate collection system. The goal was not to develop specific numeric predictions for a specific failure scenario, but rather to investigate the potential water quality and quantity effects that could occur from active dewatering and as a result of failure of a leachate collection system over time.

2. Physical Setting

2.1 Geology and Physiography

The Pebble area is characterized by relatively low topographic relief with exposed bedrock on ridges and hilltops, and thick Quaternary glacial material filling most of the valleys (Figure 1). The main ore body is drained by three streams in the Nushagak and Kvichak watersheds: the North Fork Koktuli River (NFK) and South Fork Koktuli River (SFK) drain the northwestern and southern sides of the deposit, flow south-southwest, join at approximately 25 km southwest of the deposit, and eventually drain into the Nushagak River. Upper Talarik Creek (UT) drains the eastern side of the deposit, and flows primarily southward until it drains into Lake Iliamna, approximately 25 km due south of the deposit. Lake Iliamna is in the headwaters of the Kvichak drainage, which also flows into Bristol Bay. Collectively, the Nushagak and Kvichak rivers represent two of the most productive wild salmon fisheries in the world (Ruggerone et al., 2010), and Lake Iliamna is a premier salmon nursery.

In the headwaters of the Nushagak and Kvichak watersheds, the Pebble deposit covers an area of approximately 5.5 km^2. The ore body is a porphyry copper-gold-molybdenum deposit and is divided into a shallower Pebble West Zone and a deeper and richer Pebble East Zone. The minerals of economic interest in the deposit are all sulfides. Copper occurs primarily as chalcopyrite ($CuFeS_2$); the gold is associated with the iron sulfide mineral pyrite (FeS_2) or other copper-containing sulfides; and molybdenum occurs in molybdenite (MoS). Minor bornite (Cu_5FeS_4) and tetrahedrite [$(Cu, Fe, Zn, Ag)_{12}Sb_4S_{13}$] are also present in the ore body. The shallower Pebble West deposit extends from just below the surface to a depth of 610 m, and the richer Pebble East, which extends to a depth of 1,525 m, is covered by up to 600 m of Tertiary sedimentary and volcanic rocks and Quaternary glacial material. The ore host rocks are pre-Tertiary (Cretaceous) granodiorites and mudstones, and the bedrock overlying the Pebble East Zone largely comprises Tertiary volcanic and sedimentary sequences. Bedrock throughout the deposit area is typically highly weathered and fractured in the uppermost 10–15 m (Knight Piésold, 2011; Knight Piésold et al., 2011; Ghaffari et al., 2011).

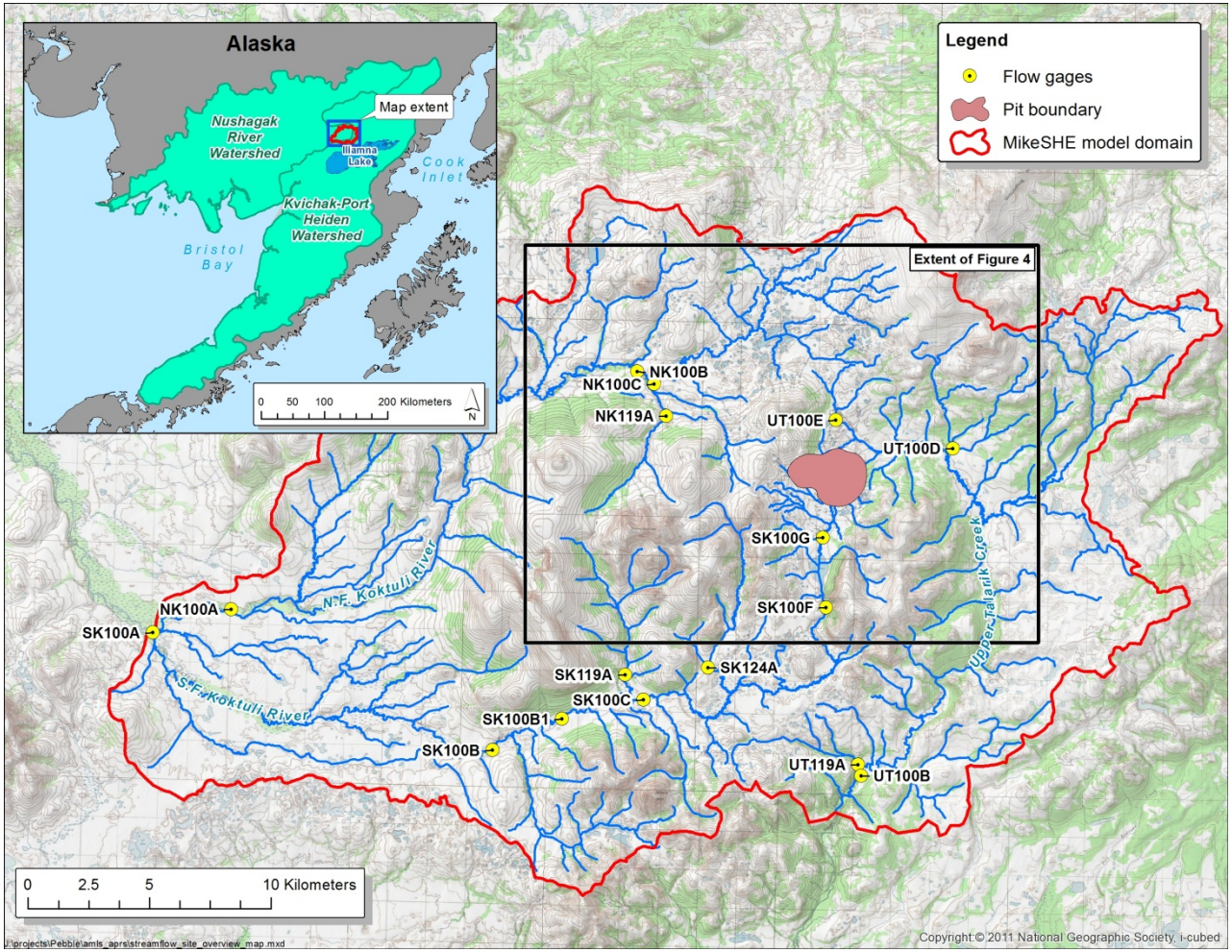

Figure 1. Location and physiography of Pebble area. Stream gages and water quality monitoring locations are labeled along SFK, NFK, and UT. Inset shows location of proposed mine infrastructure, shown in more detail in Figure 4.

Surficial deposits are characterized by thick sequences of sand and gravel outwash filling broad glacially scoured valleys. The outwash deposits are locally more than 100-m thick, with decreasing thickness along the valley walls, near bedrock outcrops, and at local constrictions in bedrock valleys. Locally, finer-grained glaciolacustrine and ice-contact deposits form low-permeability surface layers, some of which coincide with perched lakes and ponds scattered throughout the region (Knight Piésold et al., 2011).

2.2 Surface and Groundwater Hydrology

Surface water flows in the three mainstem drainages near the Pebble deposit area are characterized by a double-peak hydrograph, with peak discharges occurring during spring snowmelt, typically in May, and fall rainstorms, typically from September to October (Figure 2).

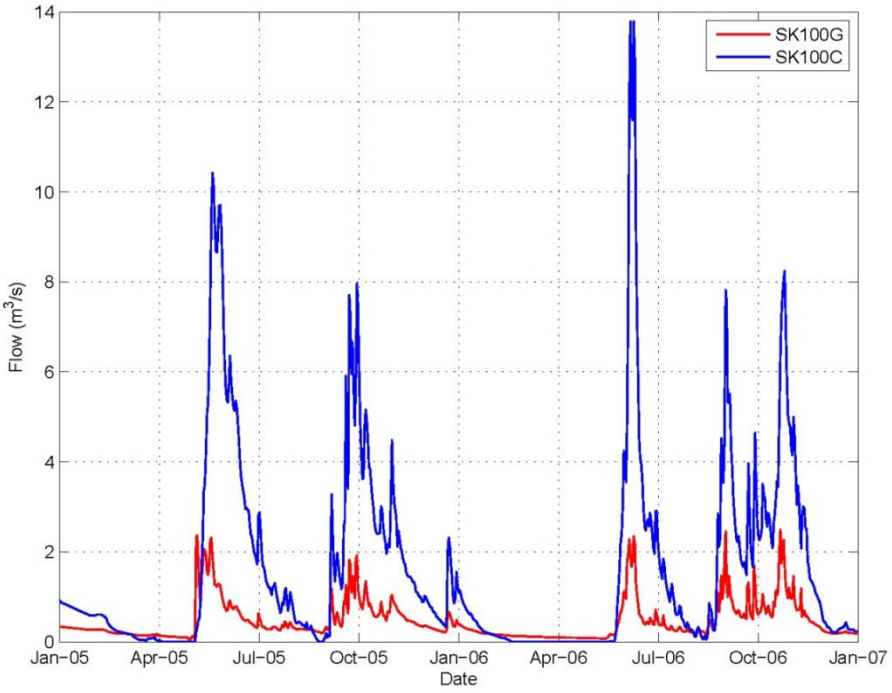

Figure 2. Typical stream hydrograph for mainstem streams draining the Pebble deposit area.

Depths to groundwater on the site range from less than 1 m to approximately 50 m below ground surface (bgs), with the majority of groundwater depths falling between 1 and 20 m bgs. Groundwater elevations vary seasonally, with many wells exhibiting seasonal variations of up to 5–10 m (Schlumberger Water Services, 2011).

In general, groundwater elevations mimic the topography, and groundwater drainage divides follow surface water divides. However, as documented in the Environmental Baseline Documents (EBD; Knight Piésold et al., 2011) groundwater migrates across surface water divides in some key locations, such as between the middle SFK and the UT drainage basin, upstream of stream gaging station UT119A (see Figure 1). Other areas of groundwater upwelling within catchments are also present in the UT and NFK watersheds. The groundwater upwelling areas provide key salmon spawning habitat because the relatively constant-temperature inflowing groundwater prevents eggs from freezing in the winter and removes fine sediment, which enhances the porosity and oxygen content of the redds (Brunke and Gonser, 1997).

2.3 Baseline Surface Water Quality

Surface water quality in the mainstem NFK, SFK, and UT is characterized by low hardness, alkalinity, and temperature; near-neutral to slightly acidic pH values; low to moderate DOC concentrations; and low dissolved copper concentrations (Table 1). Higher hardness, alkalinity, and DOC values can protect aquatic biota against the toxic effects of increasing copper concentrations (Miller and Mackay, 1980; MacRae et al., 1999; Meyer et al., 2007; Welsh et al., 2008).

DOC concentrations were measured from 2007 to 2008. In general, DOC concentrations are highest in the headwater reaches of all three streams, decrease with distance downstream, and peak during snowmelt and fall rain events (Figure 3a). The highest DOC values are in the upper reaches of UT (up to ~ 8 mg/L). During non-peak flows, DOC concentrations are typically < 2 mg/L at all locations. Hardness and alkalinity values are low in all three streams (mean values ≤ 35 mg/L as $CaCO_3$ for both parameters, with lows less than 10 mg/L as $CaCO_3$ in the Koktuli drainages) but are highest in the UT (see Table 1). Field pH values are lowest in the SFK, with minimum values below 5 at two locations (SK100F, 4.39; SK100C, 4.79). In general, pH values vary between 6 and 7 at all other locations.

Dissolved copper concentrations were in the low microgram per liter range in all drainages. Concentrations are highest in the upper reaches of the SFK over the western Pebble deposit. For example, copper values were as high as 5 µg/L at SK100G before a dry-year (2007) snowmelt peak when dilution flows were low (Figure 3b). Concentrations at this location generally peak during snowmelt and autumn rain high flows and range between 1 and 3 µg/L. Values remain above 1 µg/L between the headwaters and the middle SFK (SK100C) but decrease to 0.5 µg/L at the confluence with the SFK (SK100A; see Figure 1). Copper concentrations in the NFK and UT were lower and generally ranged between detection limits (~ 0.1 µg/L) and 0.5 µg/L (Figure 3b).

Table 1. General observed (baseline) water quality in the mainstem SFK, UT, and NFK

		Temp (°C)	pH (SU)	DOC (mg/L)	Hardness (mg/L as $CaCO_3$)	Alkalinity (mg/L as $CaCO_3$)	Dissolved copper (µg/L)
SFK	Min	-0.2	4.39	0.08	7.68	1.55	0.16
	Max	23.5	8.85	4.09	42.6	40.0	4.93
	Mean	5.3	6.68	1.58	19.7	16.5	1.57
UT	Min	-0.2	4.90	0.08	14.9	12.0	0.09
	Max	15.3	8.16	8.18	62.2	56.0	1.54
	Mean	3.9	7.08	1.38	33.9	34.6	0.43
NFK	Min	-0.2	4.99	0.69	7.52	6.00	0.17
	Max	19.0	8.36	3.37	36.4	38.0	2.94
	Mean	4.5	6.83	1.66	20.2	23.7	0.39

SFK sites: SK100G, SK100F, SK100C, SK100A.
UT sites: UT100D, UT100B.
NFK sites: NK100C, NK100B, NK100A.
Hardness, alkalinity, dissolved Cu through 2007; others through 2008.

Source: SRK Consulting, 2011a.

3. Methods

3.1 Model Selection and Description

Although single-process modeling platforms such as MODFLOW are commonly used for mine planning, the extensive surface water-groundwater exchange at the Pebble site necessitates the use of an integrated flow model. Our model was developed using the MIKE SHE/MIKE 11 modeling package developed by the Danish Hydraulic Institute (Graham and Butts, 2005).

MIKE SHE is an integrated hydrologic code that simulates flows of water within and between surface water, groundwater, and atmospheric reservoirs. One of the key advantages of MIKE SHE compared to single-process codes is that the hydrologic system is driven by external climate data, and the partitioning of precipitation among evaporation, transpiration, overland flow, and infiltration occurs dynamically at each cell according to the local physical properties (e.g., soil type, soil moisture, vegetation, temperature, relative humidity, and wind speed). Groundwater recharge is therefore not specified as a boundary condition as it is in other codes, but calculated internally and controlled by assigned unsaturated zone hydraulic properties. In addition, MIKE SHE allows for free exchanges between surface and groundwater, rather than requiring flow processes to be partitioned between different models.

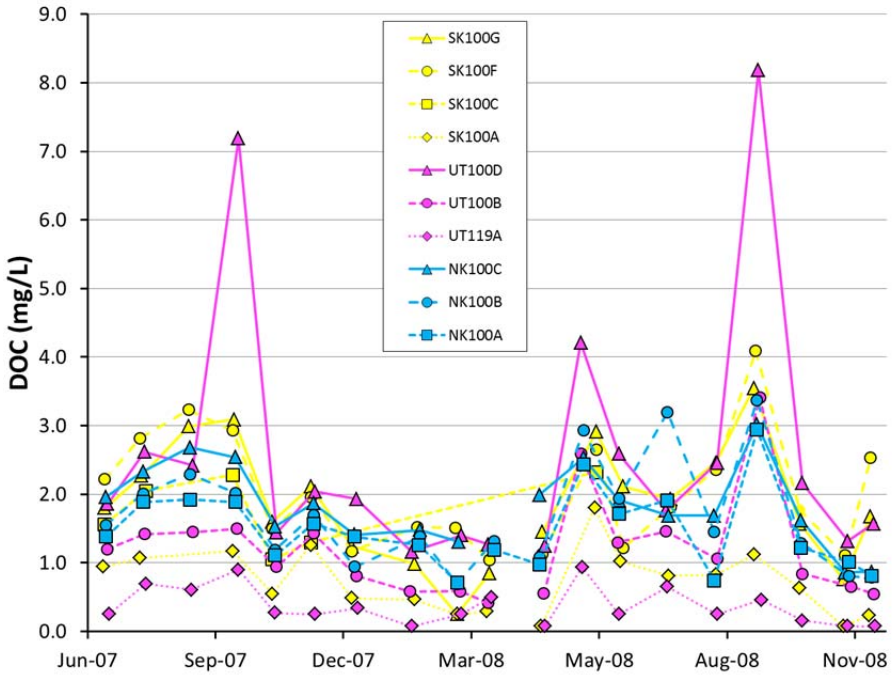

(a)

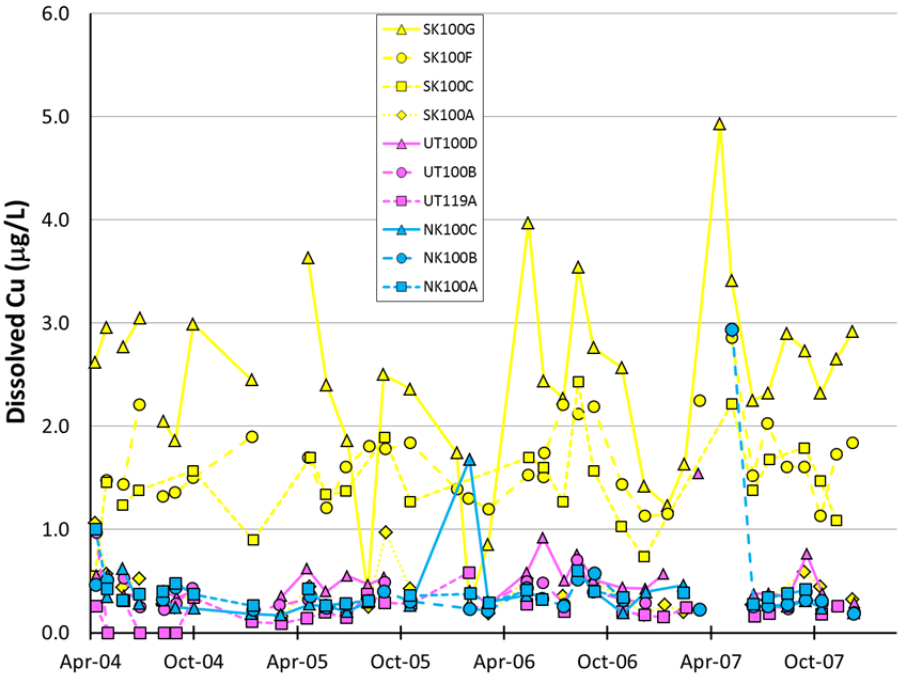

(b)

Figure 3. Temporal variability of (a) DOC (2007–2008) and (b) dissolved copper (2004–2007) in mainstem streams draining the Pebble deposit area.

MIKE 11 is a one-dimensional, fully-dynamic hydraulic and hydrology model for simulating river channel flows and water levels. Flows are calculated using a choice of fully dynamic Saint-Venant open channel flow equations, or simplifications (i.e., kinematic, diffusive, and dynamic). MIKE 11 is dynamically linked with the MIKE SHE portion of the code that simulates the remaining hydrologic processes.

MIKE SHE/MIKE 11 has been used for a variety of applications by numerous federal agencies, including the U.S. Fish and Wildlife Service (e.g., Prucha et al., 2012), the U.S. Department of Energy (e.g., Kaiser-Hill, 2002), and the U.S. Army Corps of Engineers (e.g., USACE, 2004). Applications of the model have included investigating changes in regional and local-scale fully integrated flow and contaminant transport associated with conversion of Colorado's former Rocky Flats Environmental Technology Site to a natural wildlife refuge (Kaiser-Hill, 2002), and modeling the effects of an agricultural storage reservoir on flows through the Everglades (USACE, 2004). Our model used an approach similar to that used by Prucha et al. (2012) for the Chuitna Basin, but with site-specific information from the Pebble area where available. A general description of the model inputs follows. A more complete description of the model inputs can be found in the appendix.

The model domain was chosen to maximize the use of available calibration data, while ensuring that the domain was large enough to simulate the largest possible area of potential influence from mining activities. In general, the model boundaries corresponded to drainage divides. The exit points for streamflows from the model domain were at gage site SK100A, near the confluence of the North and South Fork of the Koktuli River; and at gage site UT100B, approximately halfway between the mine site and Lake Iliamna. All of the model boundaries were specified as no flow boundary conditions, with the exception of the points where the SFK and UT crossed the model domain. A cell size of 250 m was selected as a compromise between trying to use the finest grid possible to better simulate smaller scale features (i.e., streams) and minimizing model run times. The total number of 250-m grid cells within the model domain was 13,374.

Transport simulations that were developed to track releases of copper in leachate from the waste rock piles were run on a sub-model domain nested within the larger model (Figure 4). The local-scale model also has 250-m grid spacing and the same model layers and thicknesses but runs more quickly because it is smaller in scale. Copper loads generated in waste rock leachate were tracked through groundwater and surface water within the local scale model, and fed into surface water bodies at the intersection of the local-scale model with the UT and SFK. Simulation of downstream copper concentrations was then conducted for the full model domain within the MIKE 11 modeling platform.

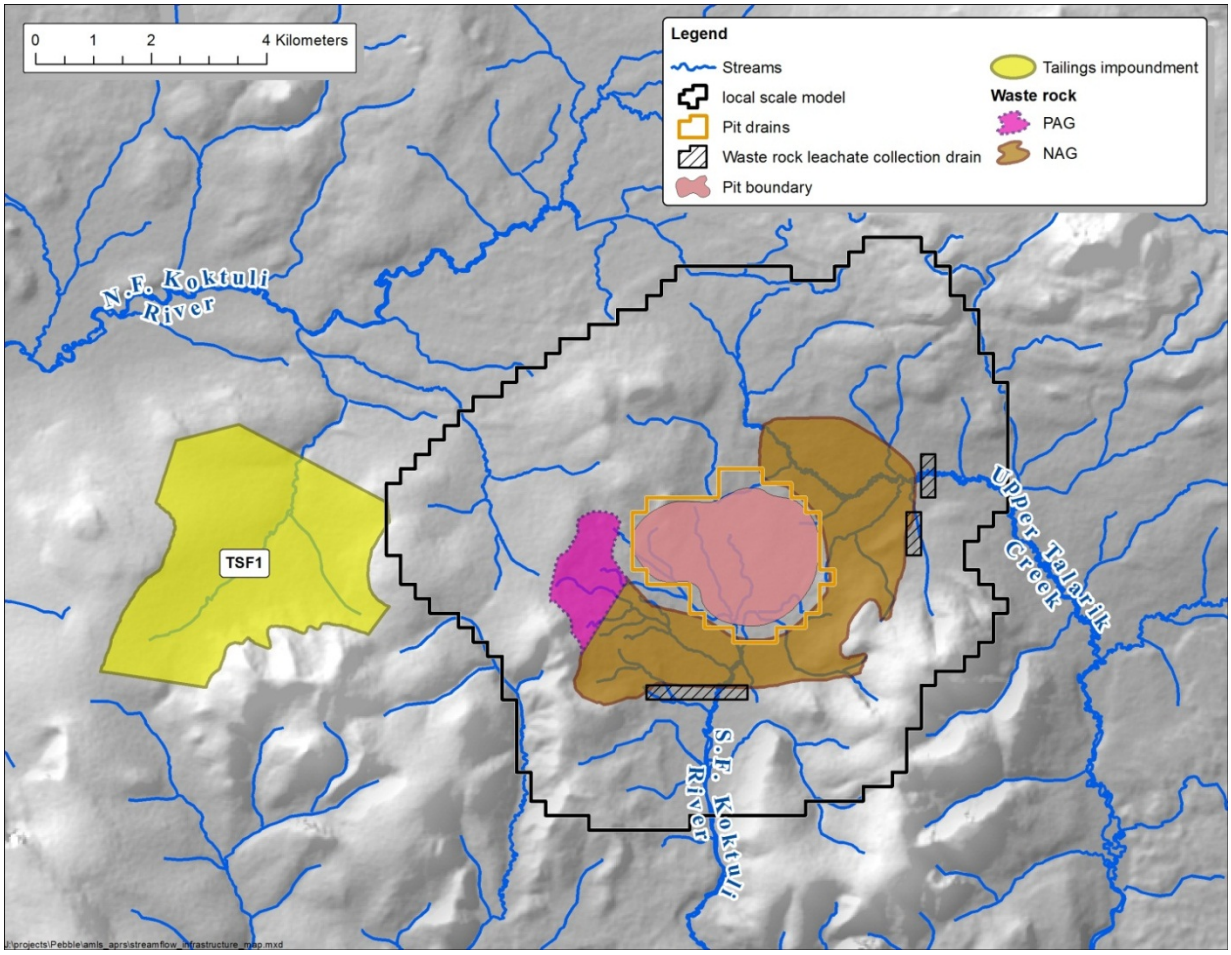

Figure 4. Mine infrastructure used for 25-year mine scenario. Open pit contours, waste rock geometry, and tailings impoundment digitized from Ghaffari et al. (2011). Overlays show model grids designated as drains, and spatial extent of local-scale model.

3.2 Model Inputs

3.2.1 Overview

The model was built using publicly available information describing the climate, topography, vegetation, soils, subsurface geology, and geochemistry of the site and potentially mined materials. The majority of these inputs were gathered from federal agencies, such as the National Oceanographic and Atmospheric Administration (NOAA), the U.S. Geological Survey (USGS), and the United States Department of Agriculture (USDA). In some cases, site-specific information was not available from these sources at the level of detail required to model the

system. In these cases, data were gathered from Pebble's EBD, which was released to the public in late 2011. Examples of the datasets extracted from the EBD include surficial and subsurface geology (which were used as model inputs) and groundwater and streamflow data (which were used as calibration targets). The geochemistry data used for the evaluation of potential mining effects were also extracted from the EBD. Information on the location and characteristics of possible mine facilities was obtained from a report to the Pebble Limited Partnership (PLP) shareholders prepared by Wardrop for Northern Dynasty Minerals Ltd. in 2011 (Ghaffari et al., 2011). A complete description of the model layers and data sources is included in the appendix.

3.2.2 Baseline conditions

Atmospheric and topographic inputs

The meteorology data used to drive the hydrologic model were obtained from the North American Regional Reanalysis (NARR) product. The NARR data include precipitation, temperature, net radiation (sum of incoming minus outgoing short-and long-wave radiation), relative humidity, wind speed, and other variables that drive the hydrologic cycle, with a three-hour temporal resolution and a 30-km spatial resolution (Mesinger et al., 2006). NARR data for three-hour time increments were extracted from the 30 km × 30 km cell overlying the Pebble deposit for the period of 1980 to 2009. The same meteorological time series was used for the baseline period and for the mine simulation period, allowing for direct comparison of hydrologic behavior between the two simulations.

Precipitation (in the form of rain or snow, depending on air temperature) drives the inflow of water into the system. Three-hourly reference evapotranspiration (RET) was calculated using a FAO56 Penman-Monteith equation using the REFET code (http://www.kimberly.uidaho.edu/ref-et/) and the associated 3-hourly NARR precipitation, air temperature, net radiation, dew point temperature, and wind speed data. The RET is used in the MIKE SHE code to calculate water loss to the atmosphere via soil evaporation and plant transpiration (or actual evapotranspiration, AET) using the Kristensen-Jenson method (Kristensen and Jenson, 1975), plant canopy, snow sublimation, and open water evaporation. Plant transpiration is calculated within MIKE SHE as a function of root depth and Leaf Area Index (LAI), which both vary in time according to the different vegetation types.

The topography used in the model was a 30-m resolution digital elevation model (DEM) from the shuttle radar topography mission (SRTM). The stream network was created from a combination of downstream flow routing using the 30-m DEM and a river and stream polyline layer from the National Hydrography Dataset (NHD). Sub-pixel details of the hydrology network, such as river meanders, were digitized from a high-resolution SPOT5 satellite image collected in 2009. The final hydrology network used in the model is shown in Figure 1.

Surficial vegetation, soil, and geology

Unsaturated (vadose) zone hydrology in MIKE SHE is influenced by vegetation and soil type, because plant roots remove infiltrating water from the vadose zone. Soil types were compiled from the STATSGO dataset from the USDA Natural Resource Conservation Service (NRCS, 2011). These data were supplemented with surficial geology data for low-permeability lacustrine and glaciolacustrine units in the three watersheds (Schlumberger Water Services, 2011). Unsaturated zone hydraulic properties were specified by soil type, as described in the appendix. Vegetation maps were imported from the national land cover dataset (NLCD), which are also available as a 30-m resolution raster dataset at http://www.mrlc.gov/ (Homer et al., 2004).

Groundwater flows in the region are strongly controlled by the thickness of unconsolidated sand and gravel deposits, which fill bedrock valleys and typically have high hydraulic conductivities (Schlumberger Water Services, 2011). The thickness of this unconsolidated material was calculated by subtracting the bedrock surface elevation from the land surface elevation at each point on the model grid. The bedrock elevations were obtained from a map included in the PLP EBD (Schlumberger Water Services, 2011), and the land surface elevations were obtained from the SRTM DEM. In areas where the bedrock surface map indicated no overlying unconsolidated material, a uniform unconsolidated thickness of 2 m was used to represent the regolith overlying bedrock. This 2-m thick regolith layer in the model was also assumed to overlie the thicker unconsolidated material filling the deeper bedrock valleys. A map showing the distribution of unconsolidated material thicknesses used in the model is included in the appendix.

Properties of hydrostratigraphic units

The model contains four layers representing discrete hydrostratigraphic units with different thicknesses and hydraulic conductivity values. A four-layer model provided sufficient flexibility to simulate what is known about the hydrogeologic conditions at the site: two unconsolidated units represented shallow regolith and deep glacial deposits, respectively, while two bedrock layers were used to represent the weathered and competent bedrock. The thickness of unconsolidated units was based on the bedrock surface map as described above, and ranges of saturated hydraulic conductivity values for initial model runs were based on hydraulic testing results summarized in Schlumberger Water Services (2011). Calibration runs adjusted these conductivity values within this range of observational constraints to optimize streamflow response. The final hydraulic conductivity values used in the model, as well as anisotropy ratios and storage coefficients, are summarized in the appendix.

The uppermost two model layers are unconsolidated material (largely glacial sand and gravel). Layer 1 is a 2-m thick upper section representing the regolith throughout the model domain; however, the 500-m wide total area around all streams was assigned a Layer 1 thickness of 5 m. Layer 2 extends from the bottom of Layer 1 to the top of the weathered bedrock. Hydraulic conductivity values for all model layers were based on the range of measured values reported in

the EBD (e.g., Schlumberger Water Services, 2011), and final values by layer were selected to optimize the streamflow response to precipitation events. Throughout the model, Layer 1 was assigned a uniform horizontal hydraulic conductivity of 1e-3 m/s, and the conductivity of the thicker unconsolidated layer (Layer 2) was assigned a value of 8e-5 m/s. A local zone of higher conductivity was created in Layer 2 of the model in the middle SFK drainage to simulate an observed interbasin transfer from the SFK to the UT catchment (e.g., Knight Piésold et al., 2011). With the exception of this local higher conductivity zone, no other separate zones were simulated in the subsurface hydraulic conductivity structure.

Underlying the unconsolidated material, the bedrock was subdivided into two layers. The uppermost bedrock layer (Layer 3) was assigned a uniform thickness of 15.2 m (corresponding to the weathered bedrock thickness of 50 ft documented by Schlumberger Water Services, 2011). This weathered bedrock was assigned a uniform hydraulic conductivity value of 5e-6 m/s, within the range of observed response test results from this unit of 4e-7 to 3e-4 m/s (Schlumberger Water Services, 2011). Below the weathered zone, the competent bedrock (Layer 4) was assigned a constant hydraulic conductivity of 1e-8 m/s. Layer 4 is 1,525 m thick and extends from the base of the weathered bedrock to the base of the model domain.

Water quality

Although a number of constituents could be released from mine activities and potentially pose a threat to aquatic biota, all water quality simulations were focused on copper as the contaminant of principal concern. Humidity cell testing results from tailings and waste rock proxies indicate that waste rock leachate will produce up to two orders of magnitude higher concentrations of copper than will tailings leachate (SRK Consulting, 2011b). Under our assumption of an impermeable dam at the base of the tailings storage facility (TSF; see Section 3.2.3), the volume of leachate escaping from the TSF under normal operating conditions is also likely to be small relative to the volumes transmitted through waste rock. We thus focused our water quality simulations on copper leachate from waste rock.

Extensive baseline water quality data are available for stream gaging locations downstream of the proposed waste rock locations for the period 2004 to 2007. To simplify the water quality simulations, copper concentrations in groundwater were assumed to be zero throughout the model domain, so that the only source of copper to the streams from groundwater was transport of leachate from the waste rock piles. Site-specific, average baseline copper concentrations in surface water were then added to the simulated copper concentrations coming from the waste rock piles to estimate water quality in receiving streams under mining conditions. Measured baseline copper concentrations in surface water reflect additions of copper from groundwater, upstream surface water, and surface runoff.

3.2.3 Mine scenarios

Mine infrastructure

The Pebble deposit is generally described as at least a 45-year and up to a 78-year resource (Ghaffari et al., 2011). However, a mine plan has not yet been released, and the preliminary mine designs currently available reflect a much smaller, 25-year mine and a "reference case" 45-year mine. In the 25-year mine scenario, the ore is extracted from a single open pit that encompasses the Pebble West Zone and the upper portion of the Pebble East Zone, and wastes are placed in a single tailings impoundment and waste rock facilities surrounding the open pit (Ghaffari et al., 2011). We focused our simulations on the 25-year mine scenario in part because the generalized mine designs are readily available, and in part because they are least likely to be superseded by alternative designs. Whereas the deeper resource in the Pebble East Zone could be extracted using underground block caving methods, "…it's certain that near-surface mineral resources within the western portion of the Pebble deposit will be most efficiently developed though open pit methods" (Ghaffari et al., 2011). The 25-year mine that we simulated will therefore be representative of the type and scale of environmental effects that could be expected from a mine in this location. However, we stress that the effects described for the 25-year mine scenario (5 billion tons mined) will likely be substantially less than those expected from the 45-year build-out (11.6 billion tons mined).[1]

In the 25-year mine scenario, the open pit is approximately 4-km wide and 800-m deep. Pit dewatering was simulated as a set of drains by layer, which were assumed to collect all water flowing from the bedrock and unconsolidated deposits intersected by the pit walls, as well as all precipitation falling on the pit footprint. The drain cell elevations were determined based on the pit geometry, which was digitized from the 25-year pit contours shown in Ghaffari et al. (2011) (Figure 4).

The 25-year design has one TSF (TSF 1) in the NFK basin and waste rock piles surrounding and just outside the southern, eastern, and western rims of the 25-year pit (see Figure 4). The dams holding back the tailings material were assumed to be impermeable (no leakage) and penetrate the entire weathered bedrock layer (Layer 3), thereby limiting infiltration through or beneath the dams. MIKE SHE cannot simulate emplacement of wet slurry into a tailings impoundment, which is how the TSF will be filled in reality. To simulate the emplacement of wet tailings, we assumed that the TSF was first filled with dry tailings with a saturated hydraulic conductivity of 2e-6 m/s (comparable to silt/fine sand) and a porosity of 46% in model year 1 (Gowan, 2006). The tailings were then filled from the top with water; although this introduces a lag in filling, a high micropore bypass value (90%) was assigned to produce a high translation rate from tailings surface to groundwater. As mining progresses, the water table rises within the tailings, based on the tailings' porosity and the rate of water inflow to the TSF (25.5 Mm^3/yr; see Water

1. Mined tonnages from Ghaffari et al., 2011.

Management section). The only loss of water from the TSF is from the head-dependent vertical leakage of tailings water to the underlying weathered and competent bedrock and as seepage beneath the dam, and evaporation from supernatant water overlying the tailings. A complete list of hydraulic properties assumed for the tailings is in the appendix.

The waste rock piles are segregated into a smaller potentially acid generating (PAG) deposit along the western side of the pit and a larger non-PAG deposit along the southern and eastern rims of the pit (Figure 4). The footprints of the waste rock piles were digitized from Ghaffari et al. (2011), and the geometry of the final piles was determined assuming that 2,379 million metric tons of non-PAG waste rock and 638 million metric tons of PAG waste rock would be generated, each with a bulk density of 2.1 metric tons/m^3. Using these values, the resulting average height of the waste rock piles was calculated to be approximately 100 m. The waste rock was assumed to have a saturated hydraulic conductivity of 3e-5 m/s. The complete hydraulic properties assumed for the waste rock are tabulated in the appendix.

The mine infrastructure was emplaced at Year 1 of the mine-scenario simulations. This modeling decision minimized the need to make assumptions regarding the rate and type of mine development, but it also leads to some uncertainty in the estimation of mining impacts. For example, because the full 25-year pit is simulated in Year 1, the modeling overestimates the effects of the mine on downstream flows in the early years as pit build out takes place. Conversely, since the cone of depression surrounding the pit will be more fully developed early in the mine simulation than in an incremental build out scenario, more of the waste rock leachate will be captured by the pit early in the model run than would occur in reality. To minimize the uncertainties created by these modeling decisions, our mine impact evaluations focus on years 20–22 of the model runs. At this point in the simulations, the hydrologic system is nearly equilibrated to the full 25-year build out, and we can be more confident that the percentages of water moving to the pit and toward streams are closer to reality than they are earlier in the simulation.

Mine water management

There are currently no detailed plans that describe water management for the proposed mine. For the MIKE SHE model, we developed a water management plan as follows. Based on the size of the resource and the duration of mining, consumptive water use from the mill and associated tailings disposal was estimated to be approximately 25.5 Mm^3/yr (U.S. EPA, 2012a). Other consumptive uses from infrastructure, such as cooling tower losses and concentrate pipeline delivery and returns, were estimated to be approximately 1.5 Mm^3/yr. Thus the total use of water from the mine was estimated to be approximately 27 Mm^3/yr for the 25-year mining scenario.

MIKE SHE was used to calculate the sources that would be available to supply these consumptive water uses, as follows. First, we used the model to estimate the average annual volume of water captured within the TSF basin. This average annual flux was approximately

12 Mm^3/yr, representing approximately 45% of the total consumptive use for the mine. The remaining 15 Mm^3/yr of consumptive water use was assumed to come from precipitation falling within the footprint of the pit and from dewatering of the aquifers, both of which would be collected by the pit dewatering system. Using the model, we calculated a total flux from pit dewatering of 18.4 Mm^3/yr, leaving an approximately 3.4 Mm^3/yr surplus. This surplus water was assumed to be treated and discharged at a constant rate and in equal proportions to upper reaches of the SFK (at SK100F) and UT (at UT100D).

Mitigation systems – operation and failure

The unconsolidated material surrounding the Pebble deposit is primarily glacial outwash (sand and gravel) with a high hydraulic conductivity. Without active mitigation systems, leachate from the waste rock piles would travel through the unconsolidated material and into downgradient waters. We simulated the transport of waste rock leachate to groundwater and downgradient surface waters, both with and without mitigation systems, to evaluate the magnitude of the potential changes in water quality that could be created from migration of waste rock leachate. In each of these simulations, all water infiltrating through the waste rock piles via incoming precipitation was assumed to take on a constant copper concentration, which was then tracked downgradient through groundwater and into surface water. For these model runs, copper was treated as a conservative tracer (e.g., we did not model precipitation or sorption of copper in groundwater or surface water). Input copper concentrations were calculated based on results from humidity cell testing, as described below.

For the mitigation scenarios, we simulated the leachate collection system as two drains – one in the SFK and one in the UT – each of which was installed to a depth of 10 m bgs. The drain in the SFK was 1.75 km long, and the drain in the NFK was 1.5 km long (see Figure 4). Each drain creates a cone of depression that intercepts ground and surface water migrating downgradient from the waste rock piles. For water balance purposes, we assumed that all water collected from the leachate collection drains would be discharged to the TSF.

In addition to simulations with and without the leachate collection drains, we conducted two simulations in which the collection system was assumed to fail for durations of one and six months. In each of these failure scenarios, our initial conditions were a fully functional collection system, and a spatial distribution of copper in groundwater calculated from 20 years of leachate transport and collection drain operation. During the failures, fully-coupled advective transport of copper in groundwater, overland flow and channelized flow were modeled to track the migration of copper downgradient and downstream of the waste pile. At the end of each failure scenario, the collection system drains were turned back on, and downgradient and downstream copper concentrations were simulated for at least one year.

Leachate chemistry

Static and kinetic (including humidity cell tests, HCTs) geochemical testing was conducted on exploration drill core samples that were designated as potential waste rock by PLP, the project proponent (SRK Consulting, 2011b). Static testing results demonstrated that nearly all the ore host rock (Pre-Tertiary) was PAG, and the majority of the surrounding rocks (Tertiary) were non-PAG. We used the results from HCTs to estimate the longer-term leaching ability of constituents in the waste rock. The HCT method was a modification of the standard humidity cell procedure (ASTM, 2001) that tested more material and larger particle sizes than called for in the standard method. Separate tests were conducted for Pre-Tertiary and Tertiary rock and for Pebble West Zone and Pebble East Zone samples.

Only copper leachate concentrations were used in the model because copper nearly always had the highest concentrations in waste rock leachate (SRK Consulting, 2011b), and salmon are known to be susceptible to low concentrations of copper, especially in low-hardness streams such as those draining the Pebble deposit area (see Section 2.3). Average stable copper release rates were used to calculate copper waste rock leachate concentrations for the MIKE SHE model. Stable copper release rates are supplied in SRK Consulting (2011b, Table 11-31 for Tertiary samples, Table 11-21 for Pre-Tertiary samples). The stable copper concentrations were calculated for each HCT sample using the following relationship:

$$\text{Leachate concentration (mg/L)} = (\text{stable release rate [mg/kg/week]}) \times (\text{kg})/(\text{L/week}) \quad [1]$$

where kg is the mass of the HCT waste rock sample (5 kg), and L is the volume of HCT leachate collected each week (2.4 L/week).

The open pit waste rock was assumed to be one-half Pebble East and one-half Pebble West, based on a cross-section of the 25-year open pit in Ghaffari et al. (2011). To estimate leachate concentrations for PAG waste rock, average stable leachate copper concentrations for all Pebble West Pre-Tertiary HCTs were averaged and then averaged with mean Pebble East Pre-Tertiary copper concentrations. Concentrations were averaged to reflect mixing of rock types in the waste rock piles under operational conditions.

The resulting leachate concentrations used in the model are likely underestimates of operational waste rock leachate concentrations for two reasons: (1) initial higher release rates and concentrations were ignored (stable rates occurred after a number of weeks of testing), and (2) the PAG HCT samples did not include waste rock with higher percent sulfur or whole rock copper concentrations. As shown in Figure 5a, initial weathering rates for copper in PAG rock are higher, reflecting the more rapid dissolution of more soluble secondary minerals such as copper sulfates (Price, 2009). Aside from these initial concentration peaks, HCTs do not reflect the weathering of secondary minerals, which often control leachate chemistry under field

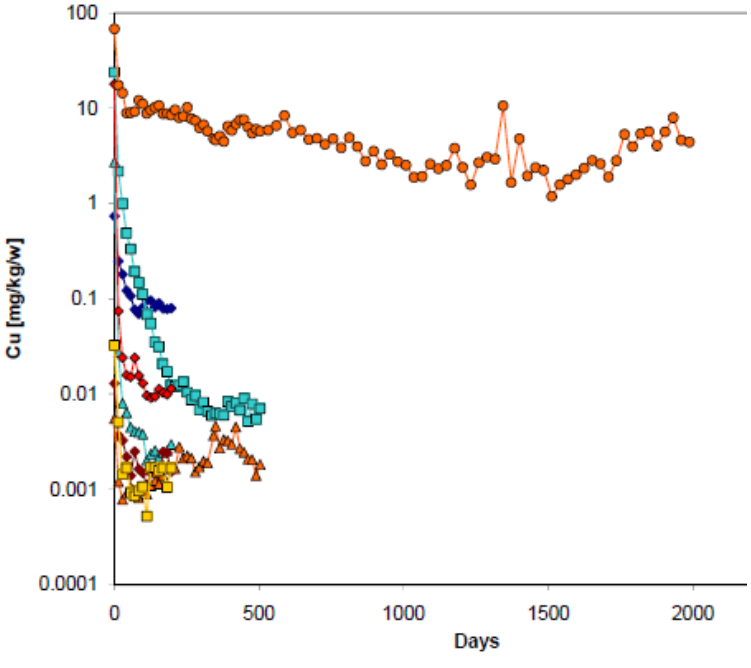

(a)

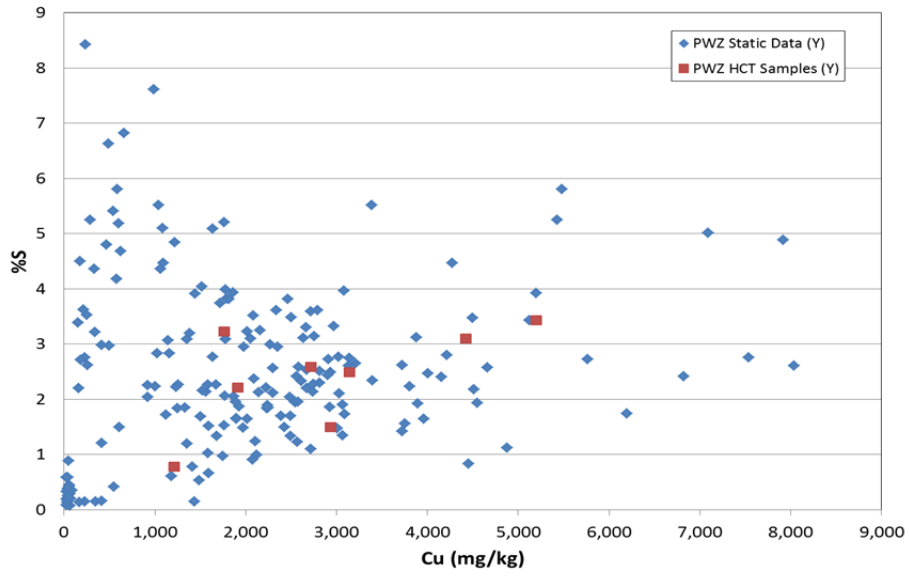

(b)

Figure 5. HCT samples. (a) Copper release rates in plutonic Pre-Tertiary waste rock samples (SRK Consulting, 2011b, Appendix 11G); [w = week; all samples shown are Pre-Tertiary plutonic rocks (primarily granodiorite); trends and copper concentrations were similar for sedimentary/volcanic Pre-Tertiary rocks (primarily mudstone)], (b) Pebble West Zone (PWZ) static and HCT comparison for samples from units containing Pre-Tertiary mudstone: % sulfur and copper (SRK Consulting, 2011b).

conditions (Price, 2009). A large study of mine waste rock seeps in Canada showed that concentrations peaks were associated with snowmelt and storm events and repeated annually (Morin et al., 1993; Morin and Hutt, 2010a, 2010b). Maximum copper leachate concentrations in the geochemical testing program (all leach tests conducted for the EBD) were as high as 1,000 mg/L, with most values between 1 and 100 mg/L (SRK Consulting, 2011b).

The second reason selected model input leachate concentrations are likely underestimated is related to the selection of samples for HCTs. Figure 5b shows the whole rock percent sulfur and copper concentrations in all PAG samples used for acid-base accounting and the subset that was used for HCTs from the Pebble West Zone. As shown in Figure 5b, the samples selected for HCT analysis did not include those with the highest percent sulfur or copper contents. Percent sulfur values are used to calculate the acid-generation potential of the samples; given the same neutralization potential and availability of acid-generating and acid-neutralizing minerals, samples with higher percent sulfur are more likely to produce acid drainage. When acid drainage forms, metal concentrations, including copper, increase substantially (SRK Consulting, 2011b). Therefore, it is likely that the HCT tests underestimate copper leachate concentrations for a portion of the rocks that would be present in the waste rock piles.

To account for the likely higher copper waste rock leachate concentrations in reality compared to the data from the HCTs, one standard deviation was added to the mean concentrations from the HCTs in Tertiary and Pre-Tertiary waste rock. As noted in Ghaffari et al. (2011), the mine plan assumes that PAG and non-PAG waste rock cannot be perfectly separated in the field and that 5% of non-PAG waste rock will be PAG. Therefore, non-PAG waste rock leachate concentrations were derived using 95% non-PAG and 5% PAG copper concentrations. In fact, 9% of the Tertiary (non-PAG) HCT samples produced acid (SRK Consulting, 2011b), and mistaken placement of Pre-Tertiary rock to the piles would only add to the percent of "non-PAG" waste rock producing acid. The resulting input values used for PAG and non-PAG waste rock in the model were 4.20 and 0.210 mg/L copper, respectively. Repeat model runs confirmed that downstream concentrations of copper scaled linearly with the assumed leachate concentrations; e.g., a doubling of assumed leachate concentrations led to a doubling of modeled stream concentrations. Using these relationships, we also estimated the percent of total waste rock leachate generated that would be required to cause copper concentrations to exceed stream water quality standards under observed streamflow conditions (see Section 4.2.2).

3.3 Calculation of Water Quality Criteria

Ambient water quality criteria for the protection of aquatic life were calculated for four locations on the SFK (SK100G, F, C, and A; see Figure 1), three locations in UT (UT100B, UT100D, and UT119A), and three locations in the NFK (NK100A, NK100B, and NK100C). Water quality criteria were calculated using the hardness-based approach (U.S. EPA, 2002) and the Biotic

Ligand Model (BLM; U.S. EPA, 2007). The U.S. Environmental Protection Agency (EPA) recommends the BLM for site-specific surface water copper standards (U.S. EPA, 2007). The BLM includes: a geochemical speciation code, CHESS (Santore and Driscoll, 1995), which calculates inorganic metal speciation; the WHAM V code (Tipping, 1994), which calculates the degree of Cu interaction with dissolved organic matter; and a biotic ligand (e.g., a fish gill) binding constant and lethal accumulation (LA_{50}) for Cu, which remains constant regardless of water quality (Di Toro et al., 2001). The main purpose of the BLM is to predict the concentration of total dissolved Cu that would cause toxicity to aquatic life under a range of site-specific water quality conditions.

Calculations for the hardness-based approach used measured calcium and magnesium concentrations for each sampling date (2004 to 2007) at the 10 locations noted above to derive a range of copper chronic and acute criterion values for each location. For criteria based on the BLM, all major element chemistry (calcium, magnesium, sodium, potassium, chloride, sulfate, and alkalinity), water temperature, pH, and DOC values are used. Measured water quality for each sampling date (2004 to 2007 for major element chemistry, pH and temperature; 2007 only for DOC because DOC was not measured prior to 2007) was used as inputs to the BLM. Water quality data were obtained from SRK Consulting (2011a).

Ranges of calculated acute [criterion maximum concentration (CMC)] and chronic [criterion continuous concentration (CCC)] hardness-based and BLM criteria for each location are shown in Table 2. The percent of the samples with baseline dissolved copper concentrations that exceed the criteria is also noted in Table 2. Note that minimum BLM criteria are always lower (more protective) than minimum hardness-based criteria, but maximum BLM criteria are often higher (less protective) than maximum hardness-based values. Overall, BLM criteria exceeded baseline (existing, background) dissolved copper concentrations at more locations and under more flow conditions than did the hardness-based criteria. The only location that did not have acute BLM exceedences under baseline conditions was UT100D, the location with the highest DOC concentrations (see Figure 3a). The exceedences of acute BLM criteria in waters that have high quality, naturally-reproducing fish and macroinvertebrate communities, with salmonid spawning reaches extending into the high headwaters areas in the NFK and UT and upstream to Frying Pan Lake in the SFK (PLP, 2011) suggests that the BLM is unreliable for the water quality conditions in the three watersheds. Therefore, the model-estimated stream concentrations for the mine effects analysis (Section 4.2) will be compared to hardness-based (rather than BLM) dissolved copper criteria.

Table 2. Calculated BLM and hardness-based chronic (CCC) and acute (CMC) criterion ranges, and percent of samples with baseline dissolved Cu concentrations exceeding chronic and acute values

Site ID	Measure	BLM CMC (µg/L)	BLM CCC (µg/L)	Hardness-based CMC (µg/L)	Hardness-based CCC (µg/L)
SK100A	Min	0.04	0.03	1.3	1.1
	Max	2.4	1.5	2.7	2.1
	n[a]	34	34	35	35
	% exceeding	26	53	0	0
SK100C	Min	0.05	0.03	1.2	1.0
	Max	8.1	5.0	3.1	2.4
	n	23	23	23	23
	% exceeding	48	70	9	22
SK100F	Min	0.07	0.05	1.3	1.1
	Max	27.8	17.3	6.0	4.3
	n	37	37	37	37
	% exceeding	27	43	8	19
SK100G	Min	0.08	0.05	1.6	1.3
	Max	3.8	7.7	5.2	3.8
	n	32	32	35	35
	% exceeding	72	81	23	46
UT100B	Min	0.08	0.05	2.2	1.8
	Max	7.7	4.8	5.1	3.7
	n	35	35	35	35
	% exceeding	9	9	3	3
UT100D	Min	1.4	0.88	2.5	2.0
	Max	18.0	11.2	8.6	6.0
	n	31	31	32	32
	% exceeding	0	3	0	0
UT119A	Min	0.05	0.03	3.4	2.5
	Max	2.3	1.4	5.0	3.7
	n	33	33	35	35
	% exceeding	9	15	0	0
NK100A	Min	0.05	0.03	1.2	1.0
	Max	8.0	5.0	3.3	2.5
	n	30	30	32	32
	% exceeding	7	13	0	0

Table 2. Calculated BLM and hardness-based chronic (CCC) and acute (CMC) criterion ranges, and percent of samples with baseline dissolved Cu concentrations exceeding chronic and acute values (cont.)

Site ID	Measure	BLM CMC (µg/L)	BLM CCC (µg/L)	Hardness-based CMC (µg/L)	Hardness-based CCC (µg/L)
NK100B	Min	0.06	0.03	1.6	1.3
	Max	17.5	10.9	4.6	3.4
	n	28	28	29	29
	% exceeding	14	21	0	0
NK100C	Min	0.12	0.07	1.8	1.4
	Max	15.9	9.9	5.2	3.8
	n	32	32	34	34
	% exceeding	6	9	0	0

Min = minimum; max = maximum; n = number of samples.

a. Samples numbers may vary for BLM and hardness-based calculations for the same location because of the number of analytes available for calculation of water quality criteria.

3.4 Calibration Procedure

The general procedure for calibration of an integrated groundwater – surface water model is similar to that used for a groundwater flow model (e.g., ASTM, 2008). However, the interactions among surface water, groundwater and the atmosphere in an integrated model make calibration more challenging than in a single-process model. In addition, the relatively long model run times (approximately 2.5 hours per year of simulation) require that calibrations are done systematically and efficiently.

Our general calibration procedure attempted to follow the "principle of parsimony" described by Hill (1998). According to this principle, model complexity should be limited to that which is required to achieve an acceptable calibration to observed data. For our purposes, streamflow was the most important calibration target. Early model runs found that the streamflows were most sensitive to choices for model layers (number and thickness) and the hydraulic conductivity of the unconsolidated material (Layers 1 and 2). Model calibration was thus focused on finding hydraulic conductivity values that were within reasonable ranges of measured values and that reproduced measured streamflow and groundwater level data throughout all model runs.

Our model calibration was iterative, following the approach outlined by Refsgaard (2007). Although our primary calibration target was the streamflow, an effort was also made to ensure

that realistic groundwater elevations were also simulated. The general calibration procedure was as follows:

1. Initial simulations were conducted on a subset of the full model domain (local-scale models) to evaluate the sensitivity of the model to particular parameters. These local watershed models were used to better understand the general hydrologic behavior of the system without the computational overhead or more complex parameter distributions of the full model, and to identify reasonable ranges of model parameters such as hydraulic conductivity, the number and thickness of unconsolidated and bedrock layers, etc.

2. Additional short-duration (five-year) simulations were conducted using the full-scale watershed model to compare model results against measured streamflows and groundwater elevations. Sensitive model parameters determined from step 1 were further refined to improve simulation of surface water flows.

3. Using the chosen model parameters, the full-scale watershed model was run for the entire period of the NARR record (1980 to 2009), without addition of any mine infrastructure. This model was used as the baseline model for further mine impact simulations.

4. Model Results

4.1 Calibration Results

Calibration of the model was evaluated based on comparisons of model outputs to measured streamflow, groundwater elevations, and areas of surface-groundwater exchange that have been observed in the Pebble deposit area. Calibration results are based on the period of overlap between NARR data and field observations, which is limited to the period from 2004 to 2007 (the only years reported in the EBD).

4.1.1 Sensitivity to model parameters

The model calibration provided a number of important insights into the sensitivity of the hydrologic system to different input parameters. First, these runs indicated that the unconsolidated material and bedrock groundwater flow systems are largely decoupled. We developed a series of model runs with a range of reasonable hydraulic conductivity values for the competent bedrock, ranging from 1e-6 to 1e-10 m/s (Schlumberger Water Services, 2011). Over the course of these runs, we found that a broad range of bedrock hydraulic conductivity values reproduced measured streamflows equally well, indicating that the behavior of the shallow hydrogeologic system is relatively insensitive to the hydraulic conductivity of the competent bedrock.

Higher bedrock conductivity values did lead to a more rapid propagation of the cone of depression and a resulting increase in dewatering rates from the pit. This has important implications for water management during mine operations and for the potential to locally dewater surface streams. The implications for water management warrant further investigations to better characterize the hydraulic conductivity of competent bedrock and to understand how faults could affect groundwater flow directions, dewatering rates, and the extent of the cone of depression. However, the relative insensitivity of the shallow hydrologic system to the bedrock conductivity in our baseline model simulations demonstrates that hydrologic connection between the overlying unconsolidated materials and the bedrock flow system is relatively limited.

4.1.2 Streamflow

Measured streamflows at gage sites in the NFK, SFK and UT watersheds are generally well simulated by the MIKE SHE model. In particular, the timing and magnitude of peak spring flows, the length of the baseflow recession, and the magnitude of simulated baseflows are well matched by the model for both small and large catchments. Figure 6 shows examples of measured and simulated hydrographs for gages in the upper, middle, and lower SFK. Calibration plots for all 15 gages are included in the appendix.

The most significant discrepancies between measured and simulated flows are during the fall, when measured peak flows are typically higher than simulated flows. This mismatch between model and observation is most likely the result of the scale at which the NARR climatology data are compiled. In contrast to the spring runoff, which integrates all winter precipitation, individual fall storms can be relatively localized and controlled by local topography. Because the NARR data are gridded at a 30-km resolution, many of these storms are likely to have been missed by the NARR dataset. Because our goal was to simulate changes in hydrology from a mining scenario, this mismatch is important only in that it limits our ability to estimate hydrologic alteration during the fall. As described below, the most substantial changes in flow predicted in the mine scenario runs were reductions in peak spring flows. However, because the model underestimates the fall peak streamflows, the model likely underestimates mine-related reductions in these flows.

4.1.3 Groundwater elevations

Groundwater elevations in the Pebble deposit area vary seasonally, in response to strong seasonality in variables such as precipitation, snowmelt, transpiration, and infiltration over the course of the year. Groundwater elevations are typically highest in the spring and fall as a result of spring runoff and fall rains, and decline in the summer and winter between these periods of recharge. We focused our calibration on the annually averaged groundwater elevation at each monitoring point.

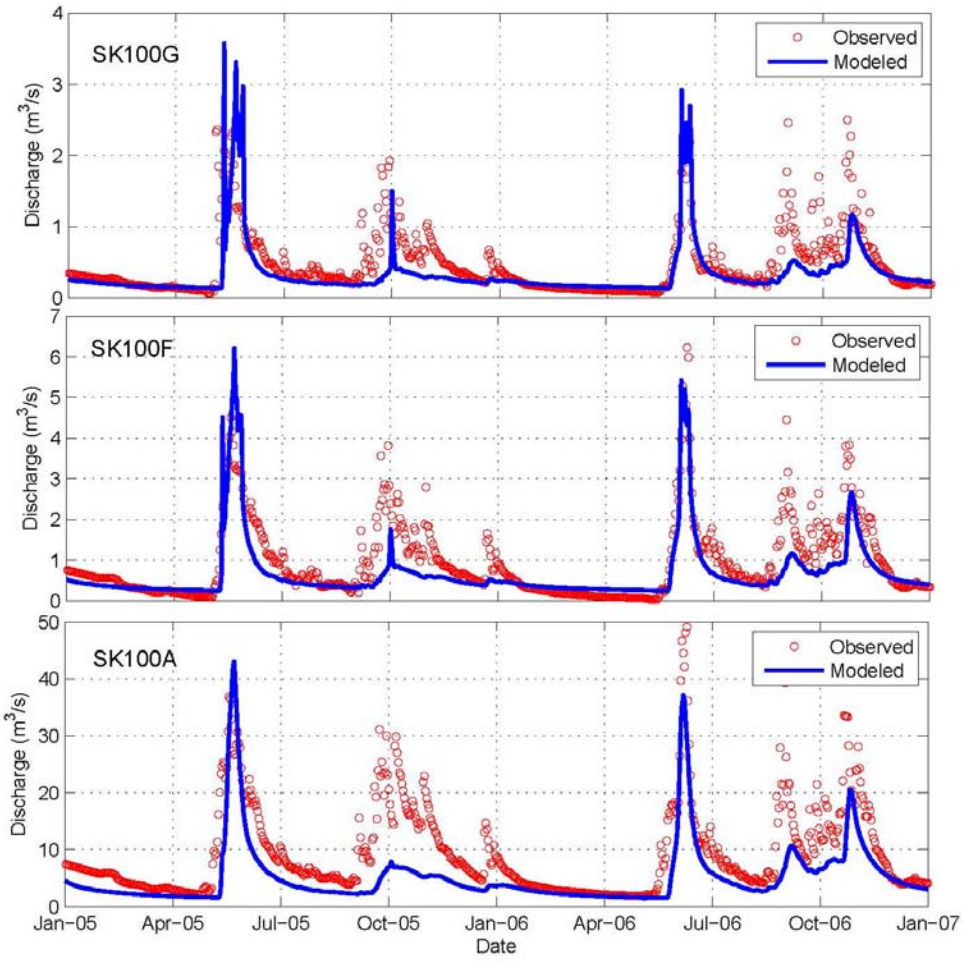

Figure 6. Examples of calibration run results for streamflow in the upper, middle and lower SFK. Note general agreement between magnitude of spring peak and baseflow, and timing of baseflow recession.

Figure 7a shows the agreement between the annually averaged measured and modeled groundwater elevations at all monitoring locations and within all aquifers. Although the agreement between simulated and observed groundwater elevations is quite good, it is important to note that much of the observed variability in groundwater elevations is a result of topography alone: groundwater typically closely follows topography, and groundwater elevations in monitoring wells high in the catchments will thus generally be higher than those at lower points in the basin. To correct for this inherent correlation between groundwater elevation and land surface elevation, Figure 7b shows the agreement between measured and simulated groundwater depths (below ground surface) across the model domain. The mean error of predicted groundwater depths is 4.5 m, with a standard deviation of 12.8 m.

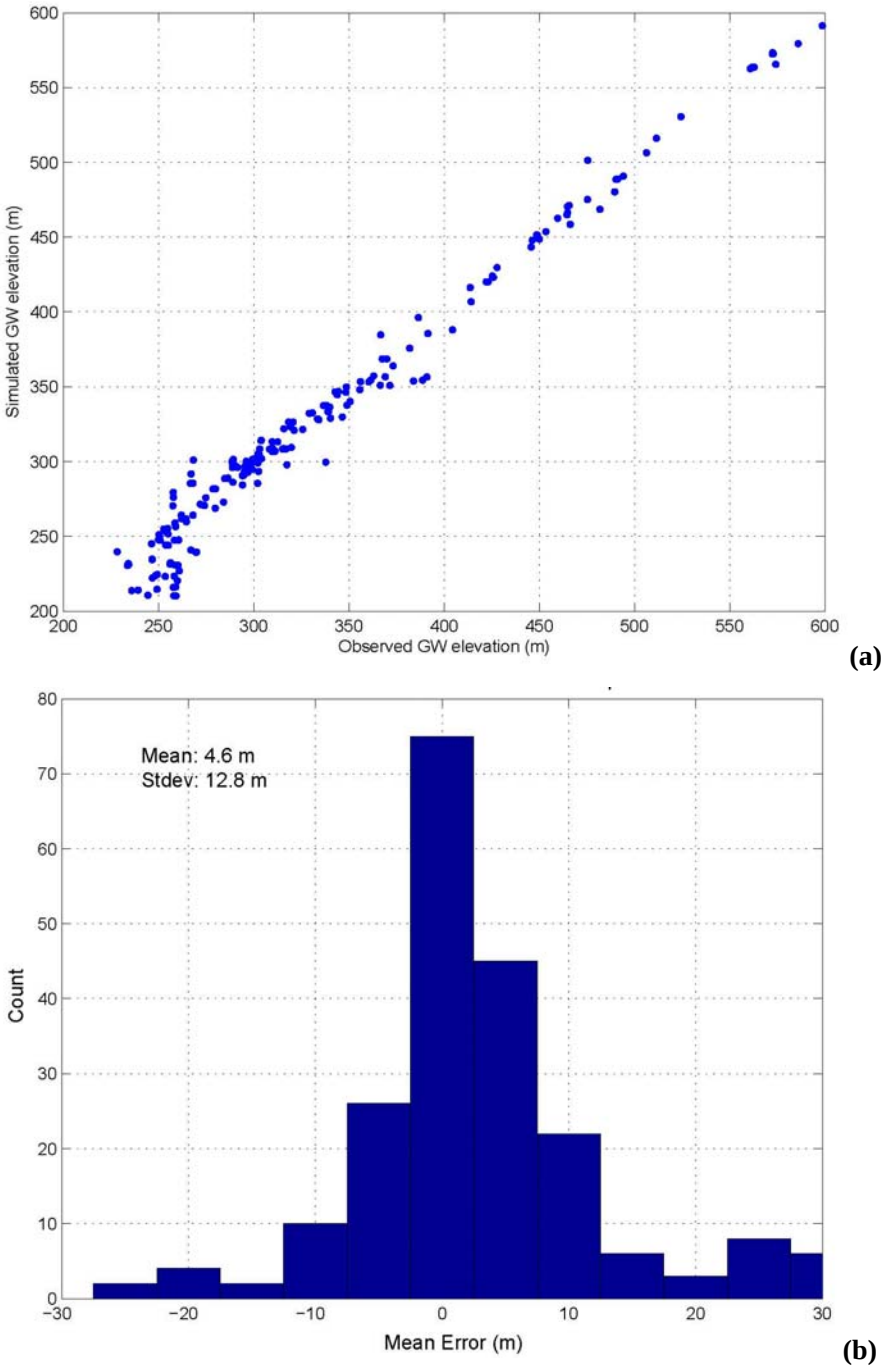

Figure 7. Groundwater calibration results. (a) Comparison of annual averages of observed and simulated groundwater elevations throughout the model, and (b) histogram of mean errors in groundwater depths from all locations.

4.1.4 Groundwater-surface water exchange

Streamflows at the majority of the gage sites were well simulated by a simple two-layer model of the unconsolidated material. Although a model with this simple set of input parameters was able to simulate flows over the majority of the model domain, these initial calibration runs were unable to match the measured flows in tributary UT119A, which has its headwaters near the middle SFK at gage SK100C. PLP studies have indicated that water from the SFK near this location feeds the UT119A tributary through groundwater, most likely via a high conductivity layer in the subsurface (Knight Piésold et al., 2011). To simulate this interbasin transfer, we incorporated a zone in Layer 2 in this region with a conductivity of 1e-3 m/s – approximately an order of magnitude higher than its surroundings. Addition of this higher conductivity zone increased leakage from the SFK to the UT watershed and improved the simulated discharge at UT119A relative to measured values.

Rate of exchange between groundwater saturated flow into surface water streams was not used as a calibration target in this iteration of the model. Nonetheless, this is a particularly important attribute with regard to life history requirements of salmon, and it is useful to evaluate the model performance in this regard. Field observations of open water channels were made by PLP from aerial surveys during the lowest-flow periods of late-winter 2006–2008 (Knight Piésold et al., 2011). During this time of year, which is after several months of extremely cold temperatures, stretches of open water are interpreted to reflect the upwelling of groundwater sufficient to prevent ice and snow cover.

As a basis for broad-scale comparison, we evaluated groundwater-surface water exchange for the lowest-flow periods of late-winter, 2004–2008 (Figure 8). The model generally supports the hypothesis of groundwater exchange from portions of SFK between SFK100F and SFK100C that flow into UT at UT119A. Likewise, the resurgence of groundwater into surface flow in the vicinity of SK100B1 and SK100A, as well as downstream of NK100B reflects the narrowing and reduction in depth of overburden in areas of the valley constriction. These results should be interpreted with caution in areas beyond the limits of detailed data on thickness of unconsolidated materials. Nonetheless, the general correspondence between simulations and open water observations suggests that the model is capturing the general patterns of surface water-groundwater exchange in these watersheds.

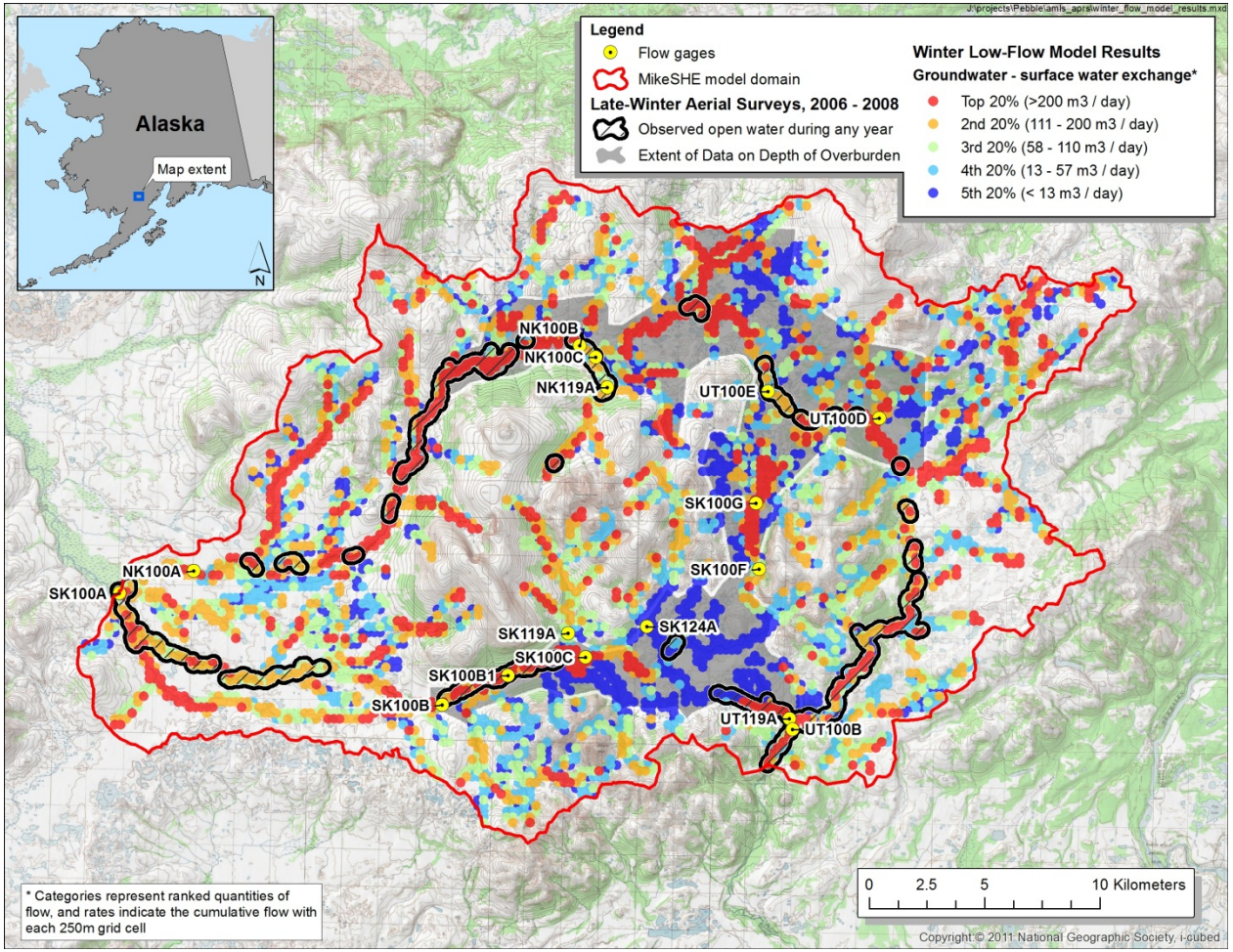

Figure 8. Comparison between MIKE SHE modeled groundwater upwelling areas and inferred upwelling areas based on PLP aerial surveys. Colored dots represent the magnitude of groundwater upwelling generated by MIKE-SHE, with red and orange colors representing the strongest upwelling. Black outlined areas show documented upwelling locations from PLP during three winter open water surveys (Knight Piésold et al., 2011).

4.2 Mine Effects Analysis

The simulated hydrologic and geochemical effects caused by mining were based on the mine scenario described in Section 3. We simulated a full 25-year mine to compare with the baseline scenario. However, we focus our discussion of hydrologic and geochemical effects on the last five years of these simulations. At this point in the simulations, the model has approached a hydrologic steady-state, where the system is largely equilibrated to the long-term effects of pit dewatering (i.e., pit dewatering rates are relatively steady in time).

4.2.1 Streamflow

Richter et al. (2011) describe two important thresholds that can determine the effects of hydrologic alteration on aquatic ecosystems. According to these authors, a 10% reduction in streamflow may lead to a "measureable alteration of ecosystem structure," while a 20% reduction in flow could create "moderate to major changes in natural structure and ecosystem functions." We focus our discussion of streamflow alterations on changes in both average annual flows and peak flows. Although the ecological effects of streamflow reductions are likely to be site-specific, both average and maximum changes in streamflow from our model are discussed in the context of the 10% and 20% thresholds.

Precipitation falling on the open pit, waste rock piles, and tailings impoundment is intercepted by these facilities and related water management operations, thus effectively eliminating runoff and groundwater recharge in these areas. As a consequence, the average annual streamflow reductions are greatest near the mine footprint in all catchments and decrease downstream as the relative proportion of drainage area covered by mine infrastructure decreases. Modeled reductions in streamflow are greatest in the SFK, since the majority of mine infrastructure is located in the headwaters of this stream. The average annual modeled reductions in streamflow ranged from less than 3% in the lowermost SFK to more than 60% in the upper SFK. Figure 9 shows the average reductions in baseflow (March) and peak flow (May) for each of the gaging stations in the model domain.

In all cases, peak stream flows associated with rainfall and snowmelt events are more significantly affected by mining than are average flows. In percentage terms, streamflow reductions are typically most substantial in the spring (May and June), and can also be large during the fall (September and October). The variability in total streamflow reduction is also greater in the wetter spring and fall months. Figure 10a shows modeled baseline and mine-affected hydrographs for the SFK near its headwaters (SK100G), and Figure 10b shows the same relationships for downstream station SK100C. As illustrated by these figures, reductions in wet-month flows (e.g., May and June) are typically much larger than those during other parts of the year. For example, while the modeled flow reduction in the middle SFK (SK100C) is

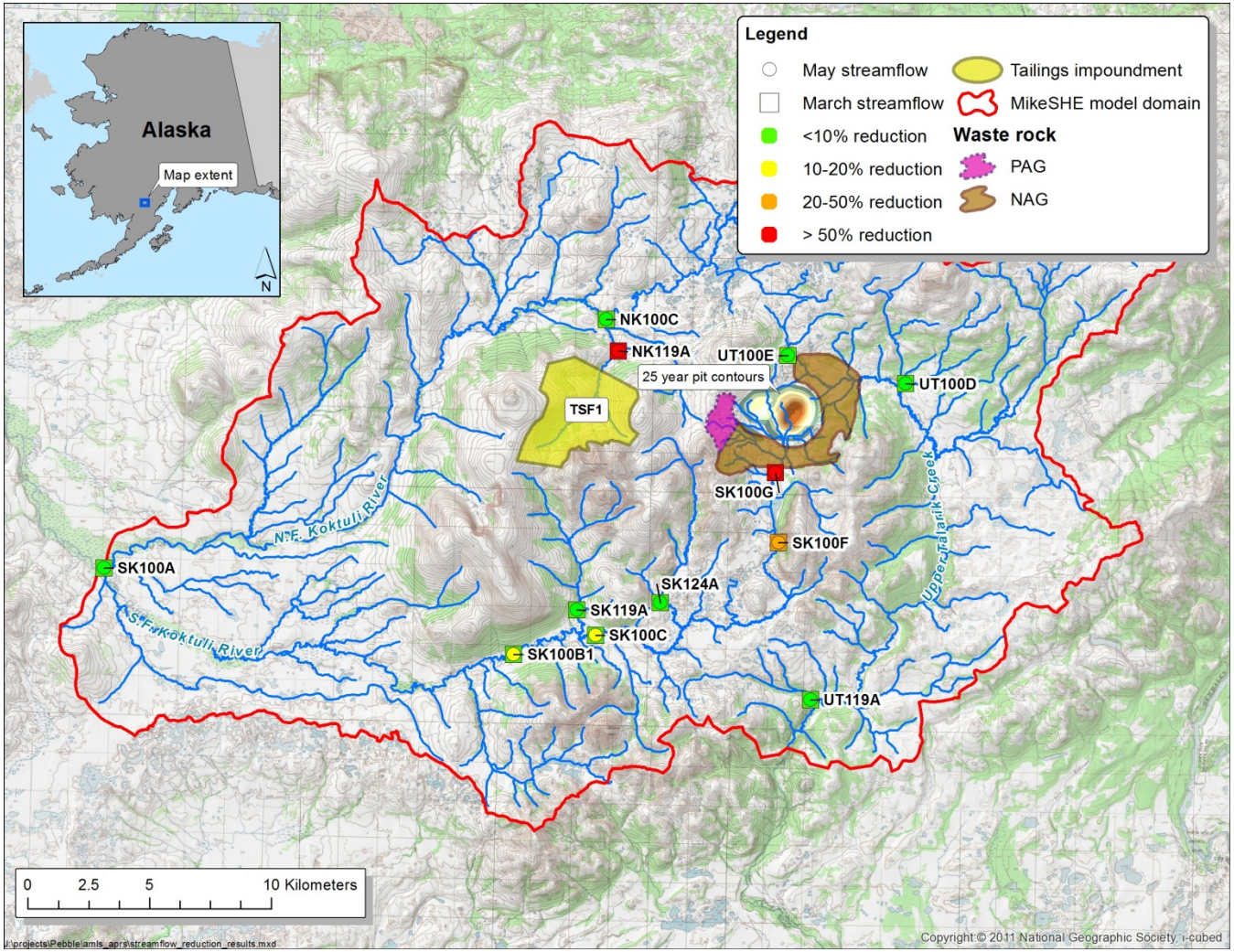

Figure 9. Map of average reductions in baseflow (March) and peak flow (May) throughout the model domain.

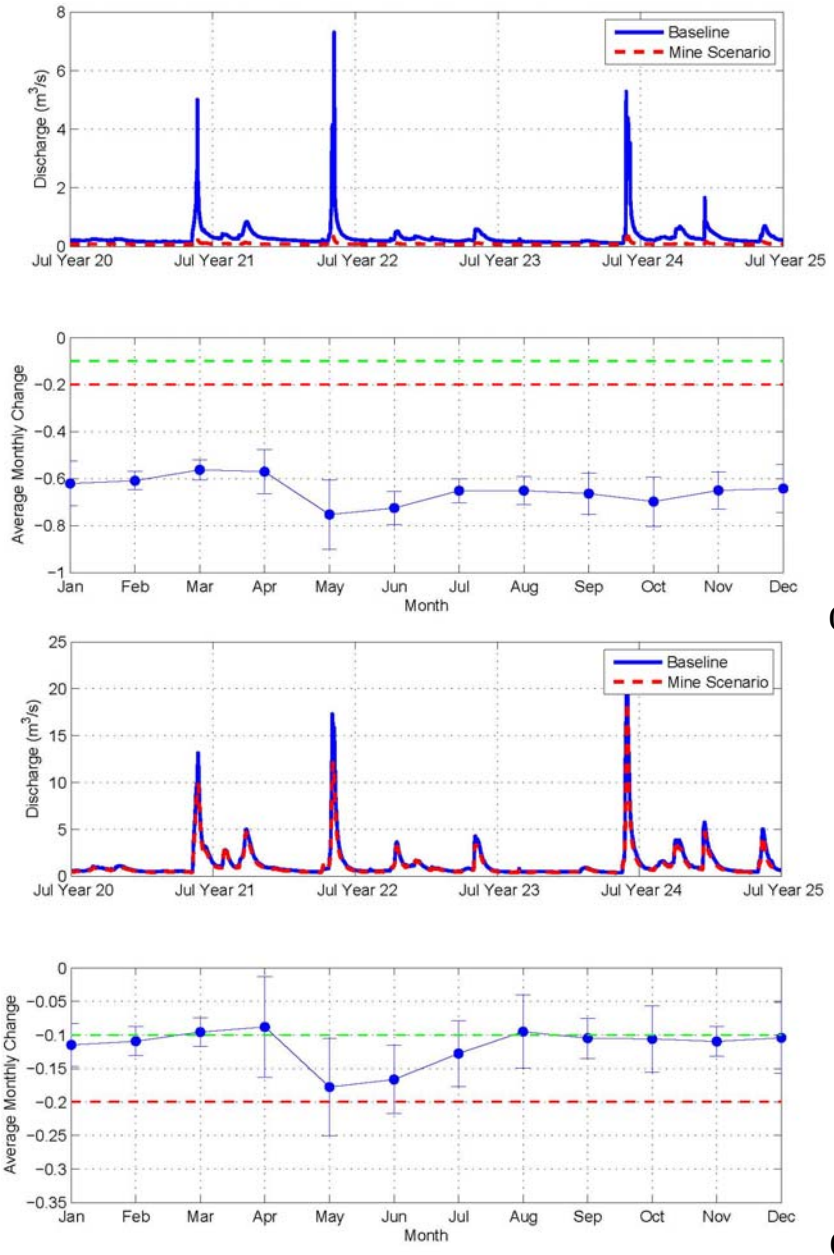

Figure 10. Hydrographs showing modeled changes in streamflow from a 25-year mine plan for (a) upper SFK (SK100G) and (b) middle SFK (SK100C). In each figure, upper plot shows pre- and post-mine hydrographs, and lower plot shows average monthly changes in flow (+ /- 1 standard deviation) over model years 20–25. Dashed green and red lines in lower plots show 10% and 20% streamflow reductions, respectively, for reference. Streamflow changes for all gages are included in the appendix.

approximately 10% during baseflow periods, the projected average flow reductions in May and June are closer to 20%, and flow reductions in the spring exceed 25% during some events. Similar effects are observed at other gages, indicating that ecological processes that depend on peak flows (e.g., cleaning of stream gravels by high-flow sediment transport) could be more significantly affected by mining than would be predicted if the impact analysis focused only on annual average flow reductions (Richter, 2009).

4.2.2 Water quality

Although the model indicates that a cone of depression propagates outward from the pit in the bedrock with continued dewatering, the orders of magnitude higher hydraulic conductivity of the unconsolidated material relative to the underlying bedrock limits the extent to which this cone of depression captures overlying shallow groundwater. In addition, the rapid infiltration through the relatively high permeability waste rock limits outward propagation of the cone of depression from pit dewatering. Thus, even though the bedrock cone of depression extends beneath the waste rock pile by the end of the 25-year model run, a substantial fraction of the waste rock leachate is transported away from the pit toward the SFK and UT. The model projects that approximately 60% of the total leachate would be captured by the pit dewatering system and approximately 40% would flow toward the two drainages.

As described above, we assumed that a leachate collection system would be installed to capture and treat waste rock leachate as it migrates downgradient to the SFK and UT. However, to evaluate the extent and severity of potential water quality alterations, we also simulated a scenario in which no mitigation system is in place and waste rock leachate that does not emerge in the pit migrates downgradient via groundwater flow to headwater streams near the deposit.

Model results from this "no mitigation" scenario (which could also be considered a "long-term failure" scenario) indicated that copper concentrations would exceed the CMC for copper under a variety of stream flows and locations in the mainstem SFK and UT drainages.[2] However, the magnitude and timing of these exceedences vary by location. For example, Figure 11 shows modeled copper concentrations in the upper and middle SFK and UT, between years 20 and 22 of mine operations. The results from these gage sites are typical in that the most significant water quality exceedences occur during winter and summer baseflows, when naturally low flows are less effective at diluting the copper emerging from the waste rock piles. Modeled copper concentrations decreased rapidly during spring and fall high flows; however, at many gage sites the modeled copper concentrations remained above the CMC throughout most of the year. Water quality results from the other gages are provided in the appendix.

2. The CMC is the highest concentration of copper that an aquatic community can be exposed to briefly without resulting in an unacceptable effect (U.S. EPA, 2012b).

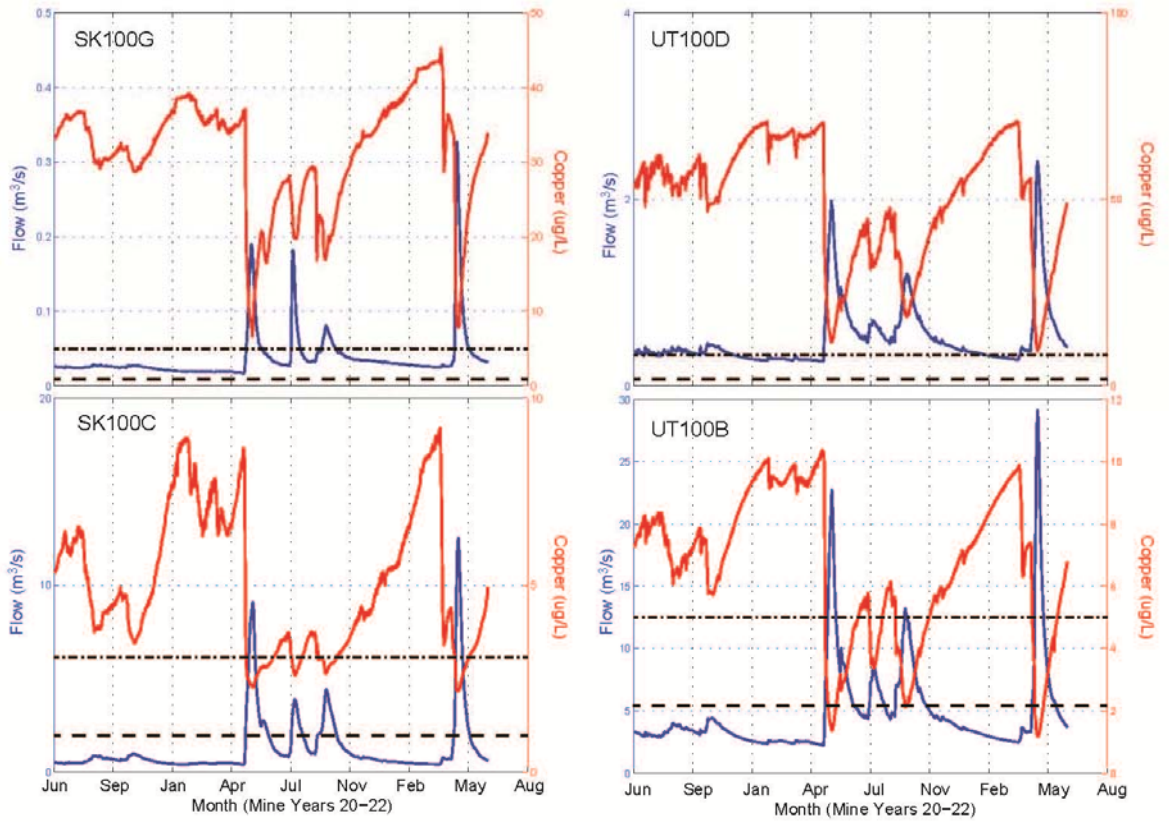

Figure 11. Estimated copper concentrations and stream discharge in years 20 to 22 with no mitigation: results in SFK (SK100G and SK100C) and UT (UT100D and UT100B). Dashed and dash-dot lines represent minimum and maximum values of acute hardness-based water quality criteria calculated using baseline water chemistry for each site.

When it is operating, the mitigation system that we simulated captures the majority of the waste rock leachate before it emerges into surface streams. As a result, copper concentrations in all streams remain near or below water quality standards while the mitigation system is operating. However, failure of the mitigation system leads to large and rapid increases in copper concentrations in downstream gages. Figures 12 and 13 show modeled copper concentrations for the upper and middle UT before, during and after 1-month and 6-month mitigation system failures. As illustrated in these plots, the mitigation system failure in the UT leads to rapid downgradient migration of copper, resulting in short-lived increases in copper concentrations in the UT that are sufficient to exceed the CMC.

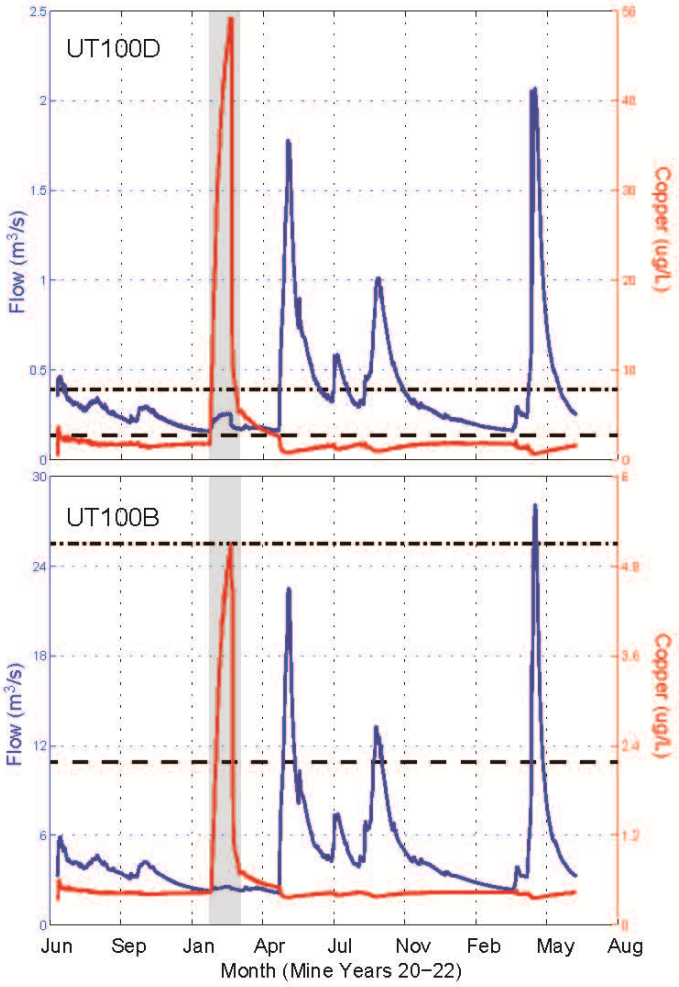

Figure 12. Estimated copper concentrations and stream discharge in years 20 to 22: results of a one-month mitigation failure in SFK (SK100G and SK100C) and UT (UT100D and UT100B). Dashed and dash-dot lines represent minimum and maximum values of acute hardness-based water quality criteria calculated using baseline water chemistry for each site. Vertical grey shading shows the duration of the leachate collection system failure.

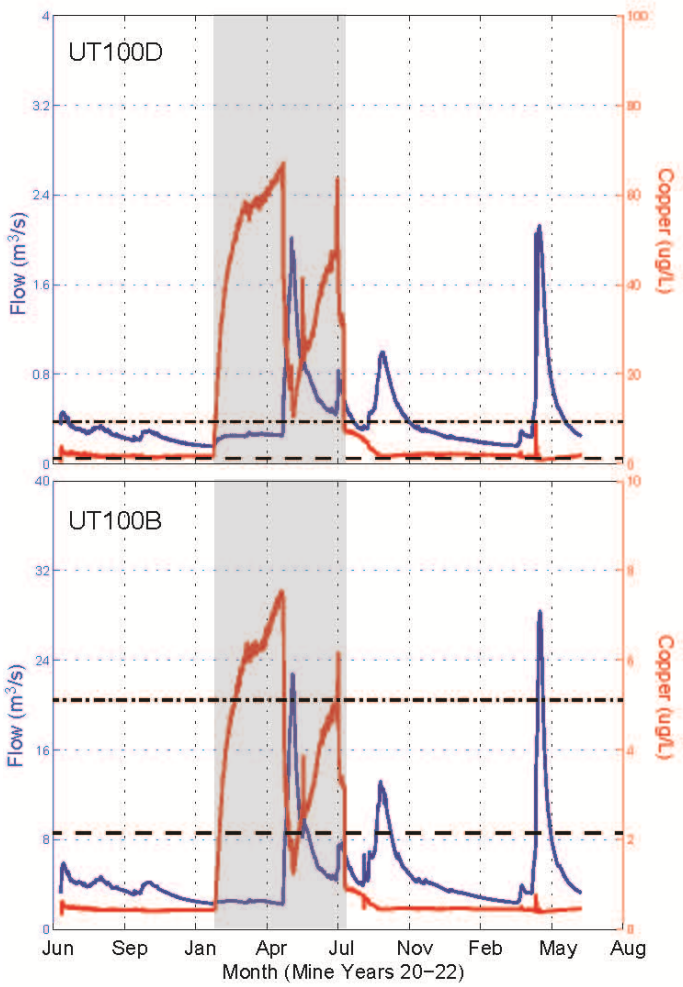

Figure 13. Estimated copper concentrations and stream discharge in years 20 to 22: results of a six-month mitigation failure in SFK (SK100G and SK100C) and UT (UT100D and UT100B). Dashed and dash-dot lines represent minimum and maximum values of acute hardness-based water quality criteria calculated using baseline water chemistry for each site. Vertical grey shading shows the duration of the leachate collection system failure.

Failure of the leachate collection system manifests itself differently in the SFK and the UT drainages, due to differences in hydrogeology between these two catchments. In both catchments, failure of the leachate collection system leads to a nearly instantaneous increase in copper concentrations in downstream waters. However, while the peak copper concentrations in the UT are nearly identical to the peak values observed without a mitigation system in place, peak copper concentrations in the SFK are approximately an order of magnitude lower than under a "no mitigation" or "long-term failure" scenario. This difference in behavior between the two catchments most likely reflects differences in the thickness and hydrogeologic properties of the glacial aquifer, the location and size of the waste rock piles in the two drainages, and differences in topographic slope between the two headwater areas, all of which create different responses to the dewatering from the leachate collection system. While a thorough sensitivity analysis of these effects was beyond the scope of this study, these differences in model predictions from the mitigation failure scenarios in the two catchments underscore some of the challenges of designing a "fail proof" mine.

The size of the waste rock pile and the relatively wet climate lead to large total daily loads of copper generated in leachate. For example, the model projects that the portion of the non-PAG pile within the UT drainage will generate an average of approximately 2 kg/day of total copper in leachate. If copper loads were lower, for example as a result of attenuation in the glacial aquifer, copper CMC values in the streams would be exceeded on fewer days. If loads were higher, for example if leachate concentrations are underestimated, less leachate would be needed to exceed copper CMC values under the same flow conditions.

We calculated the percentage of the total waste rock leachate in the UT basin needed to exceed the hardness-based CMC at UT100D and UT100B under different flow conditions using rank-ordered, 7-day minimum flow statistics (Risley et al., 2008). For example, during low flow conditions in the upper UT (95th percentile low flows), copper water quality criteria would be exceeded if as little as 3 and 4% (for chronic and acute criteria, respectively) of this leachate were to reach UT100D (Table 3). Under similar low flow conditions, chronic and acute criteria would be exceeded if 31 and 43%, respectively, of the leachate reached UT100B. Such low flows (95th percentile values) were measured during winter and early spring on 40 days at UT100D (mid-March through early May) and on 80 days at UT100B (early January through mid-April) over the periods of record. Resident fish (such as sculpin and Dolly Varden) and spawning Chinook, coho, sockeye, and chum salmon have been documented at both locations (PLP, 2011). The model results suggest that winter low flow, when salmon eggs are overwintering, and early spring, when fry are emerging, could be a critical time for potential adverse effects to aquatic biota in the UT under even a short-term leachate collection failure scenario.

Table 3. Seven-day minimum flows and percent waste rock leachate needed to exceed acute and chronic copper criteria at UT100D and UT100B

	UT100B			UT100D		
Percent flow exceedence	**7-day minimum flow (cfs)[a]**	**% needed to exceed Cu CMC**	**% needed to exceed Cu CCC**	**7-day minimum flow (cfs)**	**% needed to exceed Cu CMC**	**% needed to exceed Cu CCC**
5%	382	185%	134%	49	32%	22%
10%	306	149%	107%	37.3	24%	17%
20%	250	121%	87%	30.8	20%	14%
50%	158	77%	55%	14.7	10%	7%
80%	116	56%	41%	8.3	5%	4%
90%	95	46%	33%	6.6	4%	3%
95%	88	43%	31%	5.6	4%	3%

a. Minimum flow over consecutive 7-day periods for 6.7 years at UT100B and 3.2 years at UT100D. For example, at UT100B, a 7-day minimum flow of 95 cubic feet/second (cfs) was exceeded 90% of the time during the period of record. CMC = criterion maximum concentration (acute); CCC = criterion continuous concentration (chronic) for hardness-based copper aquatic life criteria, calculated using measured site water quality.

Much more detailed hydrogeologic characterization and modeling will be required to fully evaluate the range of mitigation options and failure scenarios that might occur. Given the combination of the rapid increases in copper concentrations from even short-term failure of the leachate collection system and the projected extent and severity of contamination in the absence of ongoing active management, our analysis suggests that large-scale mining as envisioned here poses a high level of risk to water quality and little room for error if such risks are to be consistently and effectively managed over time.

4.2.3 Model limitations and uncertainty

As with any complex model, there are uncertainties in our results that arise from the model grid scale and input assumptions. First, there are uncertainties in our assumptions related to the preliminary mine design. We defined our mine scenario on a preliminary design described by Ghaffari et al. (2011), based on a 25-year resource. However, the actual mine infrastructure will likely be much larger over time in order to capture the full 45- to 78-year resource. Depending on the final geometry of the waste rock and tailings facilities and the open pit, the spatial extent of impacts could be substantially larger than our estimates.

Second, the 250-meter grid resolution does not simulate processes that could occur at a sub-grid scale. For example, local-scale features such as topographic depressions or low-permeability lenses in the subsurface could give rise to seeps and springs that would create more direct pathways for waste rock leachate to escape than we have modeled. In this case, our model could underestimate the potential water quality effects from leachate releases. Other sub-grid geologic features, such as laterally continuous silt or fine-grained sand lenses in the subsurface, could potentially slow the migration of contaminants in the subsurface, leading to overestimates in downstream effects.

In addition, a number of other uncertainties arise from model inputs that are poorly constrained by the limited extent, resolution, and duration of baseline data (approximately three years of data for most parameters) available for the site. For example, the model lacks any parameterization of how faults could influence groundwater flow in bedrock. If faults in bedrock have higher hydraulic conductivities than their surroundings, they could substantially change the volume of water for pit dewatering, the propagation and extent of the cone of depression, and the streamflows in overlying unconsolidated materials. Faults in bedrock could also create pathways for migration of contamination from the pit or the waste facilities, which was not considered as a source of contaminants in our model. Since detailed mapping of the location and hydraulic properties of bedrock faults can be difficult, accurate prediction of contaminant migration and pit dewatering will be a substantial challenge.

As described in Section 3.2, waste rock leachate concentrations are also uncertain. We followed industry standards in using the stable concentrations from HCTs as an estimate of waste rock leachate concentrations. However, leachate concentrations could be substantially higher than we have estimated, depending on the mix of rock types present in the waste rock and the timing of releases. Since copper concentrations in receiving waters will scale linearly with our assumed input waste rock leachate concentrations, copper concentrations in streams could also be higher than we have modeled. Conversely, we treated copper conservatively in our simulations (i.e., we did not model reactive chemistry between the waste rock pile and receiving waters). Depending on the pH and redox conditions in groundwater, precipitation and/or sorption of copper along this pathway could reduce the amount of copper entering surface water.

Within the 25-year scenario that we simulated, differences in the actual water management plans could also change the timing or severity of streamflow reductions predicted by our model. For example, the pit dewatering flux could be higher than we have modeled depending on the hydraulic conductivity and extent of faults and fractures in bedrock, and the mine proponents could build surface impoundments that would allow timing of streamflow releases to better mimic natural conditions. Although these water management decisions could mitigate water quantity impacts to some degree, neither of these changes to the water management scenario would mitigate the fundamental change to headwater streams that open pit development would create.

5. Conclusions

The hydrologic system at Pebble is characterized by extensive groundwater-surface water interactions, which necessitates an integrated model such as MIKE SHE that can simulate surface water – groundwater exchange in a physically meaningful way. We developed our integrated model using publicly available information for atmospheric, topographic, and geologic conditions at the Pebble site. This model produced a very good qualitative fit to observed streamflows and groundwater elevations, suggesting that the general behavior of the hydrologic system can be characterized without extensive tuning of model parameters. Inherent uncertainties exist in any model related to grid resolution, the quality of input data, and necessary assumptions and simplifications that are required to make the modeling problem tractable. While these uncertainties limit the ability of the model to make specific numeric predictions regarding water quality or quantity impacts, the model does predict the general degree and direction of potential impacts.

Using a preliminary mine design commissioned by Northern Dynasty Minerals (Ghaffari et al., 2011), our model indicates that development of the Pebble deposit would be likely to generate substantial reductions in both streamflow and water quality. In general, these alterations arise simply because of the scale and location of the deposit, the characteristics of the mine waste, and the stream water quality, which allows only small increases in copper before water quality standards for the protection of aquatic life are exceeded. Replacement of headwater streams with an open pit creates unavoidable changes in the rainfall-runoff response of downstream rivers, and the siting of waste rock adjacent to the pit and overlying small headwater drainages creates a situation in which there is limited dilution of leachate as it enters shallow groundwater and nearby streams. Without ongoing active management, these changes to streamflow and water quality would likely result in adverse effects on aquatic biota, ranging from reductions in habitat quantity and quality to acute or chronic toxicity to aquatic organisms. The model shows that ongoing active management of waste rock leachate can reduce or eliminate the movement of leachate to streams if nearly all waste rock leachate can be captured during and after mine operations. However, if the systems fail for even a short time, copper concentrations would likely exceed relevant chronic and acute water quality criteria with potential for significant adverse effects on downstream populations of salmonids and other aquatic biota. The model results underscore the challenges that proponents of large-scale mineral development will face in predicting mine effects, designing systems that can protect habitat and water quality within salmon ecosystems, and operating in a “fail proof” mode during and after mining operations.

References

ASTM. 2001. Standard Test Method for Accelerated Weathering of Solid Materials Using a Modified Humidity Cell. D5744-96 (Reapproved 2001). American Society for Testing and Materials.

ASTM. 2008. ASTM Standard D 5981-96: Standard Guide for Calibrating a Ground-water Flow Model Application. American Society for Testing and Materials.

Brunke, M. and T. Gonser. 1997. Special review: The ecological significance of exchange processes between rivers and groundwater. *Freshwater Biology* 37:1–33.

Di Toro, D.M., H.E. Allen, H.L. Bergman, J.S. Meyer, P.R. Paquin, and R.C. Santore. 2001. Biotic ligand model of the acute toxicity of metals. 1. Technical basis. *Environ Toxicol Chem* 20(10):2383–2396.

Ghaffari, H., R.S. Morrison, M.A. Deruijeter, A. Živković, T. Hantelmann, D. Ramsey, and S. Cowie. 2011. Preliminary Assessment of the Pebble Project, Southwest Alaska. Prepared for Northern Dynasty Minerals Ltd. by Wardrop (A Tetra Tech Company), Vancouver, BC. February 15.

Gowan, M. 2006. Codisposal. Prepared by Golder Associates. Available: www.infomine.com/publications/docs/CodisposalPresentation.ppt. Accessed October 2012.

Graham, D.N. and M.B. Butts. 2005. Flexible, integrated watershed modelling with MIKE SHE. In *Watershed Models*, V.P. Singh and D.K. Frevert (eds.). CRC Press. ISBN: 0849336090. pp. 245–272.

Hilborn, R., T.P. Quinn, D.E. Schindler, and D.E. Rogers. 2003. Biocomplexity and fisheries sustainability. *Proceedings of the National Academy of Sciences* 100:6564–6568.

Hill, M.C. 1998. Methods and Guidelines for Effective Model Calibration. U.S. Geological Survey Water Resources Investigations Report 98-4005.

Homer, C., C. Huang, L. Yang, B. Wylie, and M. Coan. 2004. Development of a 2001 national land cover database for the United States. *Photogrammetric Engineering and Remote Sensing* 70(7):829–840.

Kaiser-Hill. 2002. Model Code and Scenario Selection Report Site-Wide Water Balance Rocky Flats Environmental Technology Site. Available: http://www.integratedhydro.com/CodeSelectionRFETS.pdf. Accessed September, 2012.

Knight Piésold. 2011. Geology and mineralization, Bristol Bay drainages. Chapter 3 in *Pebble Project Environmental Baseline Document, 2004 through 2008*. Prepared for Pebble Limited Partnership by Knight Piésold Ltd. December. Available: http://www.pebbleresearch.com/ebd/bristol-bay-phys-chem-env/chapter-3/. Accessed January, 2012.

Knight Piésold, ABR, 3 Parameters Plus, and Bristol Environmental & Engineering Services. 2011. Surface Water Hydrology, Bristol Bay Drainages. Chapter 7 in *Pebble Project Environmental Baseline Document, 2004 through 2008*. Prepared for Pebble Limited Partnership by Knight Piésold Ltd., ABR, Inc., 3 Parameters Plus, Inc., and Bristol Environmental & Engineering Services Corporation. December. Available: http://www.pebbleresearch.com/ebd/bristol-bay-phys-chem-env/chapter-7/. Accessed January, 2012.

Kristensen, K.J. and S.E. Jensen. 1975. A model for estimating actual evapotranspiration from potential evapotranspiration. Royal Veterinary and Agricultural University. *Nordic Hydrology* 6:170–188.

Lackey, R.T., D.H. Lach, and S.L. Duncan. 2006. *Salmon 2100: The Future of Wild Pacific Salmon*. American Fisheries Society.

MacRae, R.K., D.E. Smith, N. Swoboda-Colberg, J.S. Meyer, and H.L. Bergman. 1999. Copper binding affinity of rainbow trout (*Oncorhynchus mykiss*) and brook trout (*Salvelinus fontinalis*) gills: Implications for assessing bioavailable metal. *Environ Toxicol Chem* 18(6):1180–1189.

Mesinger, F., G. Dimego, E. Kalnay, K. Mitchell, P.C. Shafran, W. Ebisuzaki, D. Jović, J. Woollen, E. Rogers, E.H. Berbery, M.B. Ek, Y. Fan, R. Grumbine, W. Higgins, H. Li, Y. Lin, G. Manikin, D. Parrish, and W. Shi. 2006. North American Regional Reanalysis. *Bulletin of the American Meteorological Society* 87(3):343–360. doi: 10.1175/BAMS-87-3-343.

Meyer, J.S., S.J. Clearwater, T.A. Doser, M.J. Rogaczewski, and J.A. Hansen (eds.). 2007. *Effects of Water Chemistry on Bioavailability of Toxicity of Waterborne Cadmium, Copper, Nickel, Lead, and Zinc to Freshwater Organisms.* Society of Environmental Toxicology and Chemistry (SETAC) Press, Pensacola, FL.

Miller, T.G. and W.C. Mackay. 1980. The effects of hardness, alkalinity and pH of test water on the toxicity of copper to rainbow trout (*Salmo gairdneri*). *Water Res* 14:129–133.

Morin, K.A. and N.M. Hutt. 2010a. Twenty-nine Years of Monitoring Minesite-Drainage Chemistry, during Operation and after Closure: The Granisle Minesite, British Columbia, Canada. MDAG Internet Case Study #34. Available: www.mdag.com/case_studies/cs34.html. Accessed September 2012.

Morin, K.A. and N.M. Hutt. 2010b. Thirty-one Years of Monitoring Minesite-Drainage Chemistry, during Operation and after Closure: The Bell Minesite, British Columbia, Canada. MDAG Internet Case Study #33. Available: http://www.mdag.com/case_studies/cs33.html. Accessed September 2012.

Morin, K.A., I.A. Horne, and D. Flather. 1993. The appropriate geochemical monitoring of toe seepage from a mine-rock dump. In *Proceedings of the 17th Annual Mine Reclamation Symposium, Port Hardy, British Columbia, May 4–7*. Mining Association of British Columbia. pp. 119–129.

NRCS. 2011. U.S. General Soil Map (STATSGO2). Natural Resources Conservation Service, U.S. Department of Agriculture. Available: http://soildatamart.nrcs.usda.gov. Accessed December 2011.

Pinsky, M., D.B. Springmeyer, M.N. Goslin, and X. Augerot. 2009. Range wide selection of catchments for Pacific salmon conservation. *Conservation Biology* 23(3):680–691.

PLP. 2011. Fish and aquatic invertebrates – Bristol Bay drainages. Chapter 15 in *Pebble Project Environmental Baseline Document 2004 through 2008 (with updates in 2010).* Available: http://www.pebbleresearch.com/ebd/bristol-bay-phys-chem-env/chapter-15/. Accessed September 2012.

Price, W.A. 2009. Prediction Manual for Drainage Chemistry from Sulphidic Geologic Materials. MEND Report 1.20.1. Prepared for Natural Resources Canada.

Prucha, R.H., J. Leppi, S. McAfee, and W. Loya. 2012. Development and Application of an Integrated Hydrologic Model to Study the Effects of Climate Change on the Chuitna Watershed, Alaska. Integrated Hydro Systems, LLC, Boulder, CO and The Wilderness Society, Anchorage, AK. Available: http://alaska.fws.gov/fisheries/fieldoffice/anchorage/pdf/Documentation%20Report%20Climate%20Effects%20on%20Chuitna%20Hydrology%20Revised%200412.pdf. Accessed September 2012.

Refsgaard, J.C. 2007. Hydrological Modelling and River Basin Management. Doctoral Thesis. Geological Survey of Denmark and Greenland. January.

Richter, B., M. Davis, C. Apse, and C. Konrad. 2011. A presumptive standard for environmental flow protection. *River Research and Applications* doi: 10.1002/rra.1511.

Richter, B.D. 2009. Re-thinking environmental flows: From allocations and reserves to sustainability boundaries. *River Research and Applications* 26(8):1052–1063. doi: 10.1002/rra.1320.

Risley, J., A. Stonewall, and T. Haluska. 2008. Estimating Flow-duration and Low-flow Frequency Statistics for Unregulated Streams in Oregon. U.S. Geological Survey Scientific Investigations Report 2008-5126. Available: http://pubs.usgs.gov/sir/2008/5126/index.html. Accessed October 2012.

Ruggerone, G., R. Peterman, B. Dorner, and K. Myers. 2010. Magnitude and trends in abundance of hatchery and wild pink salmon, chum salmon, and sockeye salmon in the North Pacific Ocean. *Marine and Coastal Fisheries: Dynamics, Management, and Ecosystem Science* 2:306–328.

Santore, R.C. and C.T. Driscoll. 1995. The CHESS model for calculating chemical equilibria in soils and solutions. In *Chemical Equilibrium and Reaction Models*, Loeppert, R.H., A.P. Schwab, and S. Goldberg (eds.). American Society of Agronomy, Madison, WI, pp. 357–375.

Schlumberger Water Services. 2011. Groundwater hydrology. Chapter 8 in *Pebble Project Environmental Baseline Document 2004 through 2008*. Prepared for Pebble Limited Partnership. December. Available: http://www.pebbleresearch.com/ebd/bristol-bay-phys-chem-env/chapter-8/. Accessed January 2012.

SRK Consulting. 2011a. Water quality. Chapter 9 in *Pebble Project Environmental Baseline Document 2004 through 2008* (with updates in 2010). Prepared for Pebble Limited Partnership by SRK Consulting, Inc. Available: http://www.pebbleresearch.com/ebd/bristol-bay-phys-chem-env/chapter-9/. Accessed January 2012.

SRK Consulting. 2011b. Geochemical characterization, Bristol Bay drainages. Chapter 11 in *Pebble Project Environmental Baseline Document 2004 through 2008* (with updates in 2010). Prepared for Pebble Limited Partnership by SRK Consulting, Inc. Available: http://www.pebbleresearch.com/ebd/bristol-bay-phys-chem-env/chapter-11/. Accessed January 2012.

Suter, G.W., S.M. Cormier, D. Mackay, S.B. Norton, N. Mackay, L.W. Barnthouse, and S.M. Bartell. 2007. *Ecological Risk Assessment.* CRC Press, Boca Raton, FL.

Tipping, E. 1994. WHAM – A chemical equilibrium model and computer code for waters, sediments, and soils incorporating a discrete site/electrostatic model of ion-binding by humic substances. *Comput Geosci* 20:973–1023.

USACE. 2004. Central and Southern Florida Project, Comprehensive Everglades Restoration Plan. Appendix B.2, Hydrologic Modeling/Methodology Report. Available: http://www.evergladesplan.org/pm/projects/project_docs/pdp_08_eaa_store/docs_08_mod_hydr_report.pdf. Accessed September 2012.

U.S. EPA. 2002. *National Recommended Water Quality Criteria: 2002.* Document # 822-R-02-047. U.S. Environmental Protection Agency, Washington, DC. November.

U.S. EPA. 2007. *Aquatic Life Ambient Freshwater Quality Criteria – Copper*. 2007 Revision. EPA-822-R-07-001. U.S. Environmental Protection Agency, Office of Water 4304T, Office of Science and Technology. February. Available: http://water.epa.gov/scitech/swguidance/standards/current/upload/2009_04_27_criteria_copper_2007_criteria-full.pdf. Accessed September 2012.

U.S. EPA. 2012a. *An Assessment of Potential Mining Impacts on Salmon Ecosystems of Bristol Bay, Alaska. External Review Draft*. EPA 910-R-12-004a. May, Seattle, WA. Available: www.epa.gov/bristolbay. Accessed September 2012.

U.S. EPA. 2012b. National Recommended Water Quality Criteria. Available: http://water.epa.gov/scitech/swguidance/standards/criteria/current/index.cfm. Accessed October 2012.

Welsh, P.G., J. Lipton, C.A. Mebane, and J.C.A. Marr. 2008. Influence of flow-through and renewal exposures on the toxicity of copper to rainbow trout. *Ecotoxicol Environ Safety* 69:199–208.

A. Supplemental Material on Data Sources, Model Development

A.1 Summary

This document summarizes the data inputs that were used in the development and calibration of an integrated hydrologic model to evaluate the potential effects on the hydrologic regime and water quality resulting from the mining of the Pebble deposit in the Nushagak and Kvichak headwaters of Bristol Bay. The key datasets summarized in this document include the North American Regional Reanalysis (NARR) climate data, the Shuttle Radar Topography Mission (SRTM) topography data, the Natural Resource Conservation Service (NRCS) soils data, aquifer geometry using data released as part of the Environmental Baseline Documents (EBD) by Pebble Limited Partnership (PLP), and stream networks contained in the National Hydrography Database (NHD). Other inputs to the hydrologic model, including aquifer properties, soil hydraulic properties, and additional model assumptions, are also summarized here. Finally, all calibration plots and mine impact analysis plots are included here for reference, and to supplement the information contained in the body of the report.

A.2 Introduction

This report provides background information on development of a fully integrated surface water-groundwater model of the hydrologic system surrounding the Pebble deposit in Bristol Bay, Alaska. Our purpose is to describe input data sources, conceptual and numerical aspects of the hydrologic model, calibration of the model to match observed patterns of stream flow and groundwater elevations, and details of the simulation of a preliminary mine design (Ghaffari et al., 2011).

A.2.1 Study area

The study area includes 3 headwater basins in southwestern Alaska, including the North Fork Koktuli River (NFK) and South Fork Koktuli River (SFK) which drain into the Mulchatna River, a major tributary of the Nushagak River, and Upper Talarik Creek (UT) which drains into Lake Iliamna and then into the Kvichak River (Figure A.1). With elevations ranging from 131 to 930 meters, the terrain is characterized by wide valleys and rounded mountains with glacial deposits > 100 m deep in some areas. Dominant vegetation includes shrublands and dwarf scrub tundra with smaller representation of conifer and deciduous forest and barren ground at higher elevations.

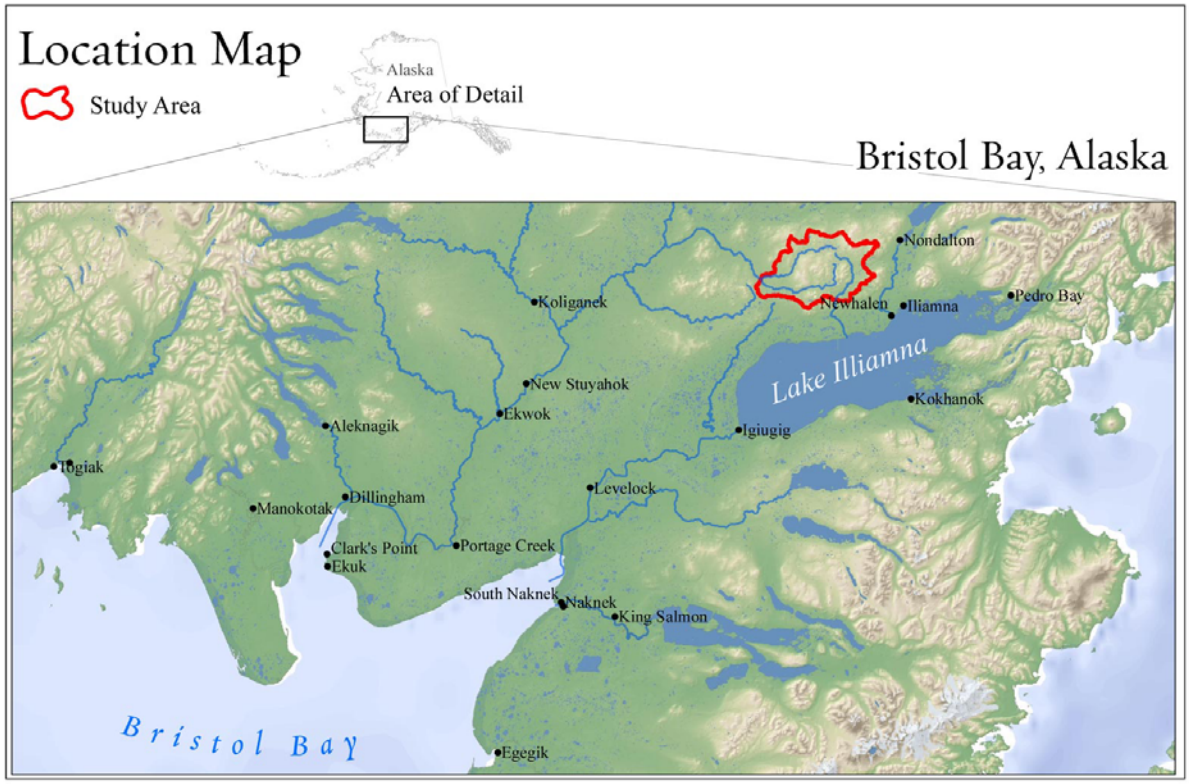

Figure A.1. The study area at the headwaters of the Nushagak and Kvichak Rivers in southwestern Alaska.

A.3 Hydrologic Characterization

The primary inputs to the hydrologic model were climatic inputs (e.g., temperature, precipitation, insolation, relative humidity), topography, surface and subsurface geology, soils, vegetation and mapped stream networks. Data used to calibrate the model were measured stream flow from stream gage stations maintained by the U.S. Geological Survey (USGS) and PLP, and groundwater elevations collected by PLP (PLP, 2011d).

A.3.1 Climate

The NARR dataset, developed by the National Center for Environmental Prediction (NCEP), is an atmospheric and land surface hydrology dataset for North America (Mesinger et al., 2006). The NARR dataset is generated by combining a high-resolution climate model (the NCEP Eta model) and the Regional Data Assimilation System (RDAS). This results in a high resolution, spatially and temporally consistent dataset that is true to all available observations. It covers the

period of 1979–present with 8 times daily (3-hourly) records for a range of climatic and hydrologic parameters at a spatial resolution of 32 km. While the spatial resolution of this dataset is coarser than other available climate data (e.g., Daly et al., 1994), the temporal resolution, the long-term record of continuous data, and the breadth of synchronized climate parameters made NARR the most useful dataset for evaluating long-term mining impacts. Parameters included in the dataset include air temperature, albedo, precipitation, dew point temperature, net solar radiation (short- and long-wave) and wind speed. We used a 30-year subset of the NARR data, covering the period of 1979–2009. In addition to the direct outputs from the NARR dataset, we calculated reference evapotranspiration (RET) every three hours.

We extracted all climate variables of interest from the 32 × 32 km NARR grid cell most directly overlying the Pebble deposit (59.92°N, 155.30°W). These variables included precipitation, air temperature, downward and upward short and longwave radiation flux, wind speed, and dew point. From these variables, we calculated an FAO56 Penman-Monteith RET every three hours using the REFET code (Allen, 2011). A brief summary of the precipitation and temperature statistics from this dataset follows.

NARR temperature summary

Mean annual air temperature based on NARR was 0.45°C, with monthly averages ranging from -10.6°C in January to +13.2°C in July. While monthly temperatures were quite variable, monthly averages were typically above freezing during May–September, below freezing during November–March, and approximately at the freezing point during April and October (Figure A.2).

NARR precipitation summary

During 1980–2009, average annual precipitation estimated from the NARR database was 980.8 mm [standard deviation (SD) = 135.2 mm], with a high of 1,233.7 in 1985 and low of 736.6 in 1984 (Figure A.3). Note that annual precipitation totals during the 2004–2008 calibration period were near the long-term average precipitation of 980 mm ($\overline{X}$ = 1001.4, SD = 40, range = 968.1–1,064.6), but did not contain years with more extreme values seen in other years over the 1980–2009 time period (Figure A.3).

The seasonal pattern of precipitation typical for this area typically includes heaviest rains during August and September, with declining precipitation delivered in the form of snowfall during winter, and lowest precipitation during March and April. The average monthly total precipitation over the 1979–2009 time period was 81.7 mm (SD = 40, range: 10.4–223.7) (Figure A.4).

Monthly precipitation during the period of calibration (2005–2008) averaged 83.1 mm (SD = 40, range: 17.5–203.6), with highest rainfall in August and September, and typically lowest during late winter (Figure A.5).

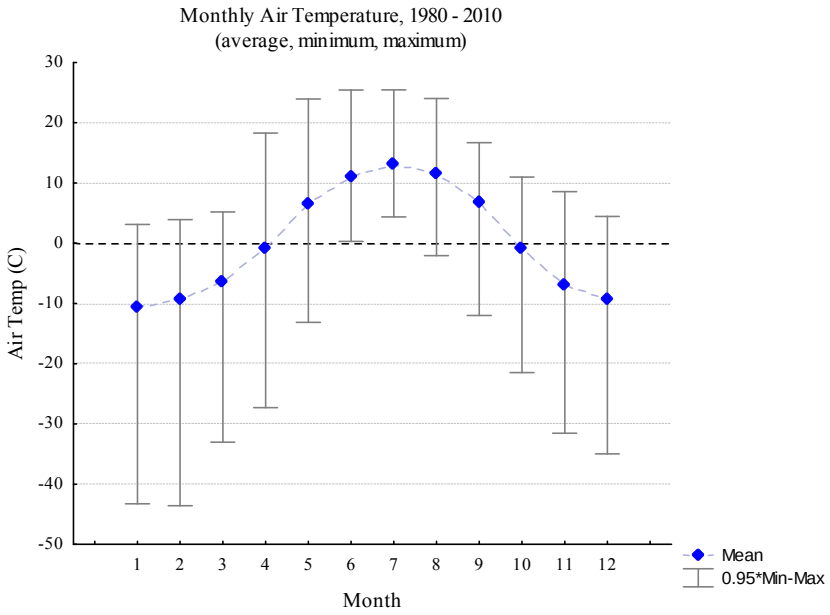

Figure A.2. Mean monthly temperature (minimum–maximum) represented in NARR climate database.

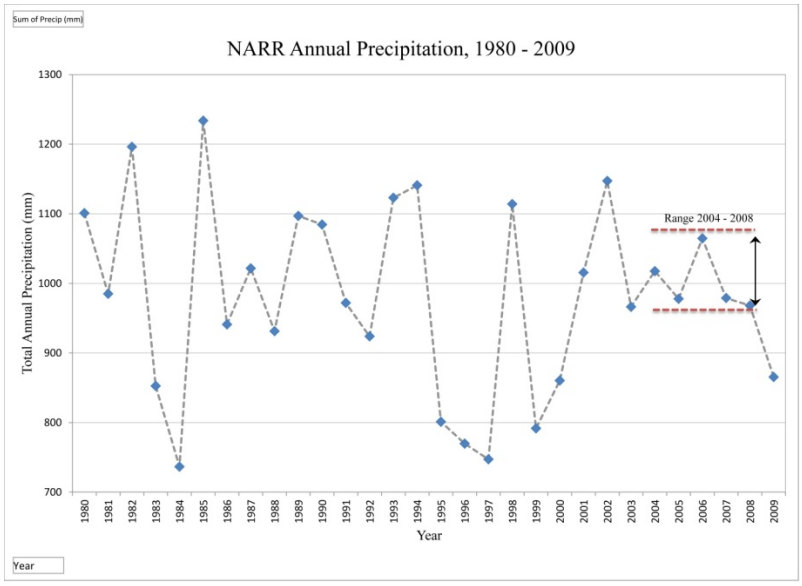

Figure A.3. Annual precipitation 1980–2009 in NARR climate database.

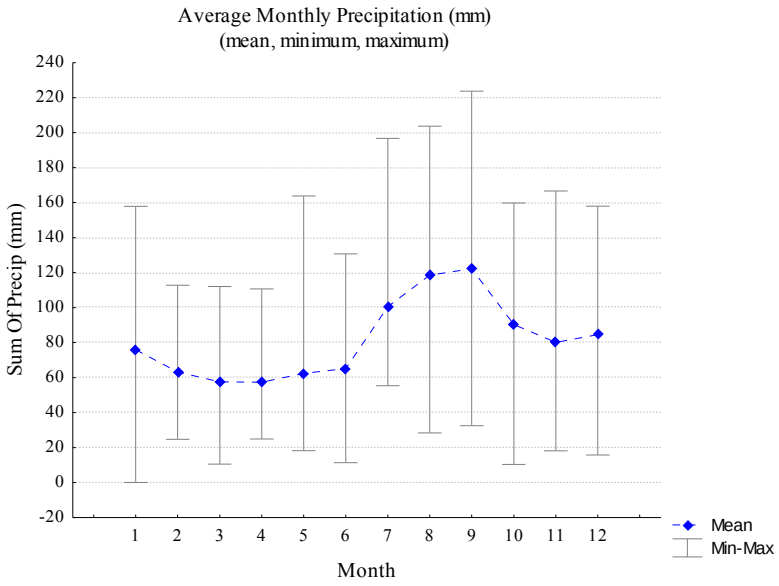

Figure A.4. Average monthly precipitation 1980–2009 in NARR climate database.

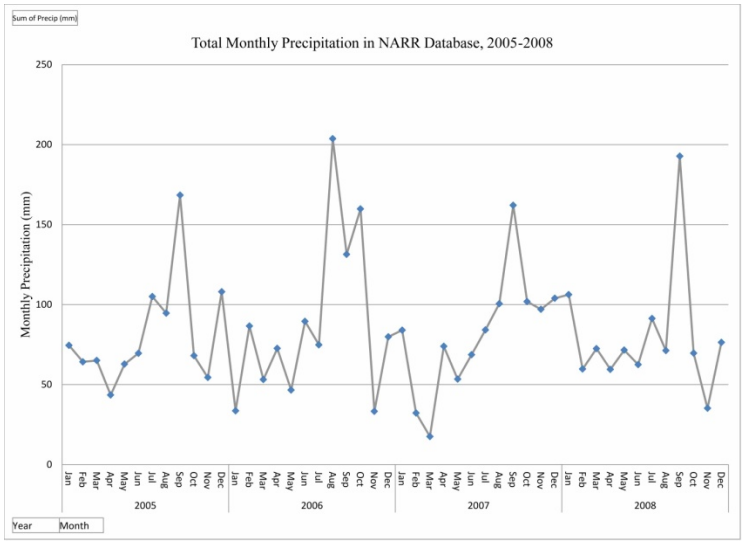

Figure A.5. Monthly precipitation in NARR data, 2005–2008.

We compared cumulative precipitation inputs reported in NARR with similar data measured at Pebble 1 weather station by PLP (PLP, 2011a) to better understand variation in observed hydrologic parameters that may reflect NARR inputs rather than model behavior. Overall, precipitation reflected in NARR was similar to precipitation measured by PLP, with a correlation of r = 0.86 among monthly totals, and an overall deviation of +9.5% in cumulative precipitation during the period July 2005–December 2007 (Figure A.6).

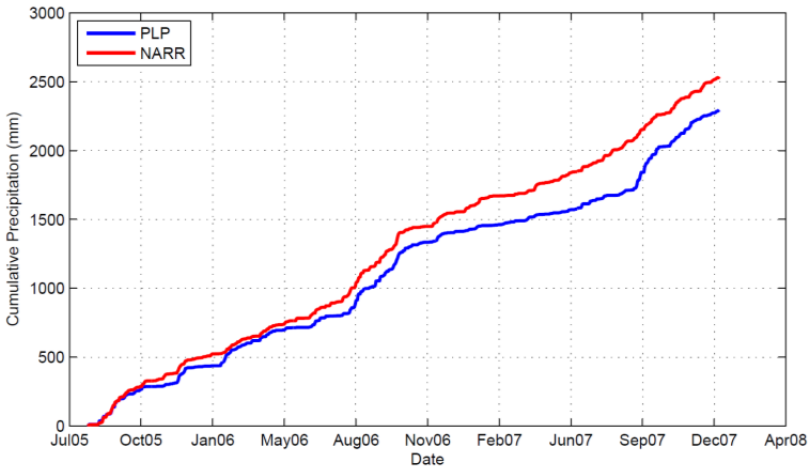

Figure A.6. Comparison of cumulative precipitation in local site observations (PLP Pebble 1 meteorological station) with NARR regional data.

A.3.2 Elevation

A digital elevation model (DEM) for this study was derived from SRTM (Rabus et al., 2003). This mission produced the most complete, highest resolution DEM of the Earth. The project was a joint endeavor of NASA, the National Geospatial-Intelligence Agency, and the German and Italian Space Agencies, and flew in February 2000. It used dual radar antennas to acquire interferometric radar data, processed to digital topographic data at 1 arc-sec resolution (approximately 29 m).

The study area is characterized by rounded mountains and broad glacial valleys, with elevations ranging from 131 m to 930 m, and broad areas of relatively low gradient terrain. 25% of lands have slope < 2.6%, which allows for extensive development of wetlands and riverine floodplain development. The lowest elevations are in UT, where the drainage is incised below the level of the SFK (Figure A.7).

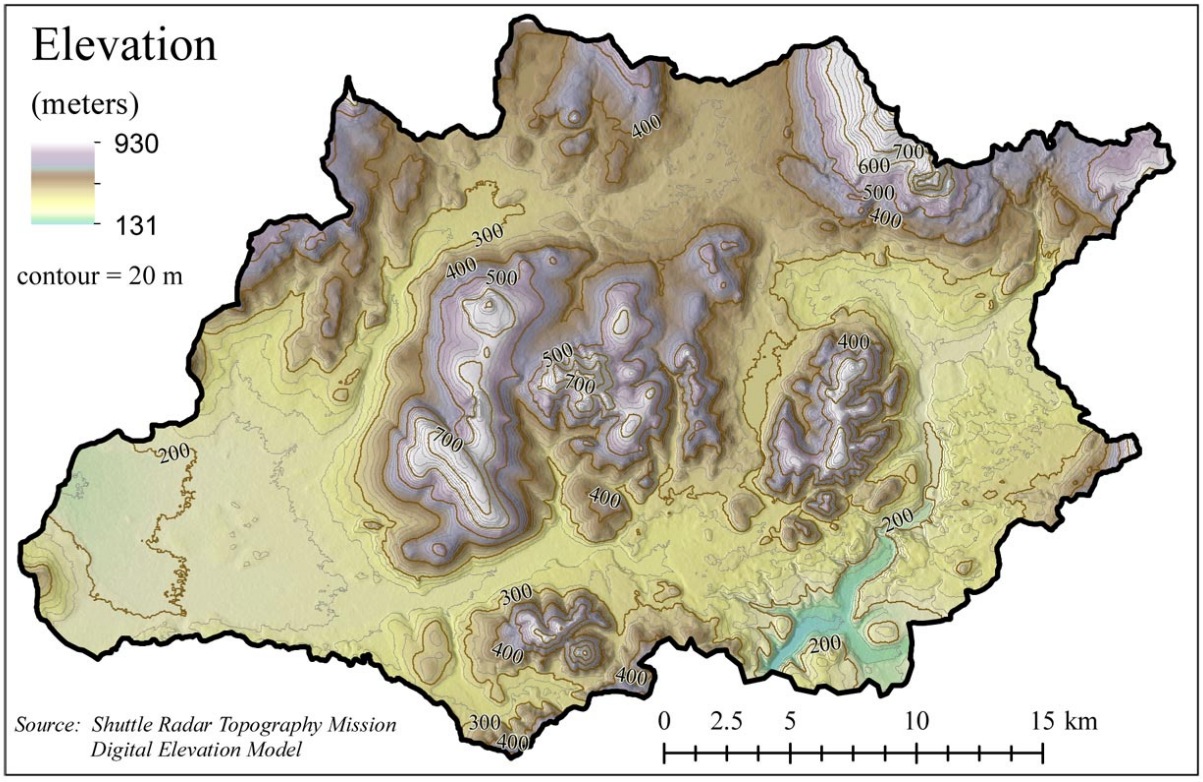

Figure A.7. Elevation within the model domain, as derived from the SRTM DEM. See Figure 1 in main text for site location.

A.3.3 Landform and soils

Coarse-scale information on landform and soils was available from the NRCS STATSGO database (NRCS, 1979). This dataset consists of digital map and attribute data derived from the publication "Exploratory Soil Survey of Alaska." The map is a broad based inventory of soils and non-soil areas that occur in a repeatable pattern on the landscape. These data were compiled at a scale of 1:1,000,000.

In addition to the soils data obtained from STATSGO, we included all surficial deposits mapped as "lacustrine" or "glaciolacustrine" in the surficial geologic map generated by PLP (PLP, 2011c). Due to the likely fine-grained nature of these lacustrine and glaciolacustrine units, they were assumed to have different unsaturated hydraulic properties than the surrounding soils (see "Unsaturated Zone Flow" section in "Model Development"). Figure A.8 shows the soil data used in the model.

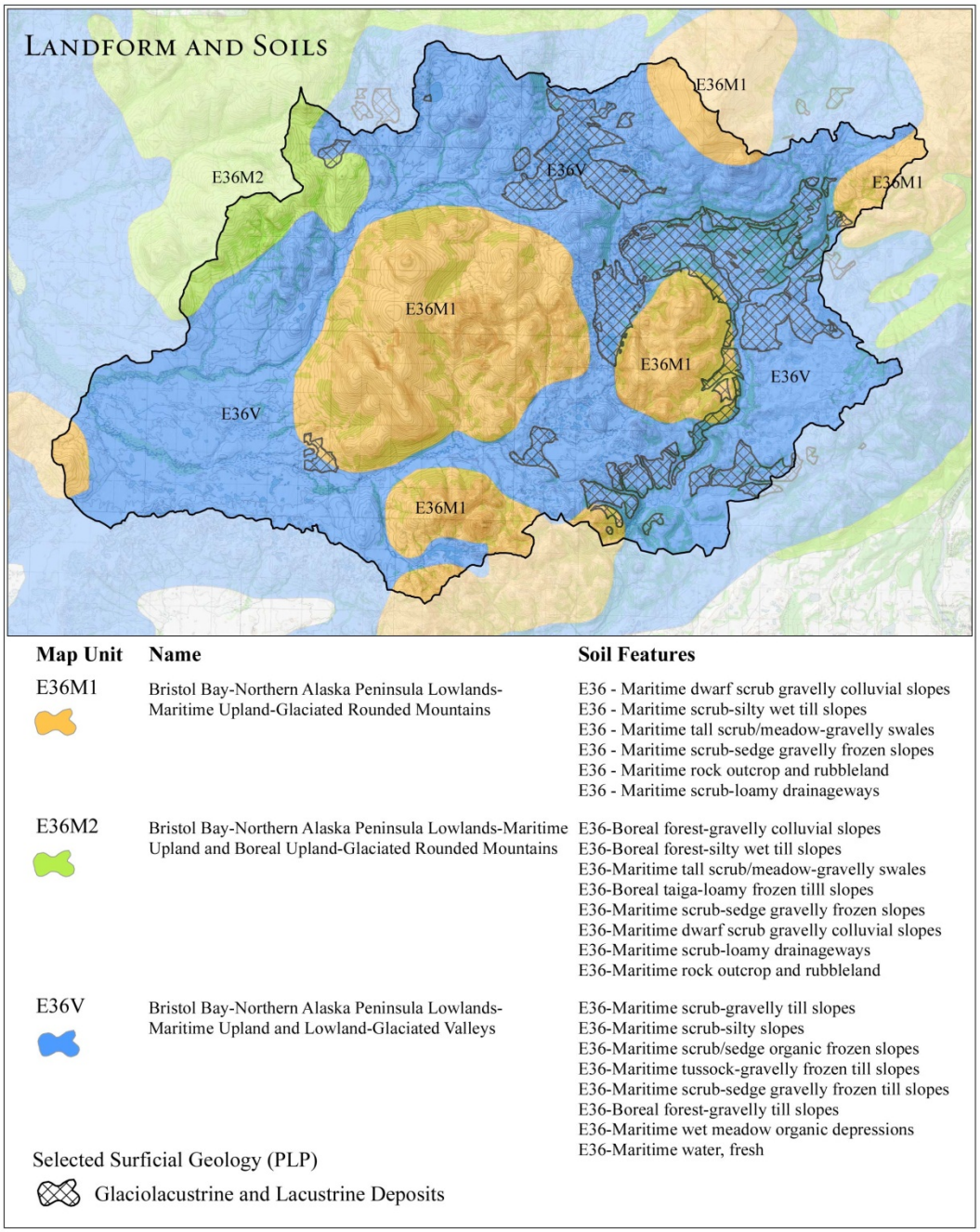

Figure A.8. Coarse-scale information on landform and soils was obtained from NRCS in the Alaska STATSGO database.

A.3.4 Depth to bedrock

The depth to bedrock (or thickness of overburden) was compiled primarily by subtracting the bedrock surface elevation from the ground surface elevation (see main text). Additional overburden thicknesses were inferred beyond the limits of the bedrock surface map, as described in the main text. The final depth of overburden used in the model is shown in Figure A.9.

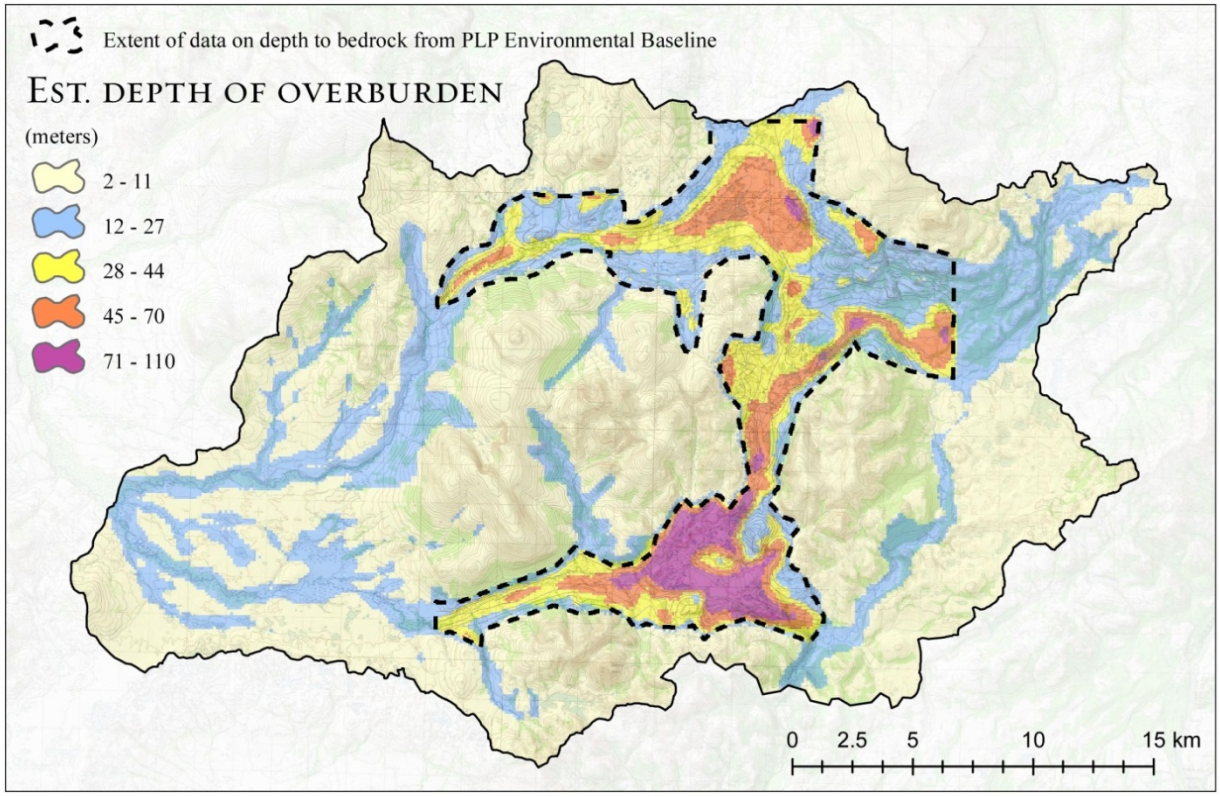

Figure A.9. Depth of overburden was based on PLP EBD (PLP, 2011d) where available, and an assumed depth of 20 m in floodplain zones (within a distance of less than 100 m of streams) and 5 m in upland zones (within a distance of greater than 100 m from streams) where EBD data were not available.

A.3.5 Vegetation and landcover

We used the National Land Cover Database (NLCD) to develop model input parameters for vegetation. NLCD products are created by the Multi-Resolution Land Characteristics (MRLC) Consortium, a partnership of Federal agencies led by USGS (Homer et al., 2004). Dominant vegetation types present within the model domain included shrublands (49.8%), dwarf shrub (44.1%), barren land (1.5%) and deciduous forest 1.0%) (Figure A.10). The two most important aspects of vegetation type for hydrologic modeling are the Leaf Area Index (LAI) and the root depth of each vegetation type. The LAI and root depth information used in the model were identical to the values used by Prucha et al. (2011) for the nearby Chuitna river system. These values are provided in Table A.1.

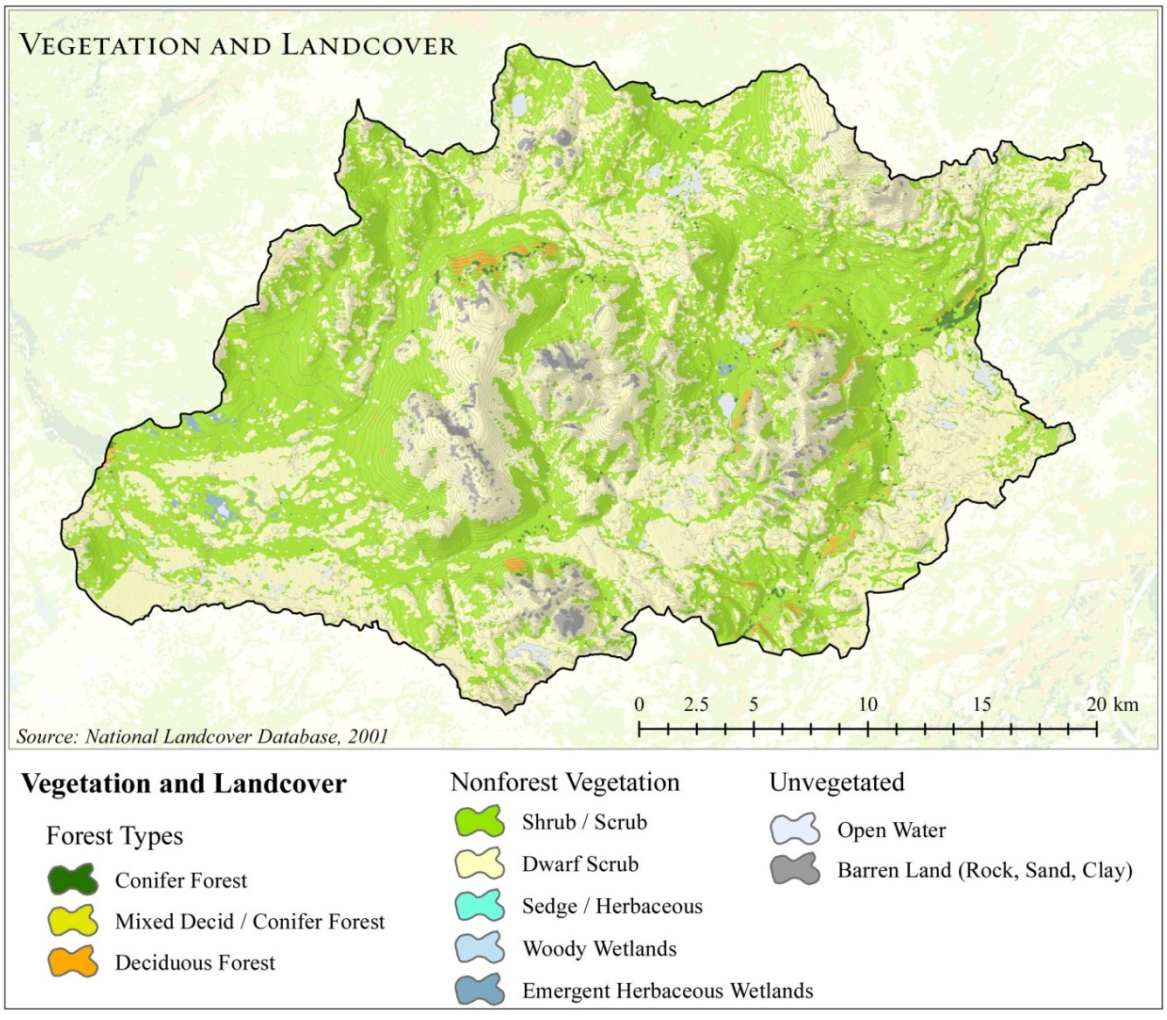

Figure A.10. Vegetation and landcover types as mapped by the NLCD.

Table A.1. Summary of leaf-area index and root depths used in the integrated hydrologic model

Cover class (NLCD)	LAI peak (SD)	Location	Sources	Root depth in cm (mean/max)
Shrub/scrub	2.24	Seward Peninsula	Thompson et al., 2004	69/123
Dwarf scrub	1.7	Seward Peninsula	Thompson et al., 2004	56/90
	5.3 (0.46)	Cook Inlet	Verbyla, 2005	
Deciduous/mixed deciduous forest	2.6 (0.7)	Boreal sites	Asner et al., 2003	75/155
	4	North America	Fang et al., 2008	
Sedge/herbaceous	1.7 (1.2)	Global grasslands	Asner et al., 2003	89/160
	1	North America	Fang et al., 2008	
Conifer forest	2.7 (1.3)	Boreal sites	Asner et al., 2003	55/101
	3.2	North America	Thompson et al., 2004; Fang et al., 2008	
Barren land	1		Fang et al., 2008	10
Water	0		NA	0
Emergent herb wetlands	1.7	Global grasslands	Asner et al., 2003	89

A.3.6 Stream network

We developed the stream network using three sources. First, the National Hydrography Dataset (USGS, 1999) was used as a preliminary guide to location of large-scale water features over the model domain. This stream layer was supplemented with smaller tributaries using hydrologic modeling tools in ArcGIS, which determine downstream flow routing based on the raw SRTM DEM. Finally, we compared the resulting outputs to high resolution SPOT imagery. In some cases we edited the stream lines to incorporate the increased sinuosity observed in this imagery. This increased sinuosity was incorporated because (1) increased sinuosity decreases streambed gradients and stream velocities due to increase in stream lengths; and (2) a longer intersection between the streambank and the adjacent shallow unconfined aquifer increases the length over which stream-aquifer flows interact.

Once the final stream network was developed using these three steps, elevation profiles for each stream were extracted from the raw SRTM DEM. In rare cases, localized pits or spikes from the raw DEM had to be adjusted to ensure that the entire channel flowed monotonically downstream. Where these situations were encountered, the new elevation of the pit or spike was calculated as the average of the next point upstream and the next point downstream on the river profile (see Figure A.11). The final stream network shown in Figure A.12 was used for the surface flow paths in the MIKE 11 surface flow model.

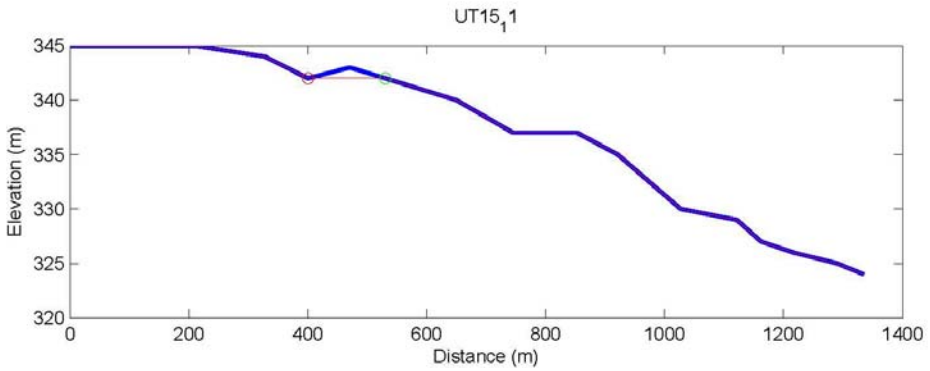

Figure A.11. Example of spike removal process for surface streams. Blue line is raw river elevation profile. Red line is corrected elevation profile. Note removal of spike at a distance of approximately 450 meters, between red and green circles.

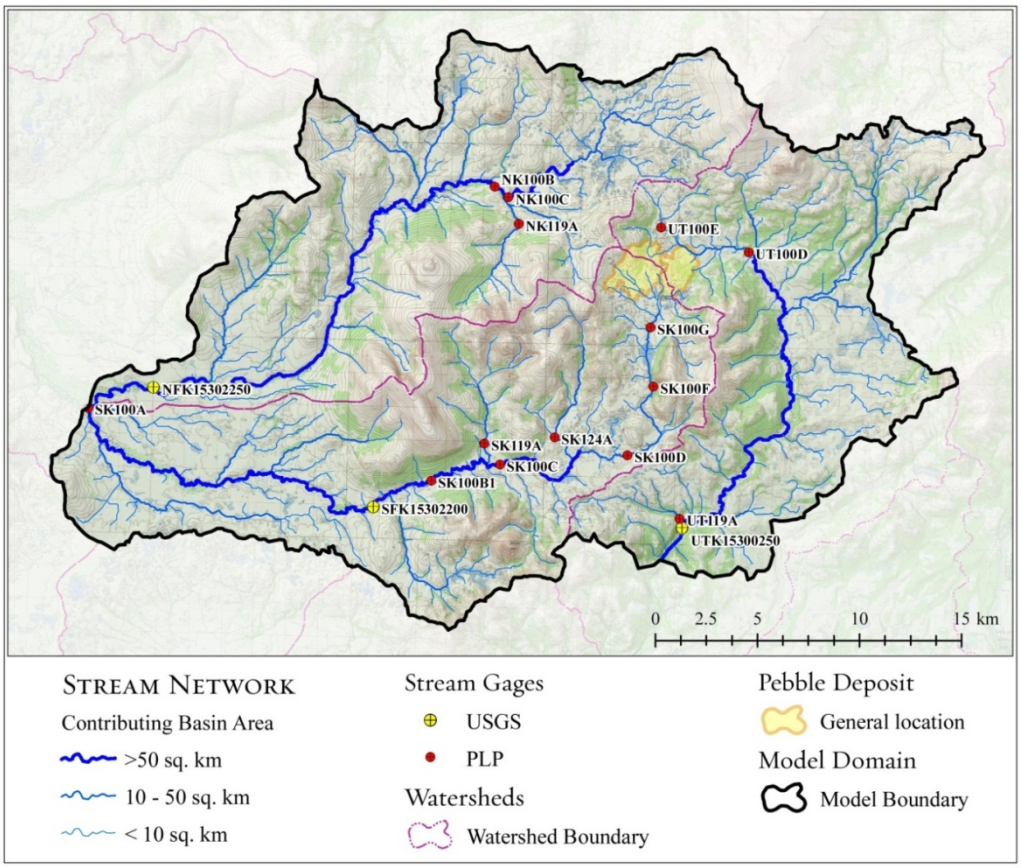

Figure A.12. Final stream network, generated using a combination of the National Hydrography Dataset, the SRTM DEM flow model, and SPOT satellite imagery. See main text for location map.

A.4 Model Development

A.4.1 Overview of MIKE SHE/MIKE 11 system

Graham and Butts (2005) summarize the use and capabilities of the MIKE SHE software (http://www.dhisoftware.com/upload/dhisoftwarearchive/papersanddocs/waterresources/MSHE_Book_Chapter/MIKE_SHE_Chp10_in_VPSinghDKFrevert.pdf). Key capabilities are shown on Figure A.13 and summarized here (Prucha et al., 2011):

- MIKE SHE/MIKE 11 is a physically-based, spatially-distributed, finite difference, hydrologic code that simulates fully coupled flows including surface flows (overland flow, channelized flow) and subsurface flows (saturated and unsaturated zone).
- MIKE 11 is a one-dimensional, fully-dynamic hydraulic and hydrology model for simulating river channel flows and water levels. Flows are calculated using a choice of fully dynamic Saint-Venant open channel flow equations, or simplifications (kinematic, diffusive, and dynamic).
- MIKE 11 is dynamically linked with the MIKE SHE portion of the code that simulates the remaining hydrologic processes.
- Overland flow is simulated using the 2-D Diffusive Wave finite difference approximation of the Saint Venant equations. DEMs can be used directly by the model to route overland flow.
- Using the Kristensen and Jensen method (Kristensen and Jensen, 1975) actual evapotranspiration (AET) is calculated based on soil evaporation and plant transpiration as a function of time-varying LAI and root depth.
- Saturated zone flow is simulated using a 3-dimensional Darcy equation and solved numerically by an iterative implicit finite difference technique.
- Unsaturated zone is simulated using a full 1-dimensional unsaturated zone flow using Richard's equation (Graham and Butts, 2005). Climate – precipitation, air temperature and RET are specified spatially and temporally at any time-step of interest.
- Snow accumulation and snowmelt are simulated using a modified degree-day model that allows wet/dry snow specification, elevation lapse rates and melting by shortwave radiation, convective air flow and advective heat from rain on snow.

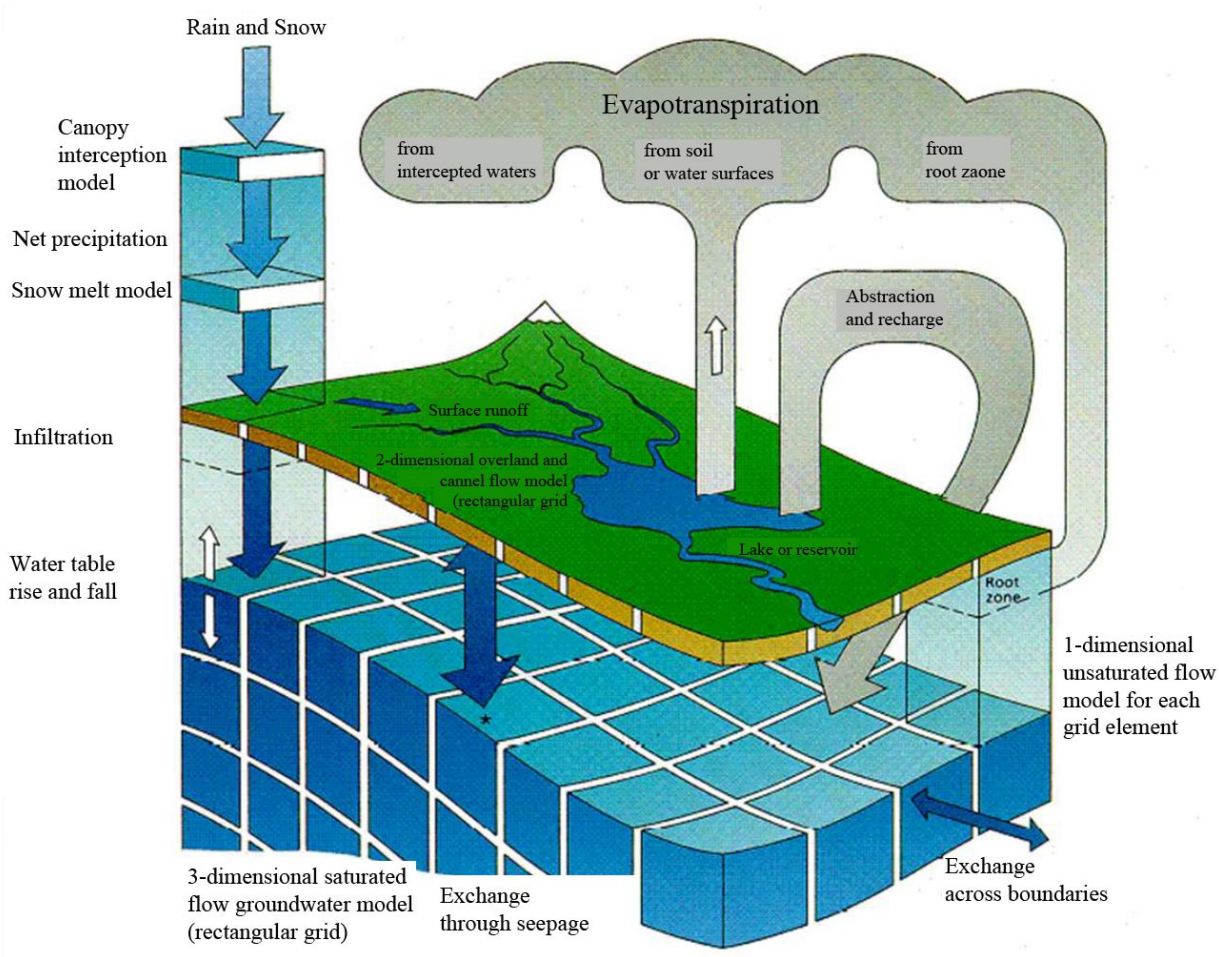

Figure A.13. MIKE SHE conceptual framework.

Source: Prucha et al., 2011.

A.4.2 Numerical model development

The numerical model was developed to simulate surface and groundwater flows through all natural media under baseline conditions, and to simulate changes in these flows under a large mine scenario. Unsaturated zone hydraulic parameters were specified for all natural soil types on site, as well as tailings and waste rock under a mine scenario (see main text). Saturated hydraulic conductivity values were specified for both unconsolidated materials and bedrock. This section describes the model grid and the values of hydraulic parameters used for each of these media.

Model domain and grid discretization

The model was developed on a 250 × 250 meter, regular grid (see Figure A.14). Model boundaries corresponded to surface drainage divides and were specified as no-flow boundaries. Details of the model domain and grid discretization are included in the main text.

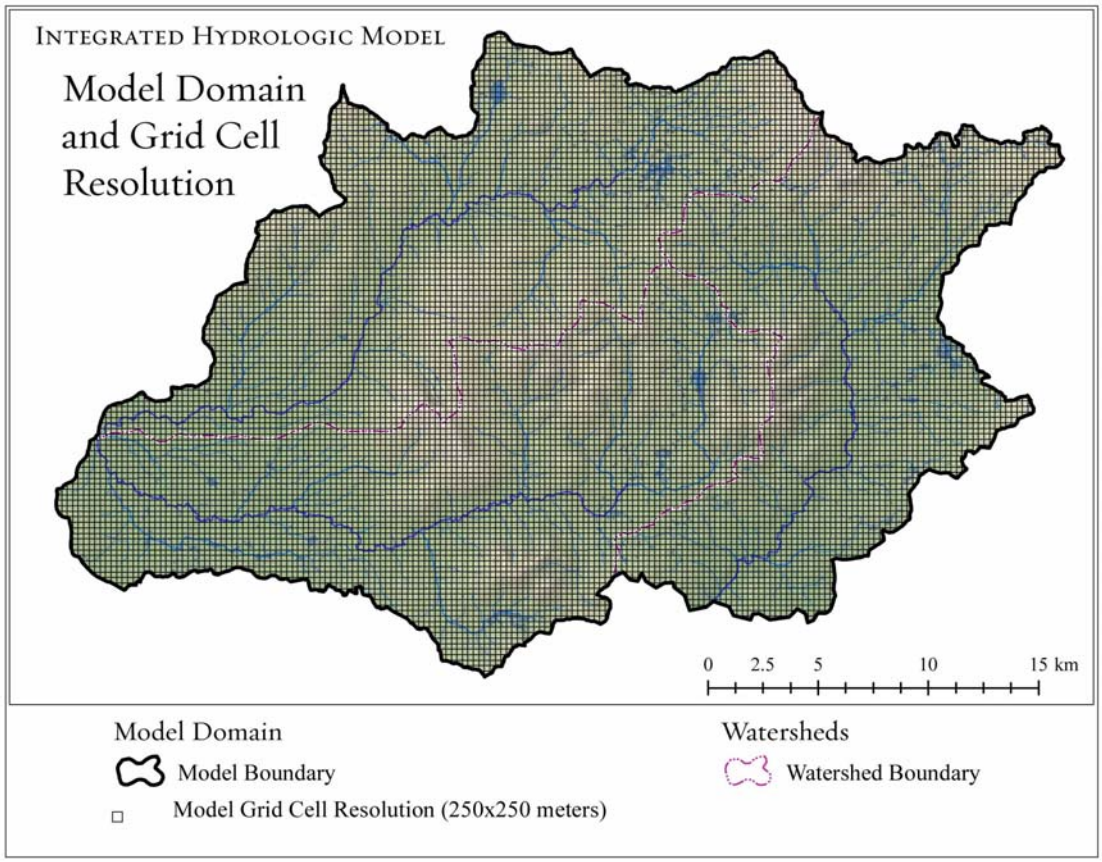

Figure A.14. The model domain was divided into a systematic grid with a cell-size of 250 m to simulate subsurface and overland flows.

Unsaturated zone flow

With the exception of unsaturated zone flow within the tailings storage facility (TSF), the vertical discretization of each soil column is the same throughout the model and starts with 2 cm high cells at the ground surface, grading to 1 m high cells below the water table. Within the TSF, cell height below the water table was increased to 4 m. Initial conditions are automatically specified in MIKE SHE as an equilibrium moisture distribution at field capacity.

Unsaturated zone hydraulic properties were specified based on soil type, as tabulated in Table A.2. Based on the coarse distribution of soil types specified in the STATSGO database, the majority of the naturally occurring soils on the site were assumed to have similar hydraulic properties, using values reported by Khaleel and Freeman (1995).

Table A.2. Unsaturated zone hydraulic parameters

Parameters	General soils	Lacustrine	TSF	Waste rock
Retention curve				
Saturated moisture content	0.2407	0.38	0.24	0.2839
Residual moisture content	0	0.1	0.01	0.0123
Field capacity moisture content	2	2	2	2
Wilting point moisture content	4.2	4.2	4.2	4.2
Van Genuchten (Alpha, 1/cm)	0.0455	0.027	0.067	0.0588
Van Genuchten (n)	1.2003	1.23	1.446	1.351
m	0.166875	0.186992	0.308437	0.259808
Hydraulic conductivity curve				
Saturated hydraulic conductivity (m/s)	1.50E-04	3.33E-07	2.00E-06	3.00E-05
Van Genuchten alpha (1/cm)	0.0455	0.027	0.067	0.0588
Van Genuchten n	1.2003	1.23	1.446	1.351
shape factor, l	0.5	0.5	0.5	0.5

Saturated zone flow

Three saturated hydraulic conductivity zones were defined for the unconsolidated Quaternary deposits (Figure A.15). As summarized in the main text, the highest hydraulic conductivities were assigned to the shallow overburden, as well as a zone of deeper overburden within the transition between the SFK and UT (Table A.3). Hydraulic conductivity was lower within other deeper overburden and weathered bedrock, and lowest in the competent bedrock. Anisotropy ratios (K_x/K_z) also varied between units, as summarized in Table A.2. Initial values were selected based on observed data from slug tests and pump tests reported by PLP (PLP, 2011d), and then adjusted to the above values during calibration against available streamflows and groundwater depths. Specific yields and storage coefficients are 0.1 and 0.00328, respectively for all unconsolidated deposits, and 0.1 and 3.28e-6 for the competent bedrock, based on values used by PLP in their numerical groundwater model (Schlumberger Water Services, 2011).

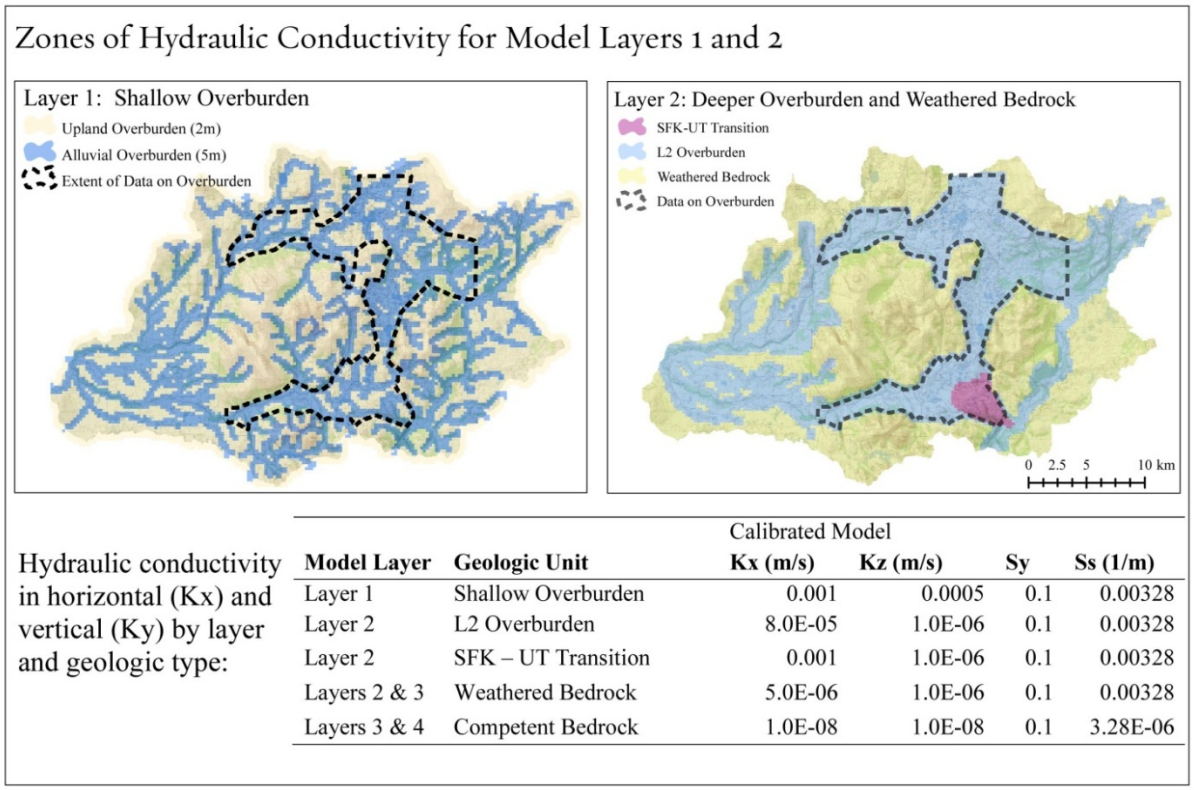

Hydraulic conductivity in horizontal (Kx) and vertical (Ky) by layer and geologic type:

		Calibrated Model			
Model Layer	**Geologic Unit**	**Kx (m/s)**	**Kz (m/s)**	**Sy**	**Ss (1/m)**
Layer 1	Shallow Overburden	0.001	0.0005	0.1	0.00328
Layer 2	L2 Overburden	8.0E-05	1.0E-06	0.1	0.00328
Layer 2	SFK – UT Transition	0.001	1.0E-06	0.1	0.00328
Layers 2 & 3	Weathered Bedrock	5.0E-06	1.0E-06	0.1	0.00328
Layers 3 & 4	Competent Bedrock	1.0E-08	1.0E-08	0.1	3.28E-06

Figure A.15. Hydraulic conductivity zones used in the MIKE SHE model. See main text for description.

Table A.3. Model layers, geologic composition and calibrated rates of conductivity in horizontal (Kx) and vertical (Kz) in the final calibrated model

		Calibrated model			
Model layer	**Geologic unit**	**Kx (m/s)**	**Kz (m/s)**	**Sy**	**Ss (1/m)**
Layer 1	Shallow overburden	0.001	0.0005	0.1	0.00328
Layer 2	L2 overburden	8.0E-05	1.0E-06	0.1	0.00328
Layer 2	SFK–UT transition	0.001	1.0E-06	0.1	0.00328
Layers 2 and 3	Weathered bedrock	5.0E-06	1.0E-06	0.1	0.00328
Layers 3 and 4	Competent bedrock	1.0E-08	1.0E-08	0.1	3.28E-06

Initial conditions were determined by running the integrated model with an initial groundwater surface equal to a depth of 10 m below ground surface. After cycling the model through a few years, relatively steady groundwater surfaces were simulated and used as the initial conditions for the actual calibration simulations. Applying the 25-year climate series available in the NARR data, we used the last 5 years (model years 21–25) for estimation of hydrologic and water quality alteration under the preliminary mine design.

Overland flow

The rate of runoff over land is controlled by slope and surface resistance. A single surface resistance value (Manning's n) of 10 was specified for the entire study area based on dense shrub cover in both uplands and floodplains (Chow, 1959). Because overland flow is rare in this system, the overall hydrologic response is not very sensitive to this parameter. As a result, it was not considered a calibration parameter and not varied during the simulations. Another parameter affecting overland flow is a threshold value controlling the amount of surface depression storage. In the model, this was set through model calibration to be a depth of 10 mm. Once ponding depths exceed this depth, overland flow can occur. The parameter accounts for small variations in the surface topography typical in catchments. This value was determined through initial calibration simulations.

Boundary and initial conditions also need to be specified in the model for overland flow. Because overland flow is a rapid process relative to subsurface flows, initial depths of overland water were set at 0 mm. Boundary conditions assumed that no overland flow occurs along any of portion of the study area boundary.

Open channel flow

Streamflow was simulated in a total of 203 streams within the study area (Figure A.11). These streams extend a total of 533.5 km (320 miles). Development of the stream network and longitudinal profiles is described above. Once streambed profiles were constructed for all streams, cross-sections along each stream were developed. The MIKE 11 code requires cross sections at the beginning and end of each segment, and one additional section every 0.5 to 2.0 km along the stream length. Our main objective in stream cross-section shape was to ensure that the cross section was wide and deep enough to convey all flow coming from upstream; calculation of flow stage and stream velocity was beyond the scope of this study. To meet this primary objective, we developed generic 5-point, compound "V" shaped stream profiles for all locations: in each cross section, the lower part of the profile had steeper side slopes, and the upper part of the profile had more gentle side slopes. The total width of all stream cross sections was 250 meters, sufficient to convey even the highest flows.

Flows were simulated using the fully hydrodynamic option in MIKE 11 (i.e., using St. Venant equations) so that backwater effects and flows in steeper slopes could be modeled. An option to use automatic time-steps was also specified. This feature helps optimize the numerical time-step required to solve the set of surface flow equations. When precipitation events occur and rapid changes in streamflow occur, the code automatically decreases the time-step to account for the shorter-term dynamics.

Precipitation and air temperature

Precipitation and air temperature obtained from the NARR dataset were input into the model from January 1, 1980 to December 31, 2009 every 3-hours. Due to the relatively subdued elevations within the model domain, we did not apply temperature or precipitation lapse rates over the model.

Snowmelt

Snowmelt parameters were based on a similar application of a MIKE SHE integrated hydrologic model in the nearby Chuitna watershed (Prucha et al., 2011), and are summarized in Table A.4. In a degree-day snowmelt model, air temperatures are used in combination with a specified threshold melting temperature and a degree-day melting coefficient to calculate snowmelt, or conversion of dry snow to wet snow. Typically, threshold melting temperatures use 0°C. Snowmelt simulations were conducted at locations with snowpack measurements to estimate the degree day coefficient. The melting coefficient for the thermal energy of rain and the factor for reducing sublimation of dry snow were also both adjusted during calibration of the Chuitna model, but snowmelt is not as sensitive to these. As dry snow melts, liquid water infiltrates down to the ground surface and is subject to loss to evapotranspiration as a surface water body. The snow's ability to store water is subject to a wet snow storage factor, which when exceeded, allows water to be treated as ponded water in the model. As ponded water, the snowmelt can either infiltrate the soils or run off, depending on soil hydraulic properties and moisture conditions. This factor is calculated as the ratio of wet storage snow water equivalent (SWE) to the sum of wet and dry storage and was adjusted to 0.6 during calibration in the Chuitna model (Prucha et al., 2011). This factor was used to adjust the rate of melting during spring melt.

A minimum snow storage is also specified that allows the model to melt snow at a reduced rate where only partial areal snow coverage exists, for example beneath trees. Melting, or freezing rates are multiplied by the ratio of the minimum snow storage to the combined dry and wet storage. The value of 0.6 specified in the model was derived through calibration.

Table A.4. Summary of model climate input parameters (basecase)

Precipitation	
Temporal frequency	Every 3 hours
Lapse rate (change with elevation)	NA
Air temperature	
Temporal frequency	Every 3 hours
Wet lapse rate	NA
Dry lapse rate	NA
RET	
Temporal frequency	Every 3 hours
Snow melt	
Degree-day coefficient	1 mm/°C/day
Threshold melting temperature	0°C
Melting coefficient for thermal energy of rain	0.15 (1/°C)
Factor reducing sublimation rate from dry snow	0.5
Maximum wet snow storage fraction	0.6
Minimum snow storage for full coverage	100 mm
Initial total snow storage	0 mm (summer start)
Initial wet snow fraction	0 mm (summer start)

A.5 Model Calibration

Primary sources of data for calibration of the integrated hydrologic model included streamflow observations at stream gages maintained by USGS (n = 3) and PLP (n = 14) (PLP, 2011b), and groundwater elevations reported by PLP (PLP, 2011d). Site data were available only for the period of 2004–2008; thus all evaluations of model calibration were based on this time period.

A.5.1 Surface flow

Complete years of record are available for most gages for calendar years 2005–2006. Visual comparison of the predictions of the calibrated model with observed streamflow for this period indicate that the model is adequately reflecting the dominant characteristics of the annual hydrologic cycle within UT (Figure A.16), SFK (Figure A.17) and NFK (Figure A.18). Correlation of daily streamflow over the entire period of available data was highest for NK100A (USGS gage 15302250) (r = 0.77), followed by UT100E (r = 0.75), SK100B (USGS 15302200) (r = 0.70), NK119A (r = 0.68), UT100B (USGS 15300250) (r = 0.66), and SK100G (r = 0.59).

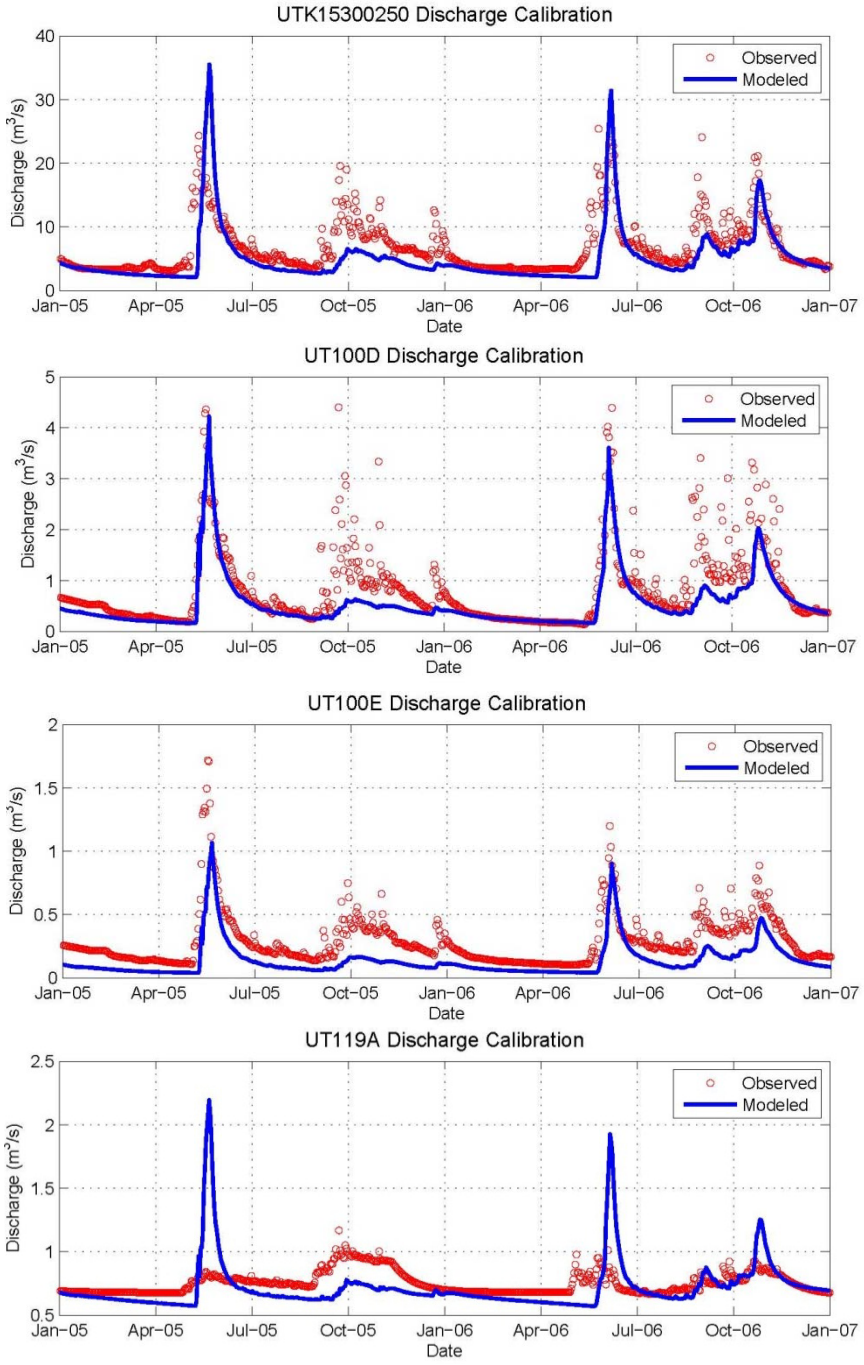

Figure A.16. Comparison of observed and predicted streamflow at UT gage stations.

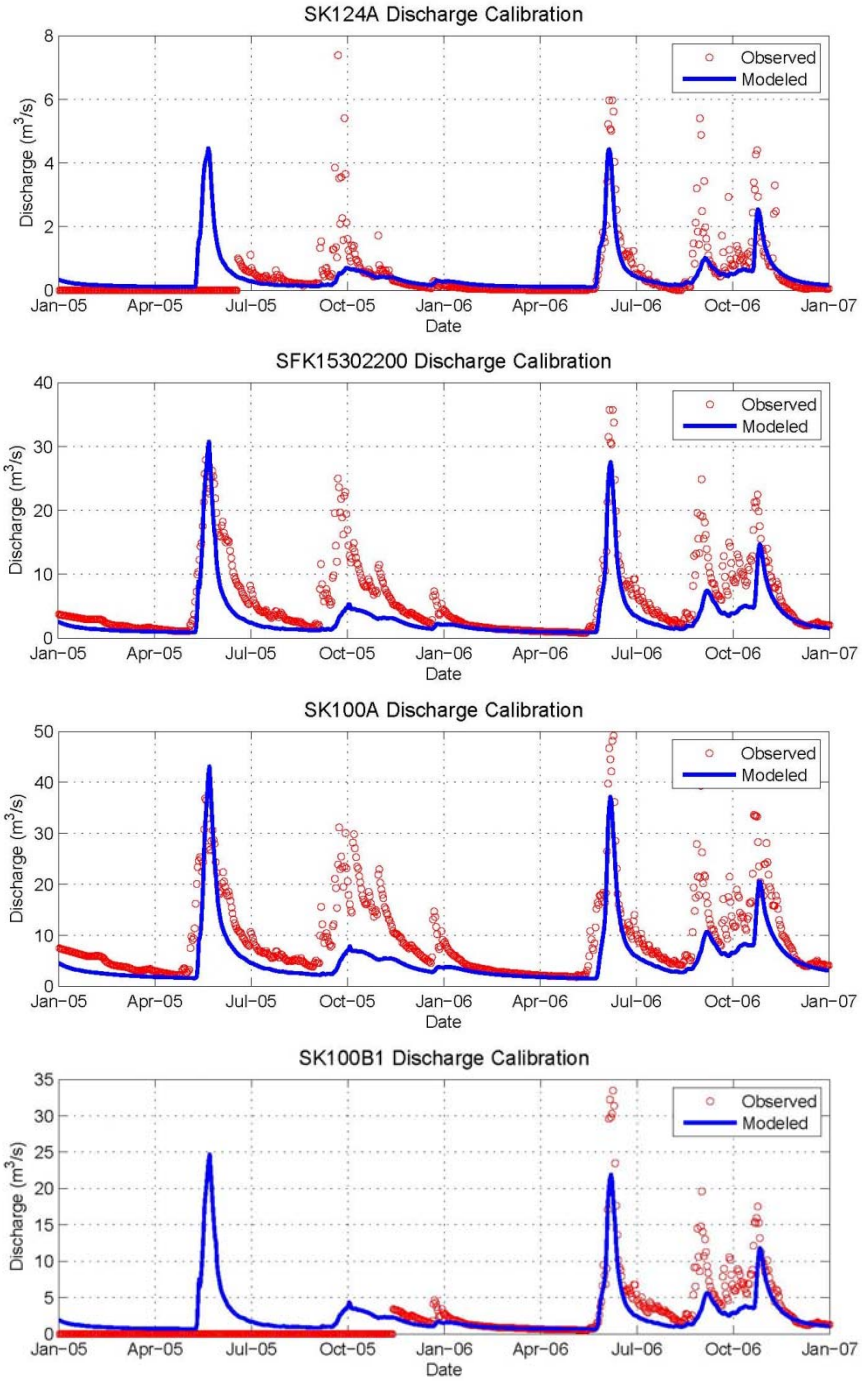

Figure A.17. Comparison of observed and predicted streamflow at SFK gage stations for calendar years 2005 and 2006. Dates with zeros for observed flows in SK124A and SK100B1 reflect days without observational data

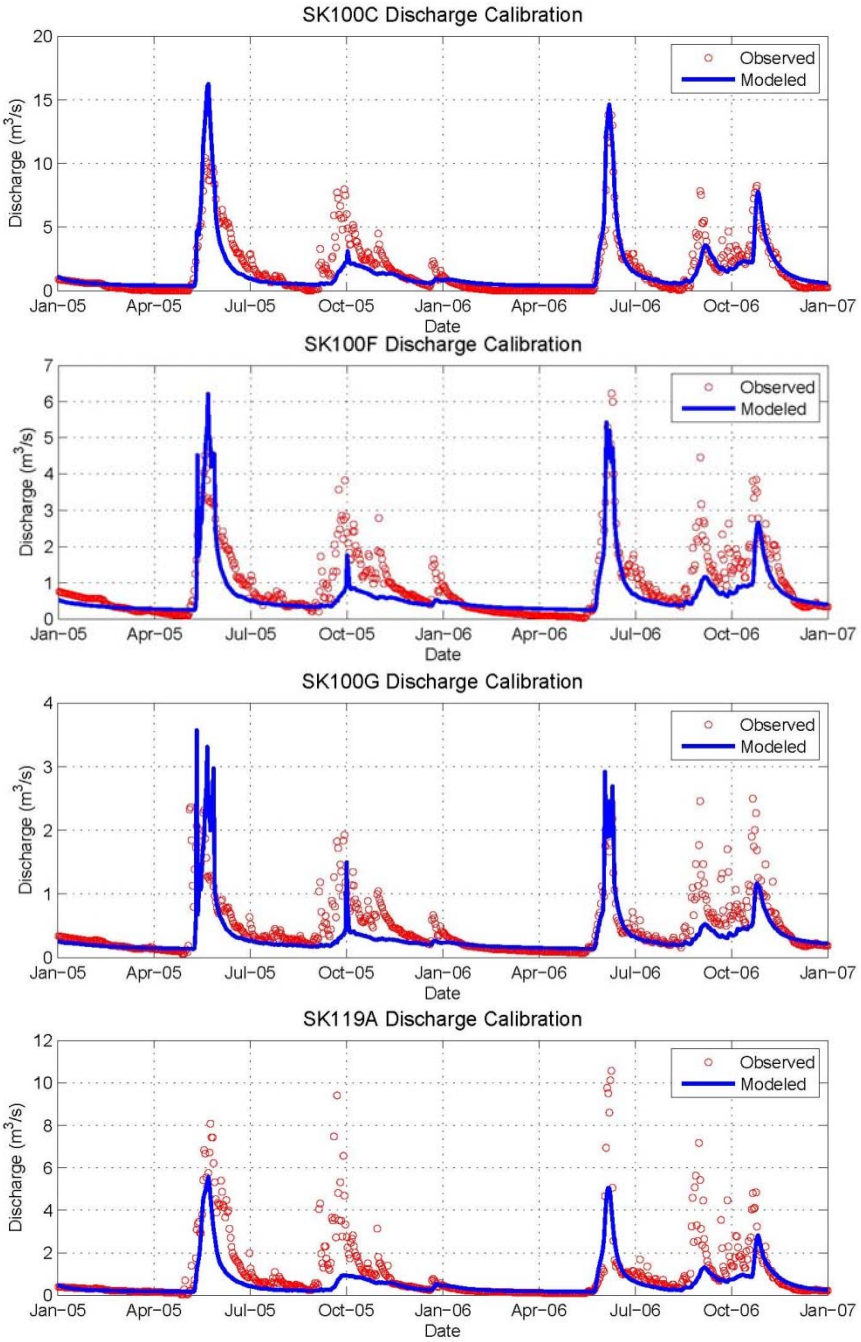

Figure A.17. Comparison of observed and predicted streamflow at SFK gage stations for calendar years 2005 and 2006 (cont.).

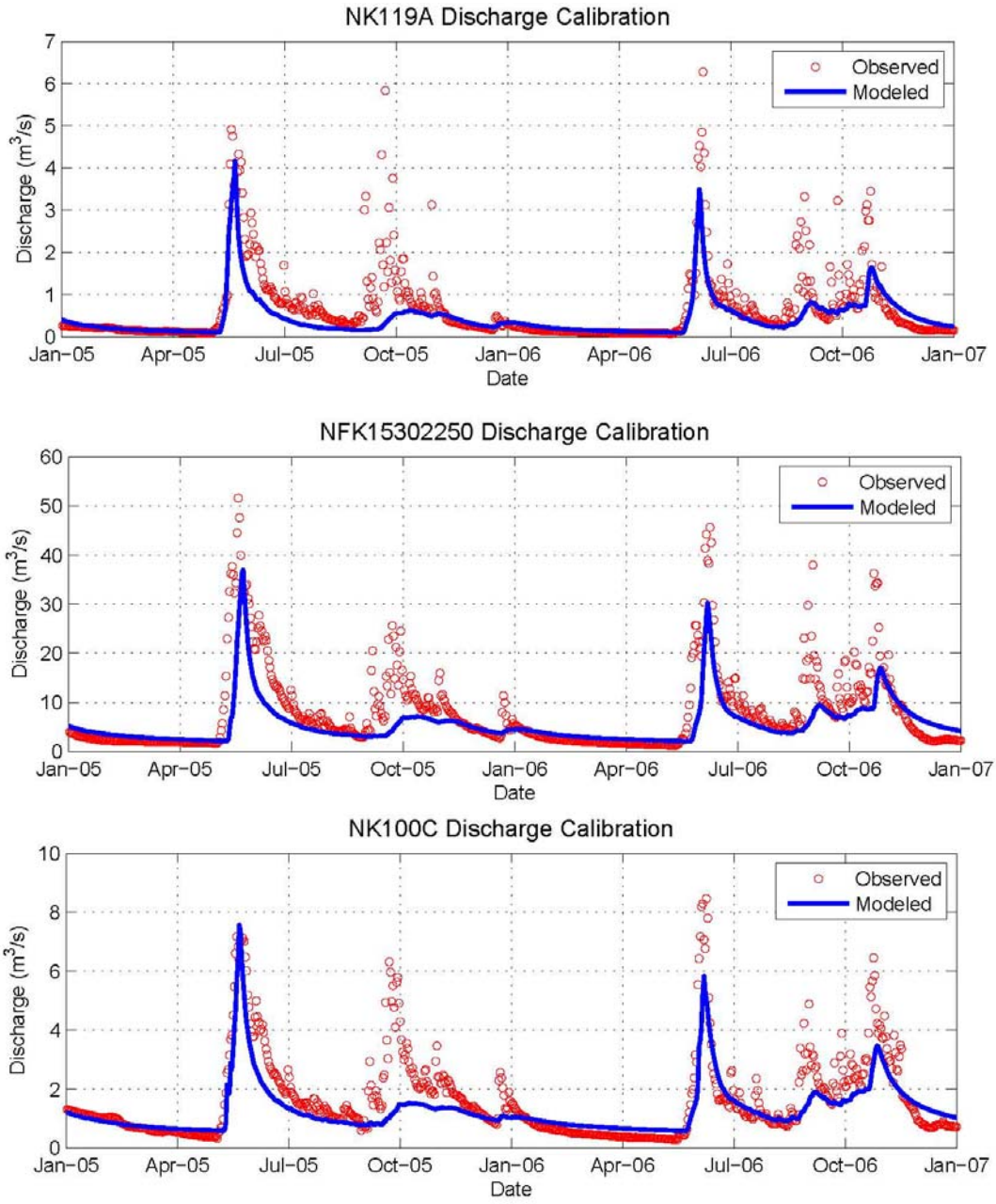

Figure A.18. Comparison of observed and predicted streamflow at NFK gage stations for calendar years 2005 and 2006.

Upper Talarik Creek

For gages UT100D and UTK15300250, baseflow (~ 0.1 m^3/sec and 4.0 m^3/sec, respectively) was represented most closely at UT100D, along with relatively close approximation of the annual recession curve of declining flows through late winter. The model was very accurate for UT100D in representation of snowmelt-driven peak flows in May 2005 and 2006 (~ 4.25 m^3/sec) as well as the much lower peak flow observed during late May 2007. The model was less accurate in representing rain-driven peak flows observed during Autumn in all years. This result was observed for all gage stations, with the possible exception of the groundwater-driven system in UT119A, which leads us to believe it is a function of the NARR precipitation inputs, rather than a result of calibration of the hydrologic model itself. As described in the main text, the NARR climatology data may be underestimating localized fall rainstorms, which is most likely the reason for this discrepancy between modeled and observed fall streamflows.

Baseflows observed at UT119A (~ 0.7 m^3/sec) were considerably higher than would be expected based on the contributing basin area of surface drainage alone, and supports the findings of earlier studies that this system is influenced by groundwater. To match observed baseflows in the calibrated model, we defined a zone of higher conductivity in the transition between SFK and UT (Figure A.15) in Layer 2 of the deeper overburden (see text).

North Fork Koktuli

Calibration results in the NFK illustrated similar patterns to those in UT, in that the timing and magnitude of snow-melt driven flow events in May predicted by the model were comparable to that of observed flow conditions (Figure A.16), but Autumn rain-driven flow events were less closely correlated. Recession curves and baseflows were most accurate for NK119A which is a relatively small, shallow headwater system. For both NK100C and NFK15302250 the peaks were somewhat underestimated and the baseflows were somewhat overestimated. Data were not available from gage NFK15302250 after June 2007, or from NK100C and NK119A after November 2007.

South Fork Koktuli

Annual patterns of flow in the SFK system were generally well correlated with observed flow. As noted throughout, underestimation of flow by the calibrated model during Autumn is relatively consistent across all gages, suggesting that this result reflects underlying precipitation inputs in the NARR data series. Peak flows following snow-melt are well approximated by the model in all cases.

Predicted base flows matched observed conditions generally well for SK100A, SK100B1, SK119A and SK100G. Predicted base flows matched observed conditions generally well for SK100A, SK100B1, SK119A and SK100G. In contrast, observed base flows for SK100C and SK100F were substantially lower than predicted, and in some cases appear to lose surface flow

altogether during late winter low-flow periods. These gages are located in the high-permeability zone near the SFK–UT transition. This result likely reflects uncertainty in the model with regard to the precise geometry and hydraulic conductivity of this high permeability zone.

A.5.2 Groundwater elevations

We compared groundwater depths predicted by the integrated model with available data published by PLP (PLP, 2011d). As illustrated in the main report, predicted groundwater elevations were relatively well correlated with observations and residuals did not appear to exhibit a systematic bias toward over or under estimation. Although groundwater elevations were not a primary calibration target for the model and these calibration results do not break out wells by aquifer, results of the groundwater calibration are reasonable, and well within the limits of +/- 10% of the mean absolute error across the entire study area. This is a standard typically applied to assess model performance (Hill, 1998).

A.5.3 Flow reduction results

Flow alterations created by the mine were calculated for gages NK100A (USGS 15302250), NK100C, and NK119A in the NFK (Figure A.19); gages SK100A, SK100B1, Sk100C, SK100F, SK100G, Sk119A, and SK124A in the SFK (Figure A.20); and gages UT100D, UT100E, UT119A and UT 100B (USGS 15300250) in the UT (Figure A.21). Plots showing all of these modeled flow changes are included below.

A.5.4 Transport simulation results: No mitigation

Copper transport simulations were conducted for the "no mitigation" scenario in gages SK100A, SK100C, SK100F, and SK100G in the SFK (Figure A.22), and gages UT100B, UT100C, UT100D, and UT119A in the UT (Figure A.23). Results from these transport simulations are included below.

A.5.5 Transport simulation results: 6-month mitigation failure

Copper transport simulations were conducted for both 1-month and 6-month mitigation system failures. Because the first month of the 6-month mitigation failure scenario was essentially identical to the full 1-month mitigation failure, we include only the 6-month failure results here. 6-month mitigation failure scenarios are shown for gages SK100B, Sk100B1, Sk100C, Sk100F, Sk100G in the SFK (Figure A.24), and gages UT100B, and UT100D in the UT (Figure A.25). In all cases, the simulated mitigation system failure occurs on February 1 of Mine Year 20, and the system is restored on August 1 of Mine Year 20.

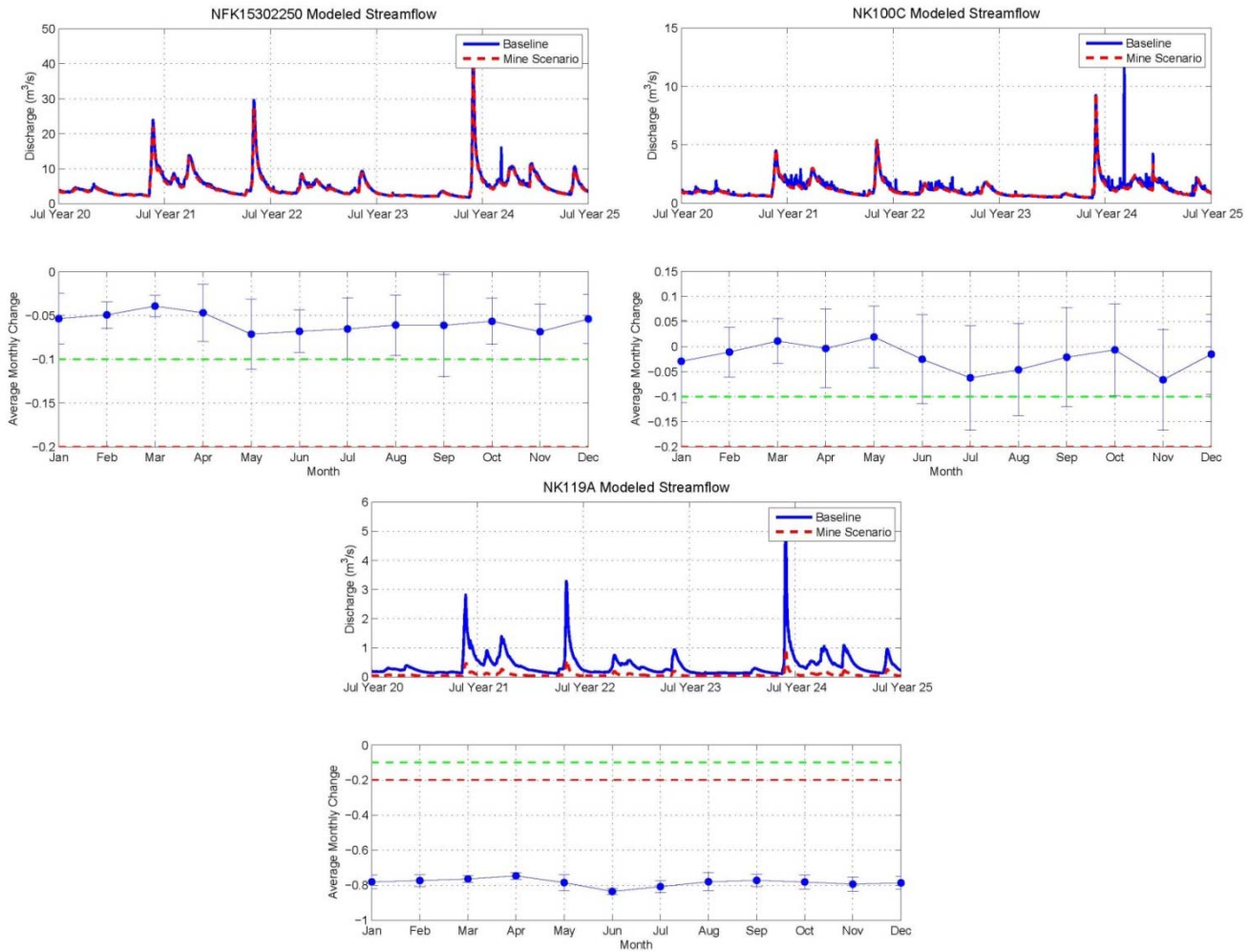

Figure A.19. Modeled flow reductions from a large mine scenario for NFK gage stations. In all figures, the upper plot shows the baseline and mine impacted hydrographs, while the lower plot shows the average flow change by month over the last 5 years of the model run (+ /- 1 SD). Green and red dashed lines in the lower plots illustrate 10% and 20% flow reductions, respectively, for reference.

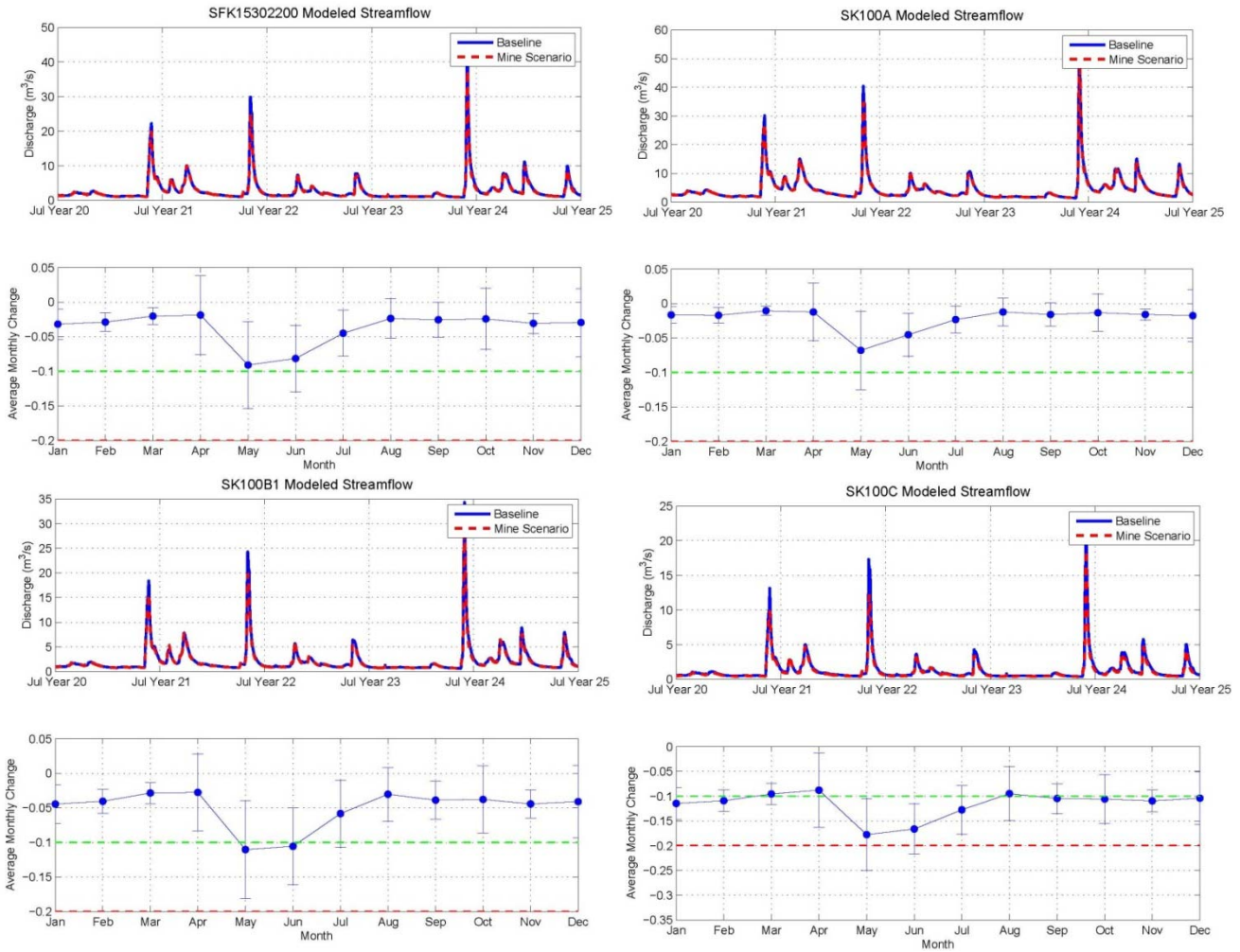

Figure A.20. Modeled flow reductions from a large mine scenario for SFK gage stations. In all figures, the upper plot shows the baseline and mine impacted hydrographs, while the lower plot shows the average flow change by month over the last 5 years of the model run (+ /- 1 SD). Green and red dashed lines in the lower plots illustrate 10% and 20% flow reductions, respectively, for reference.

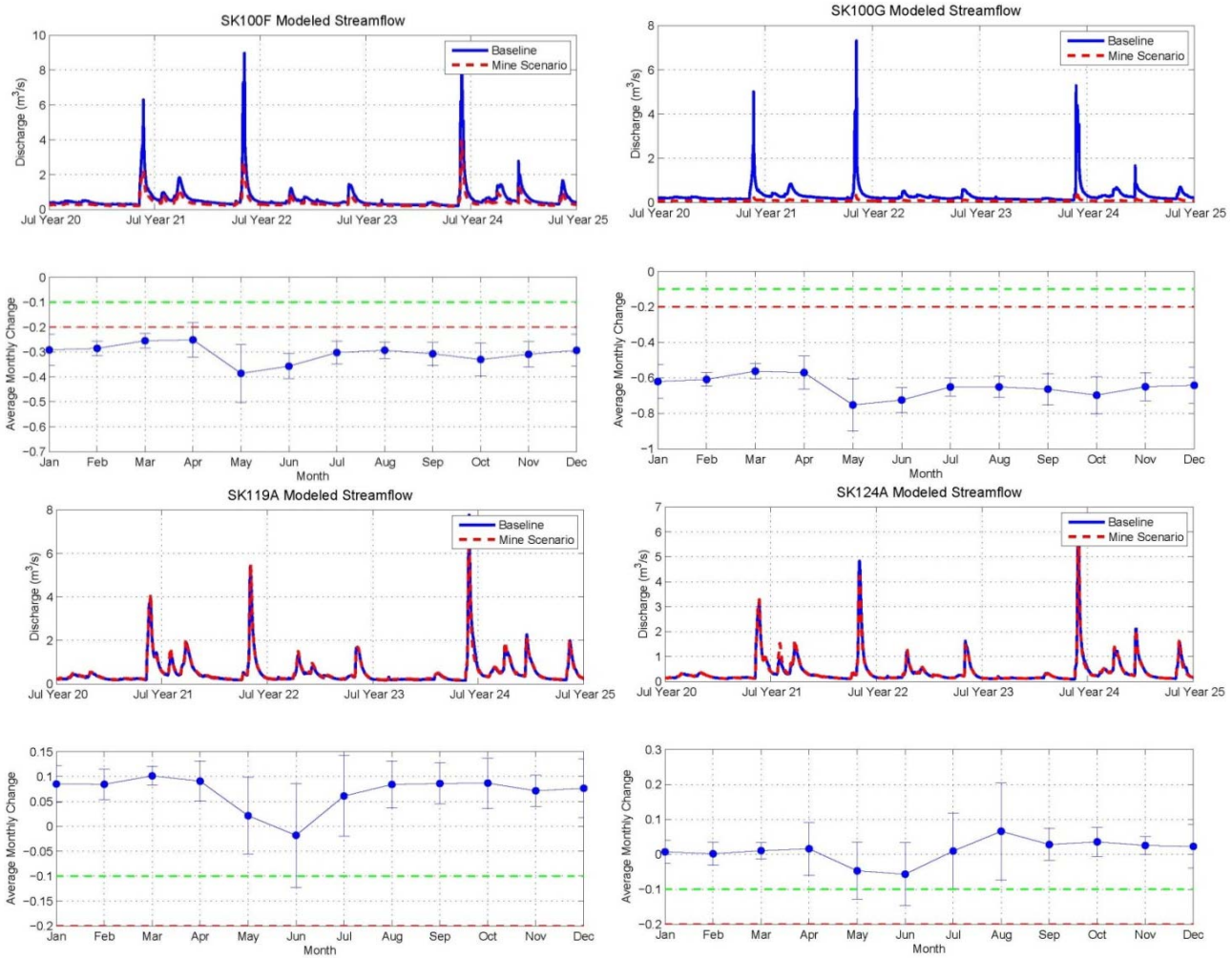

Figure A.20. Modeled flow reductions from a large mine scenario for SFK gage stations (cont.). In all figures, the upper plot shows the baseline and mine impacted hydrographs, while the lower plot shows the average flow change by month over the last 5 years of the model run (+ /- 1 SD). Green and red dashed lines in the lower plots illustrate 10% and 20% flow reductions, respectively, for reference.

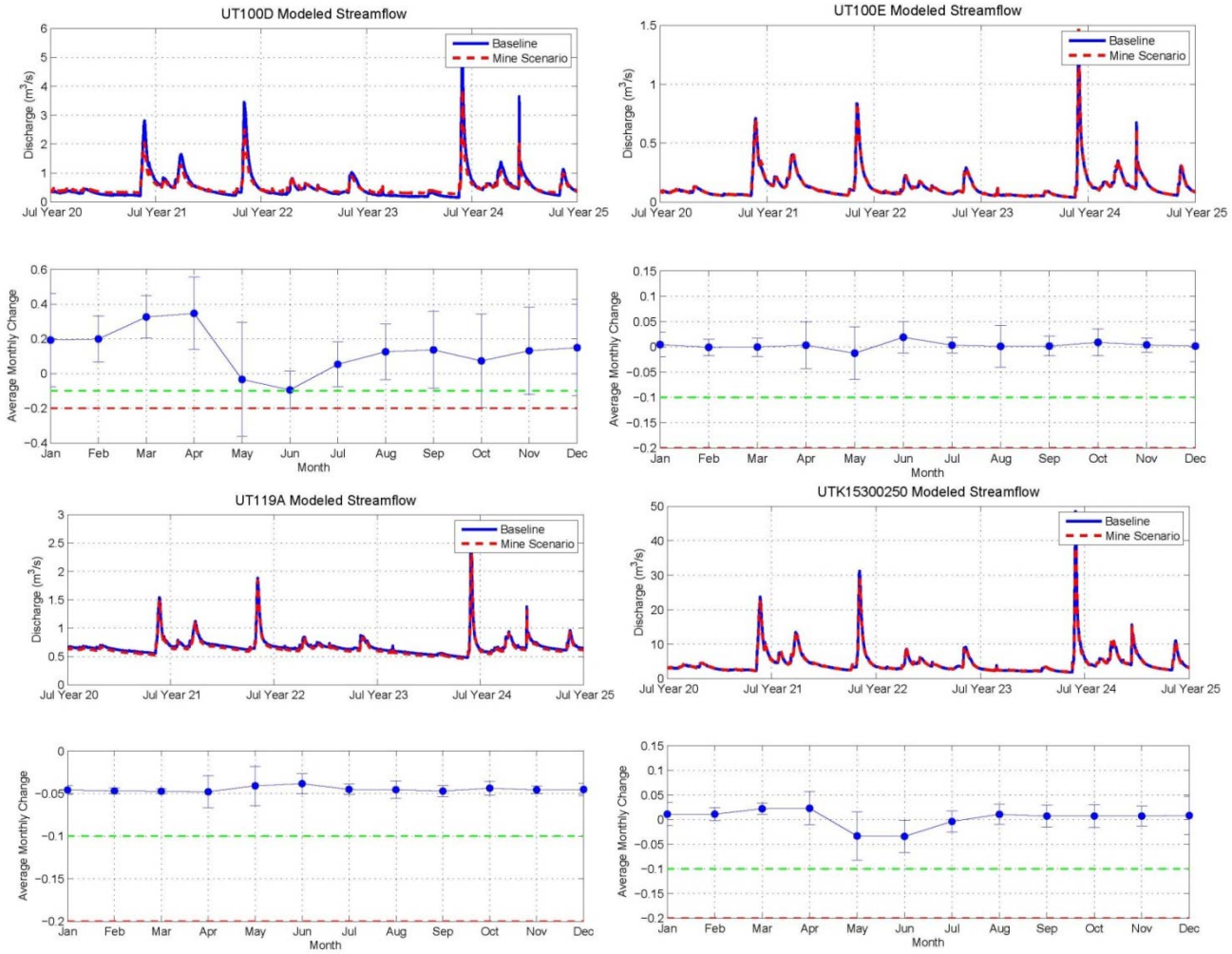

Figure A.21. Modeled flow reductions from a large mine scenario for UT gage stations. In all figures, the upper plot shows the baseline and mine impacted hydrographs, while the lower plot shows the average flow change by month over the last 5 years of the model run (+ /- 1 SD). Green and red dashed lines in the lower plots illustrate 10% and 20% flow reductions, respectively, for reference.

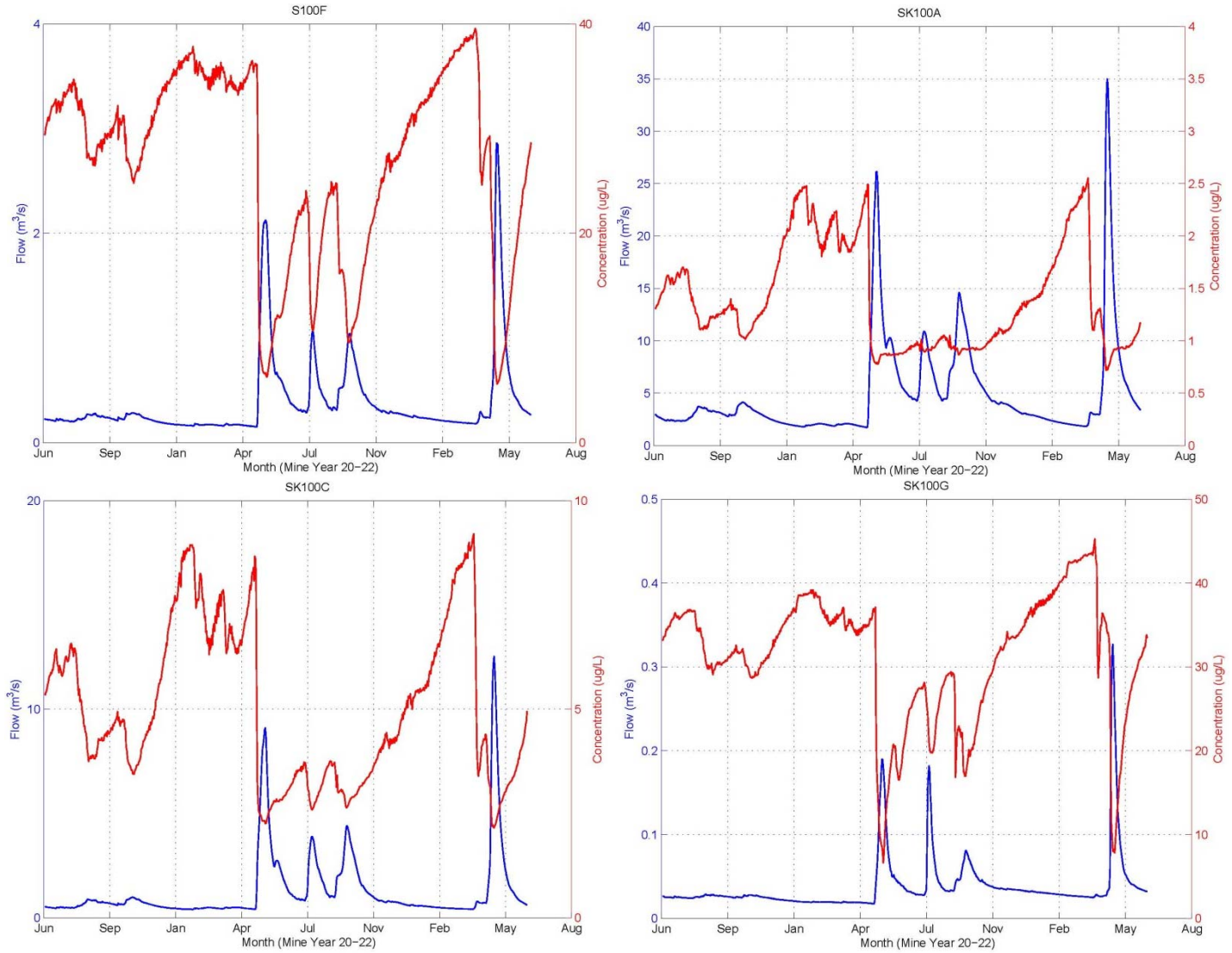

Figure A.22. Modeled copper concentrations and flows in SFK gage stations under "no mitigation" scenario.

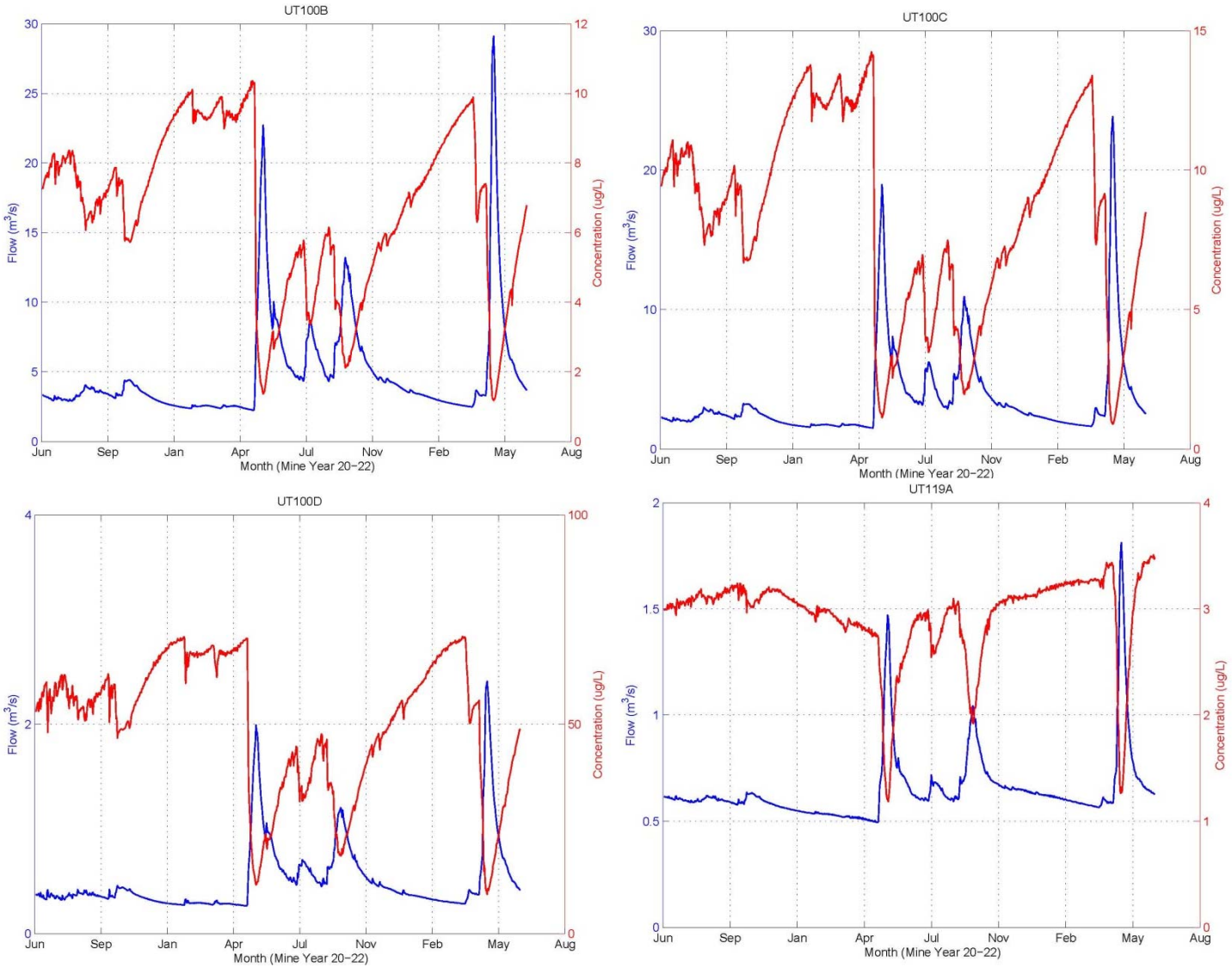

Figure A.23. Modeled copper concentrations and flows in UT gage stations under "no mitigation" scenario.

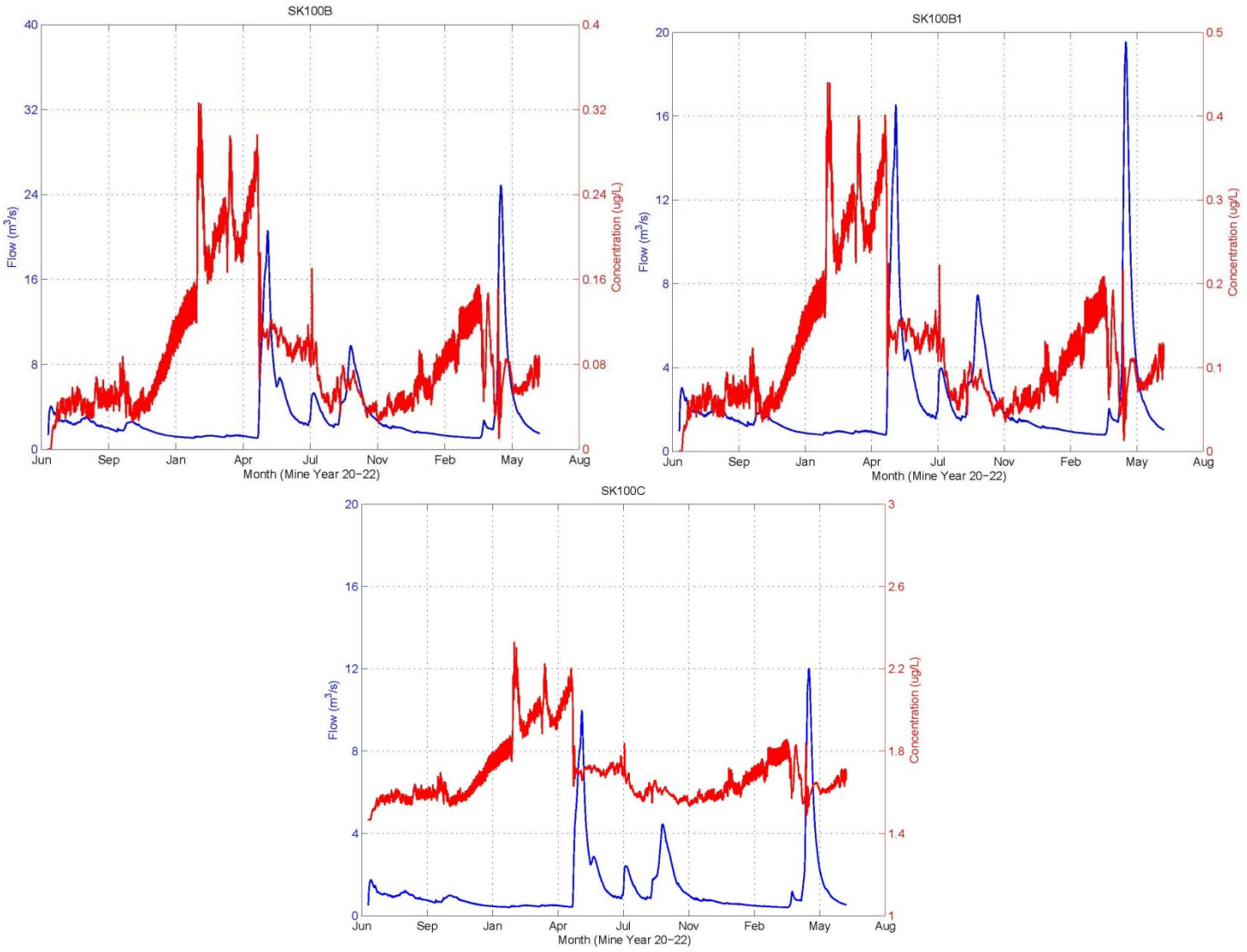

Figure A.24. Modeled copper concentrations and flows in SFK gage stations under 6-month mitigation failure scenario.

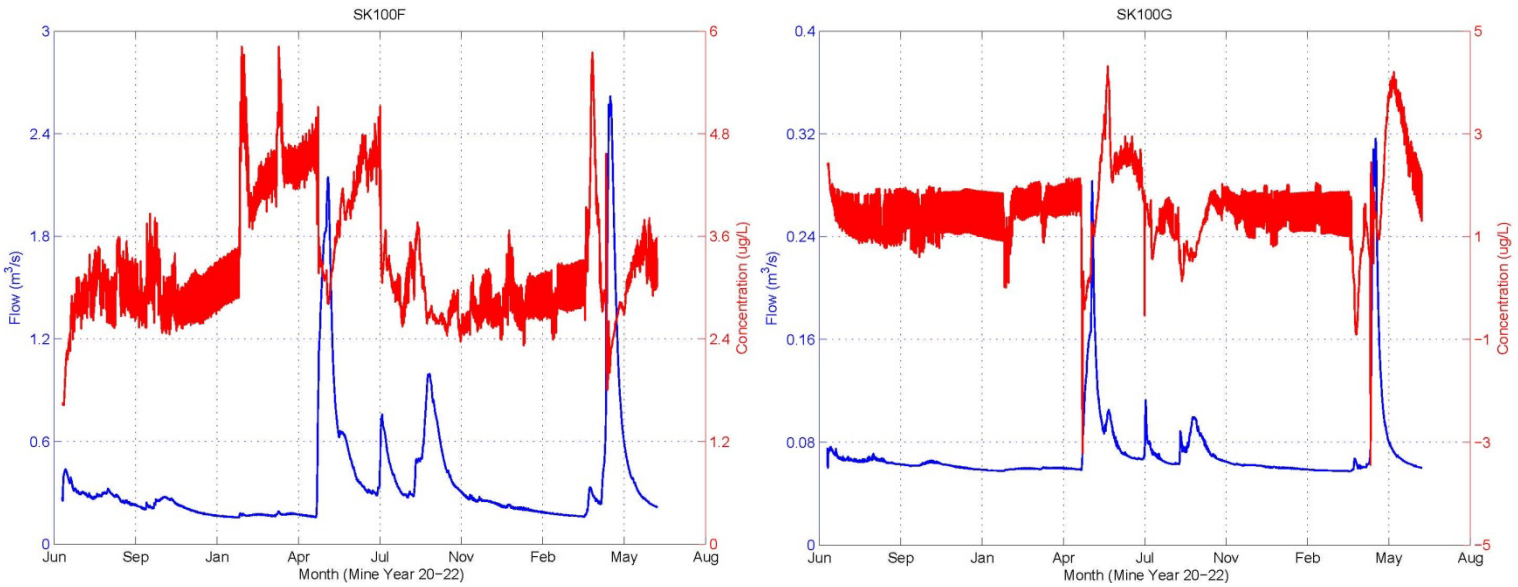

Figure A.24. Modeled copper concentrations and flows in SFK gage stations under 6-month mitigation failure scenario (cont.).

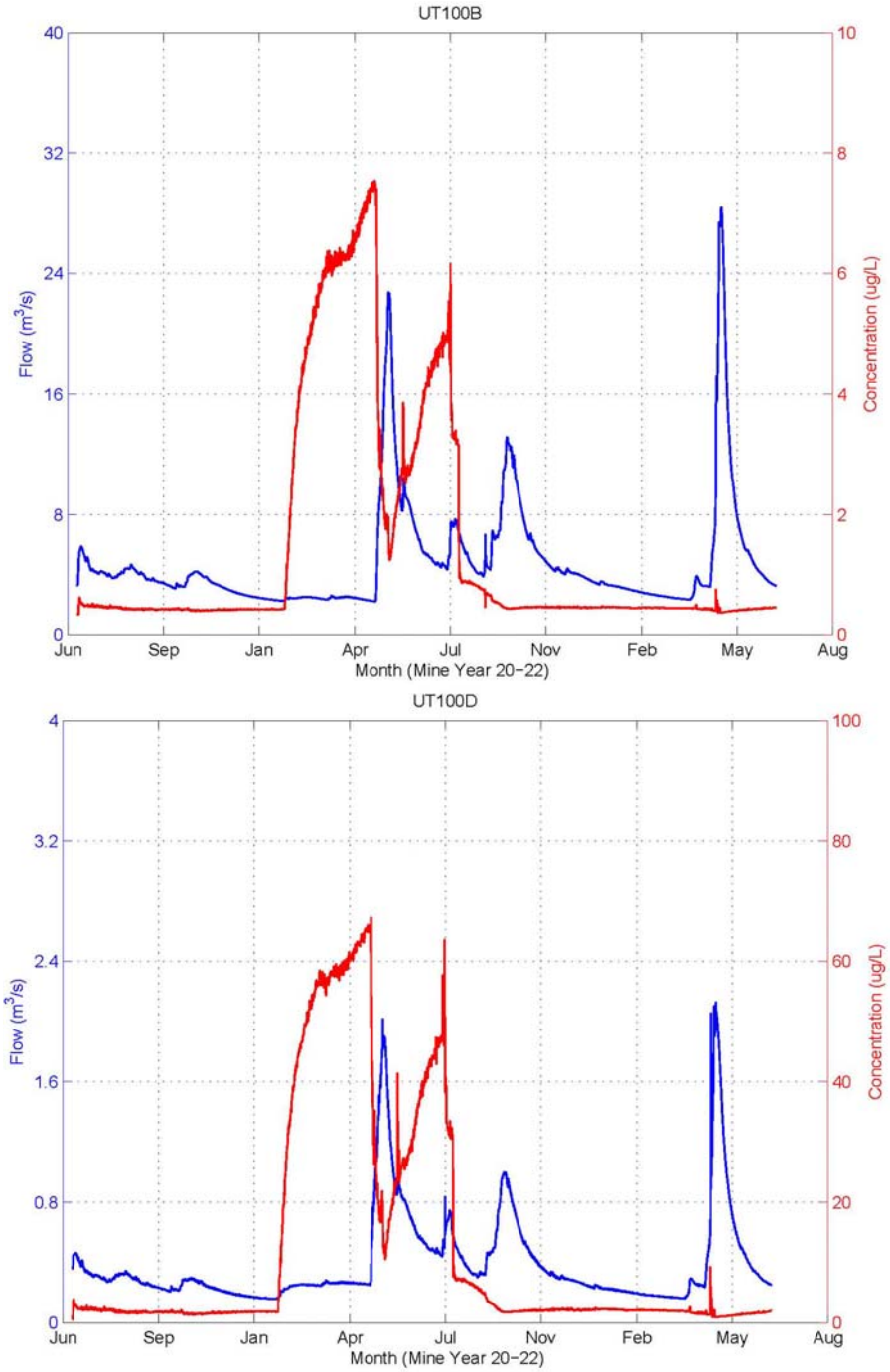

Figure A.25. Modeled copper concentrations and flows in UT gage stations under 6-month mitigation failure scenario.

References

Allen, R.G. 2011. Reference Evapotranspiration Calculator Version – Windows 3.1. July 2008, rev. July 2011. University of Idaho Research and Extension Center, Kimberly, ID.

Asner, G.P., J.M. Scurlock, and J.A. Hicke. 2003. Global synthesis of leaf area index observations: Implications for ecological and remote sensing studies. *Global Ecology and Biogeography* 12:191–205.

Chow, V.T. 1959. *Open Channel Hydraulics.* McGraw-Hill, New York, NY.

Daly, C., R.P. Neilson, and D.L. Phillips. 1994. A statistical-topographic model for mapping climatological precipitation over mountainous terrain. *Journal of Applied Meteorology* 33:140–158.

Fang, H., S. Liang, T.R. Townshend, and R.E. Dickinson. 2008. Spatially and temporally continuous LAI data sets based on an integrated filtering method: Examples from North America. *Remote Sensing of Environment* 112:75–93.

Ghaffari, H., R.S. Morrison, M.A. Deruijeter, A. Živković, T. Hantelmann, D. Ramsey, and S. Cowie. 2011. Preliminary Assessment of the Pebble Project, Southwest Alaska. Prepared for Northern Dynasty Minerals Ltd. by Wardrop (A Tetra Tech Company), Vancouver, BC. February 15.

Graham, D.N. and M.B. Butts. 2005. Flexible, integrated watershed modelling with MIKE SHE. In *Watershed Models*, V.P. Singh and D.K. Frevert (eds.). CRC Press. ISBN: 0849336090. pp. 245–272.

Hill, M.C. 1998. Methods and Guidelines for Effective Model Calibration. U.S. Geological Survey Water Resources Investigations Report 98-4005.

Homer, C., C. Huang, L. Yang, B. Wylie, and M. Coan. 2004. Development of a 2001 national land cover database for the United States. *Photogrammetric Engineering and Remote Sensing* 70(7):829–840.

Khaleel, R. and E.J. Freeman. 1995. Variability and Scaling of Hydraulic Properties for 200 Area Soils, Hanford Site. WHC-EP-0883. Prepared for the U.S. Department of Energy by Westinghouse Hanford Company, Richland, WA. October.

Kristensen, K.J. and S.E. Jensen. 1975. A model for estimating actual evapotranspiration from potential evapotranspiration. *Nordic Hydrology* 6(3):170–188.

Mesinger, F., G. DiMego, E. Kalnay, K. Mitchell, P.C. Shafran, W. Ebisuzaki, D. Jovic, J. Woollen, E. Rogers, E.H. Berbery, M.B. Ek, Y. Fan, R. Grumbine, W. Higgins, H. Li, Y. Lin, G. Manikin, D. Parrish, and W. Shi. 2006. North American regional reanalysis. *Bulletin of the American Meteorological Society* 87:343–360.

NRCS. 1979. Exploratory Soil Survey of Alaska. STATSO Publication. U.S. Department of Agriculture, Natural Resource Conservation Service.

PLP. 2011a. Climate and meteorology Bristol Bay drainages. Chapter 2 in *Pebble Project Environmental Baseline Document 2004 through 2008.* The Pebble Partnership.

PLP. 2011b. Surface water hydrology Bristol Bay drainages. Chapter 7 in *Pebble Project Environmental Baseline Document 2004 through 2008.* The Pebble Partnership.

PLP. 2011c. Geology and mineralization, Bristol Bay drainages. Chapter 3 in *Pebble Project Environmental Baseline Document 2004 through 2008.* The Pebble Partnership.

PLP. 2011d. Groundwater hydrology Bristol Bay drainages. Chapter 8 in *Pebble Project Environmental Baseline Document 2004 through 2008*. The Pebble Partnership.

Prucha, R.H., J. Leppi, S. McAfee, and W. Loya. 2011. Development and Application of an Integrated Hydrologic Model to Study the Effects of Climate Change on the Chuitna Watershed, Alaska. Integrated Hydro Systems, LLC, Boulder, CO, and The Wilderness Society, Anchorage, AK. Available: http://alaska.fws.gov/fisheries/fieldoffice/anchorage/pdf/Documentation%20Report%20Climate%20Effects%20on%20Chuitna%20Hydrology%20Revised%200412.pdf. Accessed September 2012.

Rabus, B., M. Eineder, A. Roth, and R. Bamler. 2003. The shuttle radar topography mission – a new class of digital elevation models acquired by spaceborne radar. *Photogrammatic Engineering and Remote Sensing* 57:241–262.

Schlumberger Water Services. 2011. Groundwater hydrology. Chapter 8 in *Pebble Project Environmental Baseline Document 2004 through 2008*. Prepared for Pebble Limited Partnership. December. Available: http://www.pebbleresearch.com/ebd/bristol-bay-phys-chem-env/chapter-8/. Accessed January 2012.

Thompson, C., J. Beringer, F.S. Chapin III, and A.D. Mcguire. 2004. Structural complexity and land-surface energy exchange along a gradient from arctic tundra to boreal forest. *Journal of Vegetation Science* 15:397–406.

USGS. 1999. National Hydrography Dataset. U.S. Geological Survey, Reston, VA.

Verbyla, D.L. 2005. Assessment of the MODIS Leaf Area Index Product (MOD15) in Alaska. *International Journal of Remote Sensing*. 26(6):1277–1284.

STRATUS CONSULTING

1881 Ninth Street, Suite 201 Boulder, Colorado 80302 phone 303.381.8000 fax 303.381.8200 (headquarters)

1920 L Street, N.W., Suite 420 Washington, D.C. 20036 phone 202.466.3731 fax 202.466.3732

www.stratusconsulting.com